Armin Ernst
Felix J. F. Herth *Editors*

Endobronchial Ultrasound

An Atlas and Practical Guide

Springer

Endobronchial Ultrasound

Armin Ernst · Felix J.F. Herth
Editors

Endobronchial Ultrasound

An Atlas and Practical Guide

Springer

Editors

Armin Ernst, MD
Chief, Section of Interventional
Pulmonology; Director, Clinical,
Sponsored, and Translational Research,
Interventional Pulmonology/Thoracic
Surgery, Beth Israel Deaconess
Medical Center; Associate
Professor of Medicine,
Harvard Medical School,
Boston, MA 02215,
USA

Felix J.F. Herth, MD
Professor of Medicine, Chief,
Department of Pneumonology
and Critical Care Medicine,
Thoraxklinik, University
of Heidelberg,
D-69190 Heidelberg,
Germany

Preface

Since the introduction of the flexible bronchoscope by Dr. Ikeda in Japan, bronchoscopy has been limited to the inspection of the mucosal surface of the airways. However, the airway wall and parabronchial structures, such as lymph nodes, even though frequently of crucial importance to the examination, still could not be visualized and evaluated. After decades of conventional bronchoscopy, the introduction of endobronchial ultrasound was the first really new imaging modality and it completely changed the endoscopist's capabilities. The use of EBUS can be a liberating experience, as the natural limitations of endoscopy are overcome and the mediastinal structures are open for exploration, evaluation and guided biopsy.

The editors and contributors to this book have been deeply involved in this field since its inception and have instructed hundreds of physicians in the use of this technology. Many in the field routinely asked if a book or atlas with ready instruction and helpful hints was available. Our book is intended to fill this void. We have aimed specifically to stay away from reference recitals. Our goal instead, was to create an easy-to-use book, offering technical instruction, helpful hints and an atlas all at the same time. Additionally, we have included basic staging principles, essential to the physician who embarks on mediastinal biopsy and cancer staging.

We hope you will find this book stimulating and helpful in your practice and management of your patients.

Felix J. F. Herth, MD
Armin Ernst, MD

Contents

Contributors

HEINRICH D. BECKER • *Department of Interdisciplinary Endoscopy, Thoraxklinik, University of Heidelberg, D-69190 Heidelberg, Germany*

RALF EBERHARDT • *Department of Pneumonology and Critical Care Medicine, Thoraxklinik, University of Heidelberg, D-69190 Heidelberg, Germany*

ARMIN ERNST • *Chief, Section of Interventional Pulmonology; Director, Clinical, Sponsored, and Translational Research, Interventional Pulmonology/Thoracic Surgery, Beth Israel Deaconess Medical Center; Associate Professor of Medicine, Harvard Medical School, Boston, MA 02215, USA*

DAVID FELLER-KOPMAN • *Director, Interventional Pulmonology, Johns Hopkins University Hospital, Baltimore, MD 21205, USA*

SIDHU P. GANGADHARAN • *Staff Surgeon, Section of Thoracic Surgery, Beth Israel Deaconess Medical Center; Instructor in Surgery, Harvard Medical School, Boston, MA 02215, USA*

JED A. GORDEN • *Director, Interventional Pulmonology, Swedish Cancer Institute, Thoracic Surgery Clinic, Seattle, WA 98104, USA*

FELIX J.F. HERTH • *Professor of Medicine, Chief, Department of Pneumonology and Critical Care Medicine, Thoraxklinik, University of Heidelberg, D-69190 Heidelberg, Germany*

MARK KRASNIK • *Chief Surgeon, Department of Thoracic and Cardiovascular Surgery, University of Copenhagen, Gentofte University Hospital, Copenhagen DK 2100, Denmark*

GAETANE C. MICHAUD • *Staff Physician, Interventional Pulmonology, Beth Israel Deaconess Medical Center/Harvard University, Boston, MA 02215, USA*

MANDEEP S. SAWHNEY • *Assistant Professor of Medicine, Division of Gastroenterology, Beth Israel Deaconess Medical Center/Harvard University, Boston, MA, 02215 USA*

KAZUHIRO YASUFUKU • *Assistant Professor, Department of Thoracic Surgery, Graduate School of Medicine, Chiba University, Chiba 260-8670, Japan*
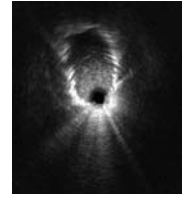
Physics and Principles of Ultrasound Imaging

David Feller-Kopman

In order to accurately interpret the images one sees on an ultrasound (US) monitor screen it is essential to have a basic comprehension of basic physics and the principles of ultrasound imaging. Several societies, including the Royal College of Radiologists *(1)*, the American College of Emergency Physicians *(2)*, and the American College of Surgeons *(3)* have developed guidelines that state the necessity of incorporating this fundamental knowledge base into one's practical training for using ultrasound at the bedside. This chapter will review some of these core principles, with key words or phrases used in the lexicon of US italicized for emphasis.

1. The Physics of Ultrasound

Ultrasound uses the transmission and reflection of mechanical waves at tissue interfaces to produce an audible or visual signal. The *wavelength* of ultrasound describes the distance between adjacent bands of compression and refraction, is measured in meters and is denoted by the symbol lambda (λ). Ultrasound *frequency* (f) is the number of wavelengths in one second and is measured in hertz (Hz) (**Fig. 1.1**). As humans can hear sound in the 20–20,000 Hz range, ultrasound is defined as sound with a frequency > 20,000 Hz, or 20 kilohertz (kHz). Diagnostic sonography for most medical applications uses frequencies of 2–20 megahertz (MHz). A key equation describing the interaction of wavelength and frequency is that *propagation speed* (c) is
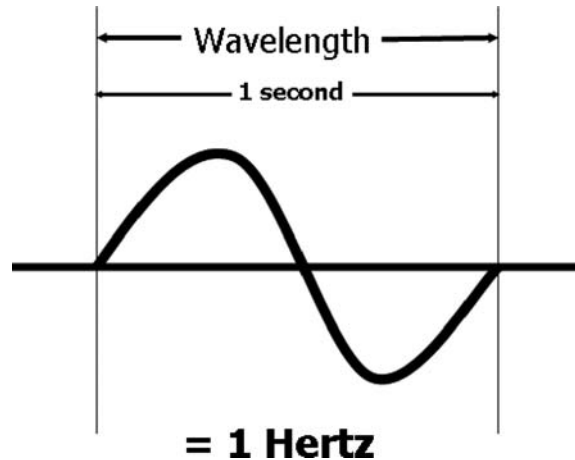
Fig. 1.1. Ultrasound wavelength and frequency. The wavelength (λ) is the distance (measured in meters) between adjacent bands of compression and refraction. Frequency is the number of cycles per second, and is measured in hertz (Hz).

equal to the frequency times the wavelength $[c = f \times \lambda]$. Frequency is determined by the sound source, and in the case of medical ultrasound, this is dependent on the thickness of the polycrystalline ferroelectric materials in the ultrasound transducer, which are typically made of lead zirconate titanates, a synthetic ceramic. Frequency is independent of the medium through which the sound travels. The propagation speed is, however, is dependent on the medium through which sound travels and, as we remember from high school physics, sound travels faster in solids, than in liquids and gasses. Non-compressible medium, such as tissue, has a wave velocity of approximately 1,540 meters/second (with different tissues having slightly different velocities), as compared to when the waves travel through air with a velocity of approximately 330 m/s. Since $c = f \lambda$, the wavelength varies inversely with the propagation speed. It is the changes in the speed of sound at tissue interfaces that result in a change of wavelength which determines image contrast and resolution.

Power and *intensity* are measures of the "strength" of the ultrasound wave. Power refers to the amount of energy passing through the tissue in a unit of time and is expressed in watts. Intensity refers to the energy per unit area per time (watts/cm^2). In the majority of handheld ultrasound units and endobronchial ultrasound units, the power is fixed. More sophisticated ultrasound units, however, have the ability to change the power settings and can actually be utilized therapeutically to destroy tissue, as is the case with high intensity focused US. For most diagnostic US the absolute intensity of the beam is less important than the intensity of the returning echo relative to the transmitted echo. Because the change in intensity is so large, due to *attenuation* of

the beam (discussed below), this relative intensity is measured in decibels (dB) which is equal to 10 log (transmitted intensity/incident intensity) *(4)*.

Medical US uses a pulse-echo approach to produce an image. A transducer converts one form of energy into another. Piezo-electric transducers convert electrical energy to mechanical energy by inducing vibration of the ferroelectric materials in the transducer head. These vibrations are transmitted through the tissue, echo back at boundaries of tissue that have different *acoustic impedance* (Z), and are again converted to an electrical signal. The transducer thus acts as an US transmitter and receiver, with the percentage of time that the transducer is transmitting referred to as the "duty factor." This is typically < 1% *(5)*. The acoustic impedance is equal to the density of the tissue (ρ) times the propagation speed ($Z = \rho c$). When the boundary between two tissues has a high acoustic impedance, most of the US is reflected back to the transducer. Typically, only a small fraction of the ultrasound pulse is reflected back, with the majority of the pulse continuing along the beam line and being scattered, refracted or transmitted. If two materials have the same acoustic impedance, their boundary will not produce an echo.

The percentage of transmitted echo that is reflected back also depends on the angle of incidence, with the angle of reflection being equal to the angle of incidence. Additionally, the continuation of the echo pulse will depend on the velocity of the beam on either side of the boundary, and is dictated by Snell's Law, which relates the angle of refraction to the speed of sound in both tissues *(4)*, and states the ratio of the sines of the angle of incidence and angle of refraction is equal to the ratio of the velocities in the two media, and opposite to the ratio of the incidences of refraction (n):

$$\frac{\sin \theta_1}{\sin \theta_2} = \frac{v_1}{v_2} = \frac{n_2}{n_1}.$$

As an US pulse (or echo) propagates through tissue, the energy contained within the beam progressively diminishes, or becomes attenuated. This results from absorption of the energy, with the energy lost as heat, as well as from scattering of the US beam. The amount of attenuation is dependent on frequency, as well as the medium through which the US beam travels. In soft tissue, US energy is absorbed and scattered, and the amount of attenuation is directly proportional to the frequency. Though liquids do not significantly absorb or scatter US energy, attenuation does occur, and is proportional to the square of the frequency *(6)*. Therefore, to image structures deep in the body, lower frequency transducers are required. Higher frequency waves, however, have better axial resolution, or the ability to distinguish two objects along the beam axis (**Fig. 1.2a**). Lateral resolution depends on the beam width as well as the focal zone (see below) of the
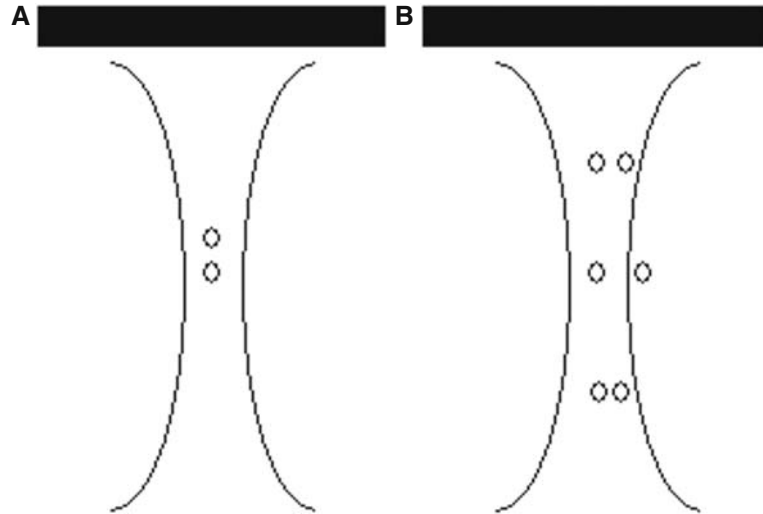
Fig. 1.2. (**A**) Axial resolution describes the ability to distinguish two points along the beam axis, and is dependent on the ultrasound frequency. (**B**) Lateral resolution is dependent on the beam-width and focal zone. The upper and lower points will be seen as one object, whereas the middle point can be differentiated from another point just lateral to it.

transducer (**Fig. 1.2b**). Axial resolution is typically between 2 and 4 wavelengths, whereas lateral resolution ranges between 3 and 10 wavelengths *(6)*. One would ideally like to use the transducer with the highest frequency (best resolution) while being able to obtain images from the desired depth (**Fig. 1.3**).
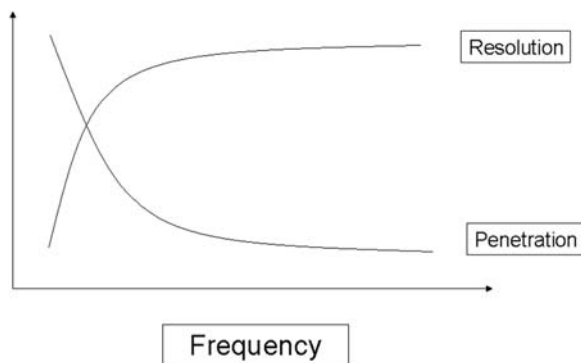
Fig. 1.3. The general relationship between frequency, resolution and penetration.

Ultrasound beams do not pass through tissue in a continuous, parallel fashion, but like a camera, have a certain focal zone. The beam is cylindrical in shape close to the transducer and becomes conical at a "transition zone." Additionally, there are several low intensity sound beams located peripheral to the main axis of the ultrasound beam that are called *side lobes*, which can interfere with

lateral resolution *(7)*. To compensate for this, the ultrasound beam can be focused. The focal zone of an ultrasound transducer can be adjusted mechanically with an acoustic lens that is part of the US transducer, or electrically. The area between the transducer and the focal zone is called the "near" or "Fresnel" zone, whereas the area more distant to the focal zone is called the "far" or "Fraunhofer" zone *(5)*. Almost all modern ultrasound units/transducers can continuously change the focus as echoes are received from deeper structures, thus always keeping the beam in focus.

The visual representation of the echo signal is referred to as brightness mode (B-mode) (**Fig. 1.4** top), or motion mode (M-mode) (**Fig. 1.4** bottom), which displays the motion (Y axis) of the echo reflection over time (X axis) on a single line of the B-mode image. M-mode allows for precise measurements of size and distances, especially with rapidly moving structures such as cardiac valves. In both B- and M-modes, it is the amplitude (measured in decibels) of the returning echo signal that
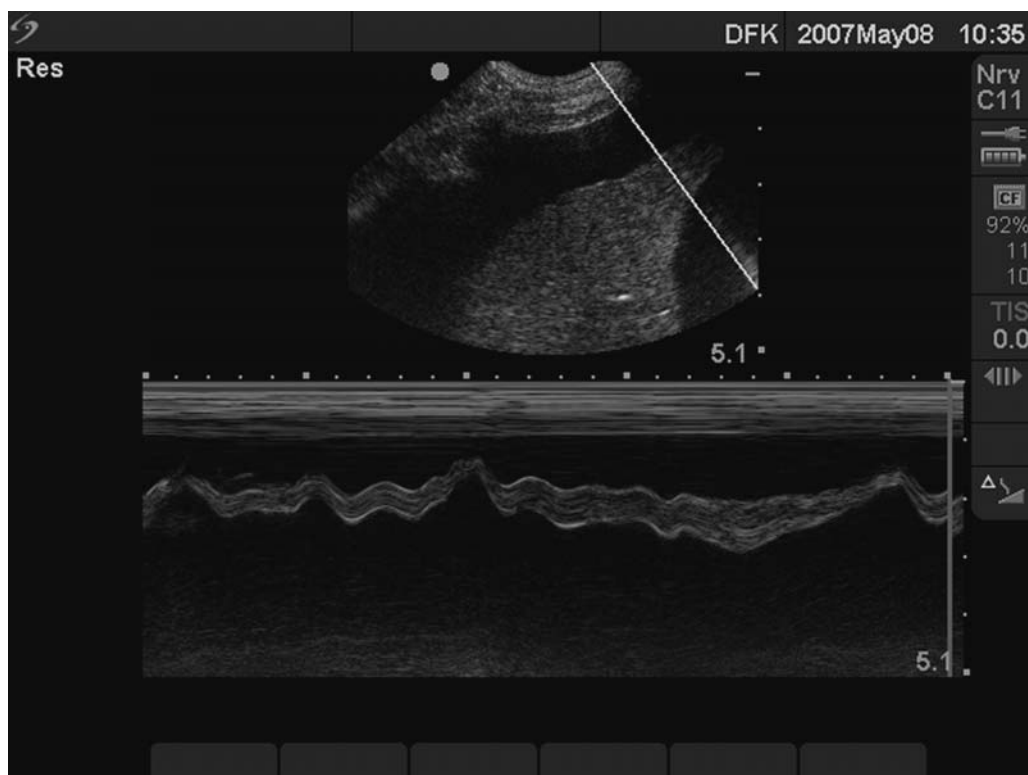
Fig. 1.4. B-mode (*top picture*) and M-mode imaging of a pleural effusion. With chest ultrasonography, cranial is to the *left* of the screen, caudal to the *right*, deep tissues are towards the *bottom* and superficial tissues are towards the *top* of the screen. The B-mode image shows normal lung in hypoechoic pleural fluid. This can be seen on the M-mode image as well, producing the 'sign-wave' sign, and confirms the hypoechoic area as fluid with the lung 'floating' in it.

determines the brightness on the screen, and the amount of reflected echo is a function of the density and nature of the target, as well as angle at which the sound wave is reflected. The B-mode image is produced by sweeping the US pulse perpendicular to the axis of the US beam, and as this occurs at rates of 20–40 frames per second *(8)*, it is seen as a continuous image by the human eye.

In addition to uniform preamplification of the received echo, the user can also adjust the *gain*, or the overall amplitude of the received echo, to make the picture appear more white or black. This is analogous to adjusting the volume on a radio receiver – the received signal is amplified prior to being transmitted to the speaker. The only ways to increase the brightness of an image are to either increase the power out of the transducer or increase the gain once the echo is received. As increasing power may lead to tissue destruction, many units do not allow the user to control this setting and, thus, they need to rely on adjusting the gain. *Time-gain compensation* is the ability to adjust the gain at varying depths such that equally reflective structures appear to have similar brightness, despite the fact that the echoes from deeper structures undergo more attenuation.

Echogenicity is the tissue's ability to reflect the pulsed echo. This is primarily determined by the density and acoustical impedance of the tissue. By convention, tissues such as the liver and kidney are said to be isoechoic. Tissues that reflect more US waves back to the transducer are hyperechoic, whereas fat, blood, and fluid tend to absorb more of the US energy and are hypoechoic. The *gray scale* of B-mode imaging is the range of echo strength on the black-white continuum. Bone is a significant absorber, and scatterer of US energy (see below). Since air reflects nearly 99 percent of the ultrasound waves, the ultrasound transducer needs to be coupled to the tissue in order for the waves to penetrate more deeply. This can be done with coupling gel on the outside of the body, or with a water-filled balloon, as is done with endobronchial ultrasound. Even with coupling, however, it is very difficult to image beyond the periostium (the internal components of bone) or air filled structures such as the lung.

All frequencies have associated *harmonics*, or integral multiples of the fundamental frequency. For example, a second harmonic has twice the frequency as the 1st harmonic (fundamental frequency). As US waves travel through tissues, they become slightly distorted from the true sine-wave shape to a sharper, more sawtooth shape, which contains frequency components comprised of higher order harmonics *(8)*. Since the harmonics are of higher frequencies than the fundamental, they are subject to more attenuation. *Tissue harmonic imaging* (THI) utilizes these features to minimize the reflections and scattering created by the superficial structures with the fundamental frequency and improves lateral resolution.

The *Doppler effect*, named after the 19th century Austrian mathematician, describes the changes in frequency and wavelength as perceived by an observer moving relative to the sound source. As the sound source moves closer to the receiver, the wavelengths become compressed. Likewise, as the sound source moves farther from the receiver, the wavelengths lengthen. Because wavelength is inversely proportional to frequency (when velocity is constant), the observer will detect a perceived frequency that is different from that emitted by the source when the relative velocity is zero. Because medical US uses the pulse-echo approach, there is a Doppler effect as the US beam hits its target, as well as when it bounces back from the target *(9)*.

There are several US modes that utilize the Doppler effect, including *continuous wave, pulsed-wave, color flow*, and *power* Doppler US *(7, 9)*. Continuous wave Doppler uses the continuous generation and sensing of the reflected echo. Because it is not possible for a single transducer element to simultaneously transmit and receive the Doppler signal, two separate crystals are required. As the signal is analyzed continuously, this modality is primarily used for looking at high velocity movement, such as flow through stenotic valves. Pulsed-wave Doppler uses the standard pulse-echo mechanism and is able to analyze the Doppler characteristics at a given region of flow, depending on the time delay between sound transmission and receiving (called the pulse repetition frequency, PRF). If the region of interest is close to the transducer, the PRF is short, and if the target is further away, the PRF is longer. This property makes pulsed-wave Doppler ideal for looking at flow and velocity at a given point. Due to the intermittent nature of transmission and receiving, there is a velocity limitation beyond which the US will misinterpret velocity and direction of flow. The term *aliasing* is used to describe an apparent reversal of direction that is caused by the relatively low sampling rate.

Endobronchial US utilizes either color flow or power Doppler to help distinguish blood vessels from lymph nodes. Color flow Doppler uses the pulsed-wave Doppler echoes to produce an image that shows both the velocity and direction of flow. By convention, flow moving toward the transducer is colored red-orange and flow moving away from the transducer is colored blue. This is important to remember, as the novice ultrasonographer may interpret red to mean arterial blood and blue as venous blood, when in fact the colors are purely dependent on the direction of flow relative to the transducer. In addition, if the movement of the target is perpendicular to the US beam it will not give rise to any Doppler frequency shift *(6)*. As red blood cells are the primary source that generates the Doppler signal, and as they are much smaller than the ultrasonic beam, one will see a single color if all the cells flow in the same direction, as is the case with purely laminar flow. With turbulent flow, a broad spectrum of frequencies is

obtained. The technological requirements for color Doppler are more complex and, in order to allow for the accurate measurement of the Doppler frequencies, a longer pulse duration is sometimes used. This may increase the pixel size and reduce spatial resolution. In order to overcome this, many units will acquire Doppler images on only a portion of the B-mode image so they can be acquired at the appropriate frame rate. The Doppler window can be moved to any desired location on the screen, typically with a trackball or other controller. Power Doppler, on the other hand, solely relates information about velocity, and not the direction of flow. An advantage of power Doppler is that it is more sensitive than color flow Doppler for detecting slower flow rates and smaller vessels. Clearly, all types of Doppler imaging will show any movement relative to the transducer. In the case of endobronchial ultrasound, a hypoechoic lymph node may appear to be a vessel to the novice sonographer due to normal respiratory or cardiac induced motion.

2. Basic Instrumentation

All US units have an electrical source, a piezoelectric transducer, and a computer processor that will turn the energy from the received echo into a visible picture. Ultrasound transducers come in several varieties, including simple single element disc transducers, annular, linear, sector, phased arrays, and radial probes. The differences in these probes lie in the way the beam is focused, the beam pattern, and the ability to electronically steer the beam.

Each of these transducers generates an "A-line," that is one beam or pulse that is directed in the axial plane of the US. The B-mode image is produced by sweeping the A-lines along the transducer to produce a *footprint* that is square/rectangular, trapezoidal or circular, depending on the probe. As mentioned above, the amplitude of the echo determines the brightness of the pixel, and the position of the pixel on the screen is determined by the depth from which the returning echo originates. Most all transducers, aside from radial probes, have some mark on them that corresponds to a mark on the screen so the operator can correlate what they are seeing to the orientation of the probe. Ultrasound units have several knobs, buttons and dials, and a recently coined term, knobology, describes the understanding of what these controls do. The sophistication of the computer processors has actually allowed many of the functions to be preset, or set automatically depending on which transducer is connected. As such, power and focus controls are not on many of the smaller units, and defaults for gain, depth and contrast are already

calibrated. Most US units have ways to enter pertinent patient data (name, medical record number) and means to control depth, contrast, gain and provide basic measurements such as distance or more complex measurements such as gestational age, volume and cardiac output. Ultrasound units also may have the ability to store pictures or movies.

3. Important Ultrasound Artifacts

Much of what is seen on B-mode imaging relies upon the accurate interpretation of ultrasound artifacts. This is especially true when ultrasound in used for thoracic imaging. As mentioned above, fluid does not significantly attenuate ultrasound energy. As such, structures that are deep to a fluid filled space may show some relative *acoustic enhancement*, that is they appear brighter than one would expect based solely on tissue characteristics and depth. This can be used clinically, as it lends support to the probability that the hypoechoic material proximal to the area of enhancement is indeed fluid. *Acoustic shadowing* is the effect opposite to enhancement and is seen when an intervening structure strongly attenuates the US energy. This is classically described for rib shadows, gallstones, and more solid tumors. It should be noted that not all strong reflectors will induce shadowing. Macro-calcifications, which are generally the size of an ultrasound beam, will be reflected and cast a shadow. Microcalcifications, on the other hand, are smaller than the US beam and will not induce shadow. They will just be seen as hyperechoic dots.

When a strong echo is obtained – as is the case with bone, air, the diaphragm or a needle – the reflector can continue to give rise to the echo even as the US transducer sweeps the beam laterally. This generates a long, curved, hyperechoic line called a *side lobe artifact*. These artifacts have a radius of curvature that corresponds to the distance between the transducer and the strong reflector *(6)*. A *mirror image artifact* also results from the US beam encountering a strong reflector such as the diaphragm, and produces a false image equal in distance, and deep to the reflector, that disappears with subtle changes in transducer positioning *(10)*.

Reverberation artifacts are usually seen as bright parallel lines occurring at regular intervals, and are commonly seen in the chest *(11)*. "A" lines are hyperechoic horizontal lines that may be seen between rib shadows and are equally spaced with a distance equal to the skin-pleural distance. "B" lines, or comet tail artifacts, originate from the pleural surface, and spread vertically to the edge of the screen without fading. By definition, they erase

A-lines and move with respiration. "E" lines that appear similar to B-lines, however, are due to subcutaneous emphysema and, therefore, originate just under the skin surface *(11)*.

Refractive shadows can occur when the sound beam hits the boundary between two media with different acoustic impedances at an oblique angle. If the beam path travels from a higher velocity medium (soft tissue) to a lower velocity medium (fluid), the US beam converges, whereas the beam diverges if traveling from a low velocity to a high velocity medium *(10)*. If the ultrasound beam is relatively wide in reference to the imaged target some of the beam may be interacting with a fluid filled target and the other portion of the beam with adjacent soft tissue. This *beam-width artifact* can create spurious echoes within the target.

Finally, though not truly an artifact, the operator should be aware of poor image quality due to inadequate coupling gel, or anatomic limitations such as obesity or surgical dressings. One may need to position the patient in a way to bring the target closest to the transducer, and scan in multiple planes in order to obtain a satisfactory image.
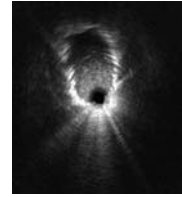
4. Summary

Prior to incorporating the use of ultrasound into one's daily practice, it is essential to understand the basic physics and principles of ultrasound imaging. In order to obtain the best image, one should position the target tissue as close to the transducer as possible, and use the highest frequency transducer that will penetrate to the desired depth. Some "golden rules" of ultrasound imaging include: '(1) Never make an interpretation on a single image… (2) Because a feature is displayed it is not necessarily real… (3) Because a feature is not displayed it is not necessarily not there.' *(6)* It is only through practice, and repeated imaging that one develops the skills necessary to fully reap the benefits of ultrasound imaging.

References

1. Board of the Faculty of Clinical Radiology TRCoR. Ultrasound Training Recommendations for Medical and Surgical Specialties. Royal College of Radiology. 2004. 11-6-2006. Ref Type: Electronic Citation.
2. American College of Emergency Physicians. Use of ultrasound imaging by emergency physicians. Ann Emerg Med 2001; 38(4): 469–470.
3. American College of Surgeons. Ultrasound Examinations by Surgeons. http://www.facs.org/fellows_info/statements/st-31.html. 1998. 3-15-0006. Ref Type: Electronic Citation.

4. Aldrich JE. Basic physics of ultrasound imaging. Crit Care Med 2007; 35(5 Suppl): S131–S137.

5. Smith RS, Fry WR. Ultrasound instrumentation. Surg Clin North Am 2004; 84(4): 953–971.

6. Kossoff G. Basic physics and imaging characteristics of ultrasound. World J Surg 2000; 24(2):134–142.

7. Lawrence JP. Physics and instrumentation of ultrasound. Crit Care Med 2007; 35(8 Suppl):S314–S322.

8. Hangiandreou NJ. AAPM/RSNA Physics Tutorial for Residents: Topics in US: B-mode US: Basic Concepts and New Technology. Radiographics 2003; 23(4):1019–1033.

9. Boote EJ. AAPM/RSNA Physics Tutorial for Residents: Topics in US: Doppler US Techniques: Concepts of Blood Flow Detection and Flow Dynamics. Radiographics 2003; 23(5):1315–1327.

10. Scanlan KA. Sonographic artifacts and their origins. Am J Roentgenol 1991; 156(6): 1267–1272.

11. Lichtenstein DA, Meziere G, Lascols N et al. Ultrasound diagnosis of occult pneumothorax. Crit Care Med 2005; 33(6): 1231–1238.

Chapter 2

Relevant Thoracic Anatomy

Jed A. Gorden

1. Central Airway Anatomy

This section outlines the basic anatomy of the tracheobronchial tree, including lengths and diameters (**Fig. 2.1**). This serves as a reference for bronchoscopic procedures because a critical understanding of airway anatomy is vital to the planning of any airway procedure. Knowledge of airway anatomy allows the bronchoscopist to correlate radiographic findings with endoluminal anatomy, ensuring accurate biopsies and lavage specimens. In addition to specimen acquisition, anatomic accuracy is essential when communicating with surgical, oncology and radiation oncology colleagues. In addition, comfort with bronchoscopic landmarks will prevent the operator from becoming disoriented during the procedure and give them the confidence and flexibility to perform bronchoscopy from multiple positions including head of the bed, facing the patient or other positions that best serve the patient and operator's needs. This chapter hopes to familiarize the reader with common bronchoscopic anatomy and landmarks that will enhance performance, accurate specimen acquisition and communication with colleagues.

2. Upper Airway

The central airways may be accessed with the bronchoscope either through the nose or the mouth; each has its own unique anatomy and each serves as a conduit to the central airways below.
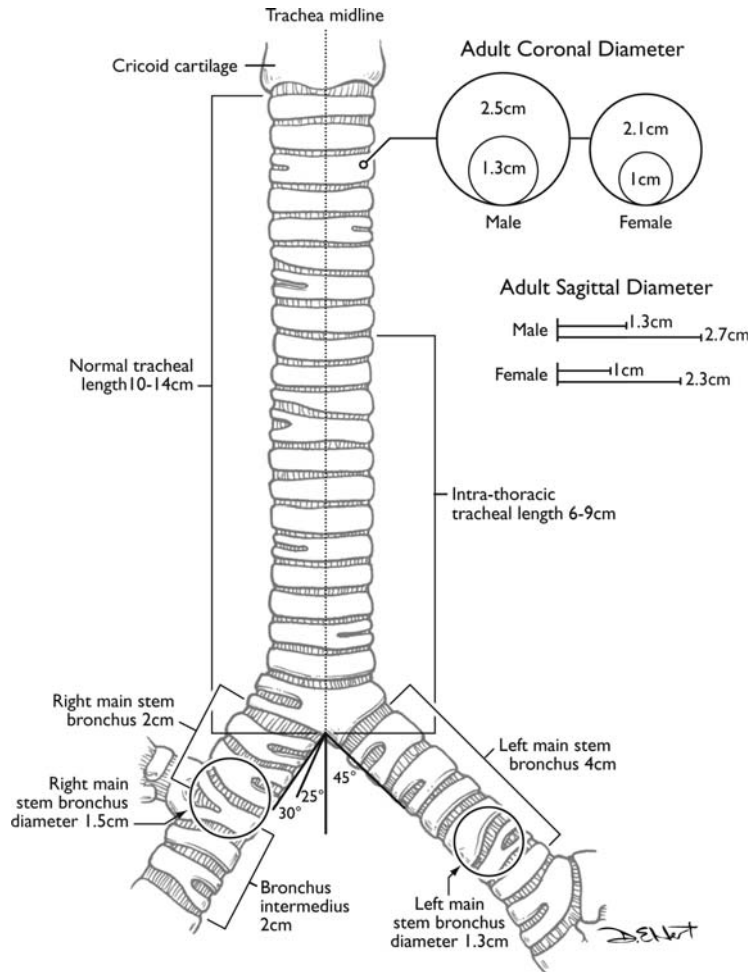
Fig. 2.1. Basic anatomy of the tracheobronchial tree. Reprinted with permission from Gorden JA, Wood DE. Rigid bronchoscopy. In: Simoff MJ, et al. (eds). Thoracic Endoscopy. Oxford: Wiley-Blackwell; 2006: 121–133.

Bronchoscopy can be performed through the left or right nares. The nasal passage is composed of the external nares, nasal cavity and nasal pharynx. The medial border of each nostril is the nasal septum, the lateral border is the turbinate and the inferior border is the hard palate which separates the nares from the mouth *(1)*. When viewing the larynx through the bronchoscope the most prominent structure is the epiglottis. When performing bronchoscopy from the head of the bed the epiglottis is a prominent curved flap that lies in the anterior and superior position and projects out into the posterior pharynx (**Fig. 2.2**). Advancing the bronchoscope under the epiglottis allows the operator to visualize additional structures of the larynx. The most inferior structure before the esophagus is the interarytenoid notch bounded by the Corniculate tubercule and Cuneiform tubercle,

Fig. 2.2. Bronchoscopy performed from the head of the bed with the patient supine. Prominent central structure is the epiglottis.

respectively. Tethered between the epiglottis superiorly and the interarytenoid notch inferiorly are the vocal folds (true vocal cords) medially and the ventricular folds (false vocal cords) laterally. When the vocal cords are open the bronchoscopist has a view into the proximal portion of the trachea (**Fig. 2.3**); when they are closed the vocal cords should be in apposition at the midline with the false cords stretched to close the opening (**Fig. 2.4**).

The larynx is an important point of inspection for the bronchoscopist. Lack of movement of either of the vocal chords can be a clue to recurrent laryngeal nerve damage or a hidden tumor in the mediastinum below.

3. Trachea

The origin of the trachea is defined as the inferior aspect of the cricoid cartilage at the approximate level of the 6th or 7th cervical vertebra. The distal margin of the trachea is the main carina

Fig. 2.3. Bronchoscopy performed from the head of the bed with the patient supine. View of the larynx with the vocal chords abducted with the proximal trachea visualized below.

marking the bifurcation of the right and left main stem bronchi at the approximate level of the 5th thoracic vertebra. The trachea is divided into the extra- thoracic trachea, which lies above the suprasternal notch approximately one-third of its total length, and the intrathoracic trachea, which falls below the suprasternal notch making up two-thirds of its total length. The length of the normal adult trachea is 10–14 cm. Computed tomography (CT) guided measurements of the intrathoracic tracheal length range from 6–9 cm in adults. The coronal diameter of the normal trachea in adult males ranges from 1.3 cm to 2.5 cm; the sagital diameter ranges from 1.3 cm to 2.7 cm. The coronal diameter of the normal trachea in women ranges from 1 cm to 2.1 cm, the sagital diameter 1 cm to 2.3 cm *(2–4)*. The length of the pediatric trachea is the same for males and females representing similar gender growth rates from birth to adulthood. At age 14 the female trachea ceases to grow while the male trachea continues to enlarge, but not lengthen until maximum adult diameter is achieved *(5)*. The trachea maintains its structure with the rigid structural support of 18–24 C-shaped cartilaginous anterior rings. The posterior wall of the trachea is a membranous band and lacks cartilaginous support

Fig. 2.4. Bronchoscopy performed from the head of the bed with the patient supine. View of the larynx with the vocal chords adducted. The central stripe is the true left and right vocal chords in apposition. At the 12 o'clock position is the base of the epiglottis.

(**Fig. 2.5**). The presence of the membranous trachea allows the diameter of the intrathoracic trachea to be dynamic, expanding with inspiration and recoiling upon expiration.

The structural difference of the anterior and posterior trachea is critical to maintaining orientation during bronchoscopy. The experienced bronchoscopist is required to be facile, performing bronchoscopy from the patient's front and with the patient supine from the head; knowing that the cartilaginous portion of the trachea is anterior and the membranous portion is posterior ensures correct orientation of the left and right mainstem bronchi, regardless of bronchoscopic position.

4. Main Carina

The main carina denotes the first branching of the airway. The main carina marks the bifurcation of the trachea into the right and left main stem bronchi (**Fig. 2.6**). For orientation the membranous

Fig. 2.5. Bronchoscopy performed from the head of the bed with the patient supine. This view is of the distal trachea with the main carina in view. Prominent cartilaginous rings form the anterior structure; the membranous trachea is seen forming the posterior wall.

portion of the airway remains posterior and the cartilaginous rings support the anterior structure; this is critical to confirm right and left orientation during bronchoscopy. Anatomically the main carina relates to the manubriosternal junction or the 5th–6th thoracic vertebrae. There is wide variability in the accepted normal subcarinal angle, with mean angles ranging from 56–61 degrees *(2)*. In adults the left main stem bronchus branches at a more obtuse angle relative to the midline trachea in contrast to the right main stem bronchus. In the pediatric population, ages birth to 15 years, there is no statistical difference in the right and left main stem bronchial angles when measured from the midline trachea *(2)*.

5. Right Bronchial Tree

5.1. Right Main Stem Bronchus

The right main stem bronchus (RMSB) is defined at its proximal end by the main stem carina and at its distal end by the right upper lobe orifice. In adults the course of the right main stem bronchus

Fig. 2.6. Bronchoscopy performed from the head of the bed with the patient supine. The main carina forms the central structure. The *left* and *right* main stem bronchi are in view. The length of the *left* main stem bronchus is well illustrated. Continuation of the anterior cartilaginous support and membranous posterior wall is well represented in this view of the *left* main stem bronchus.

off the trachea is more direct than that of the left main stem bronchus. The right main stem bronchus diverges off the trachea at an angle of 25–30 degrees from the midline. The approximate diameter of the right main stem bronchus is 1.5 cm. The approximate length of the right main stem bronchus is 2 cm *(2–3)*.

5.2. Right Upper Lobe Bronchus

The right upper lobe bronchus is the first airway visible off the right main stem bronchus. The origin of the RUL is the lateral wall of the RMSB. The rapid branching of the right bronchial tree with its short RMSB distinguishes it from its left-sided companion and serves as another anatomic clue of left and right orientation. Upon entry, the right upper lobe immediately trifurcates into the anterior, apical and posterior segments (**Fig. 2.7**). From the mouth of the right upper lobe the anterior segment is at the nine o'clock position, the apical at 12 o'clock and the posterior at three o'clock.
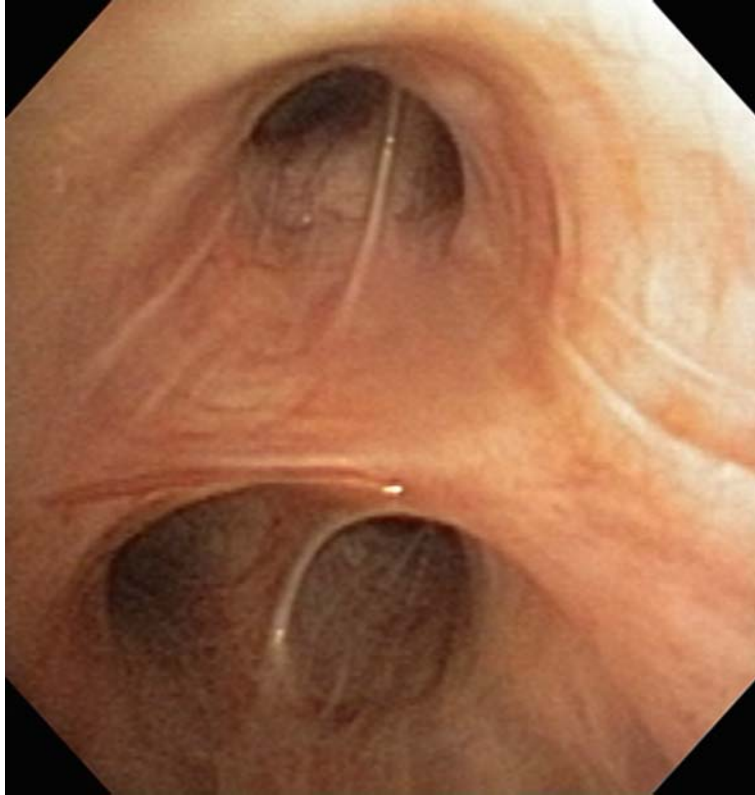
Fig. 2.7. Bronchoscopy performed from the head of the bed with the patient supine. The trifurcation of the right upper lobe is illustrated in this image. The anterior segment is inferior and 9 o'clock, the apical segment is at 12 o'clock, the posterior segment is inferior and at 3 o'clock.

Entry into the RUL from the RMSB comes at an acute angle and often requires a clockwise rotation of the bronchoscope and flexion of the bronchoscope tip.

5.3. Bronchus Intermedius

The bronchus intermedius is the continuation of the right bronchus distal to the right upper lobe take off. The proximal border is the right upper lobe bronchus, and the distal border is the right middle lobe and right lower lobe bifurcation. The length of the bronchus intermedius is approximately 2 cm long *(2)*.

5.4. Right Middle Lobe

The right middle lobe orifice is found on the medial and slightly anterior aspect of the right bronchial tree (**Fig. 2.8**). The opening of the right middle lobe is often described as having a fishmouth appearance. The right middle lobe forms the distal border of the bronchus intermedius. The right middle lobe bronchus is 1–2 cm in length and then bifurcates to form the medial and lateral branches.
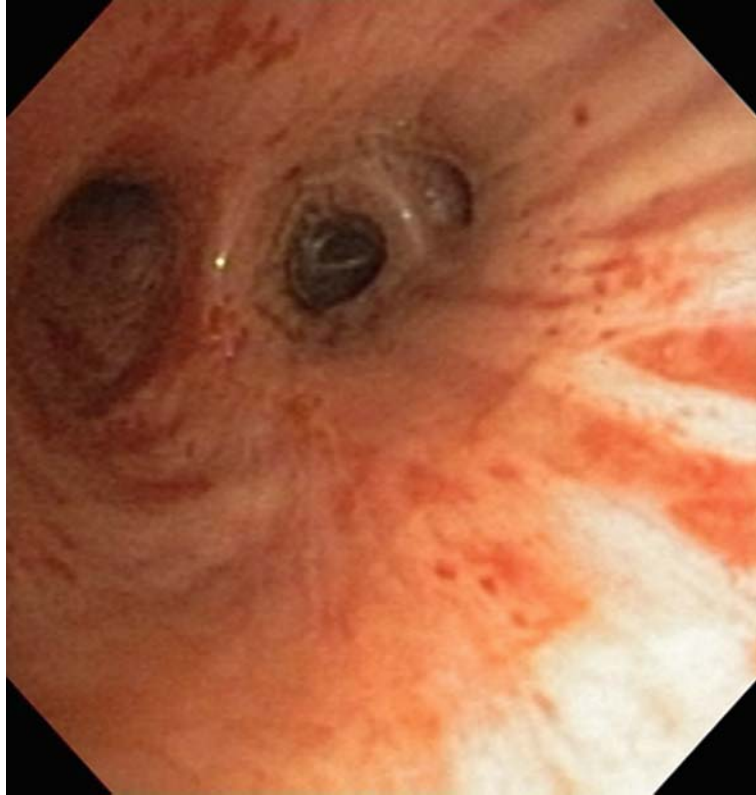
Fig. 2.8. Bronchoscopy performed from the head of the bed with the patient supine. For this image the bronchoscope is positioned in the bronchus intermedius. The right middle lobe is the large orifice at 9 o'clock, in the middle the distal lower lobes are visualized and at 9 o'clock the superior segment of the lower lobe is in view.

5.5. Right Lower Lobe Basilar Segments

The posterior wall of the bronchus intermedius gives rise to the airway supplying the superior segment of the lower lobe, which is nearly directly across from the right middle lobe orifice. Distally the right lower lobe divides into the medial basilar, anterior, lateral and posterior segments *(2)* (**Fig. 2.9**). The medial basilar segment is the next orifice after the superior segment of the lower lobe; its origin is the medial wall of the airway inferior to the right middle lobe. The more distal anatomically accessible airways are the anterior, lateral and posterior segments. These segments often go by the acronym ALPs, meaning (A) anterior, (L) lateral and (P) posterior segments. There is often normal anatomic variation to the positioning of these structures, but in most cases these three orifices fall in the same linear plane with the anterior segment in the most medial and anterior position, the lateral segment falling in the middle and the posterior segment being the most lateral and posterior structure.
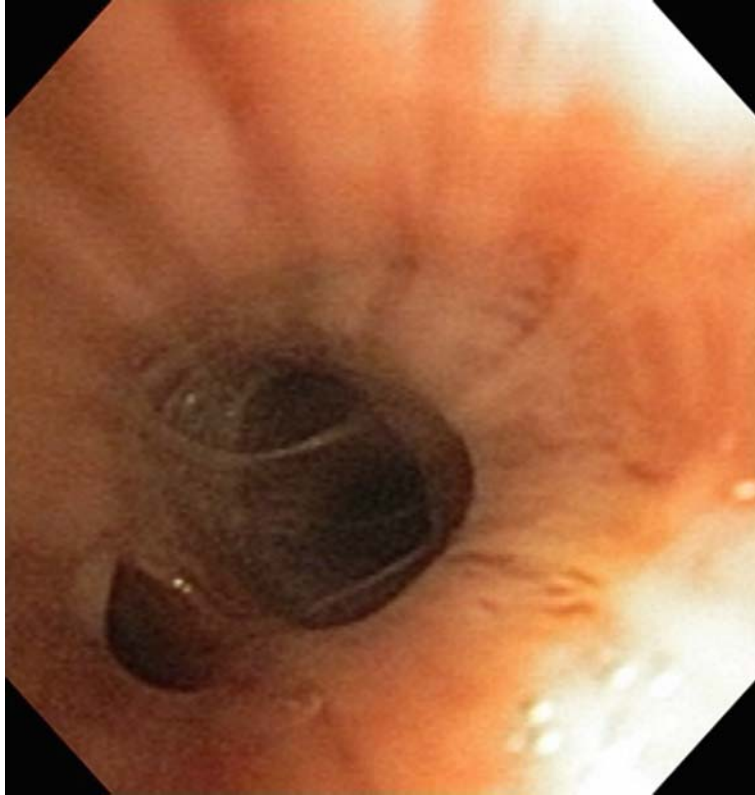
Fig. 2.9. Bronchoscopy performed from the head of the bed with the patient supine. Right lower lobe segments. At the 8 o'clock position is the entrance to the medial basilar segment. Centrally the ALPs are visualized. At 11 o'clock (A) anterior segment, in the middle position sits the (L) lateral segment, and the most posterior orifice is the (P) posterior segment.

6. Left Bronchial Tree

6.1. Left Main Stem Bronchus

The left main stem bronchus (LMSB) rises off the trachea and forms the origin of the left bronchial tree. In adults the left main stem bronchus forms a more obtuse angle of divergence from the midline trachea than the right main stem. The left main stem bronchus diverges from the midline trachea at an approximately 45-degree angle. The diameter of the left main stem is approximately 1.3 cm, and the length is approximately 4 cm. The boundaries of the left main stem bronchus are the main carina at its proximal end and the branching of the left upper and lower lobes at its distal end *(2)*. The left main stem bronchus is considerably longer than its right main stem counterpart, and this is a critical anatomic feature to help maintain orientation. The distal boundary of the LMSB bronchus is the carina dividing the left lower lobes and left upper lobe and lingual.

**6.2. Left Upper Lobe
and Lingula**

The left upper lobe and lingual orifice open anterior to the left lower lobe, often in a roughly 12 o'clock to six o'clock relationship (**Fig. 2.10**).
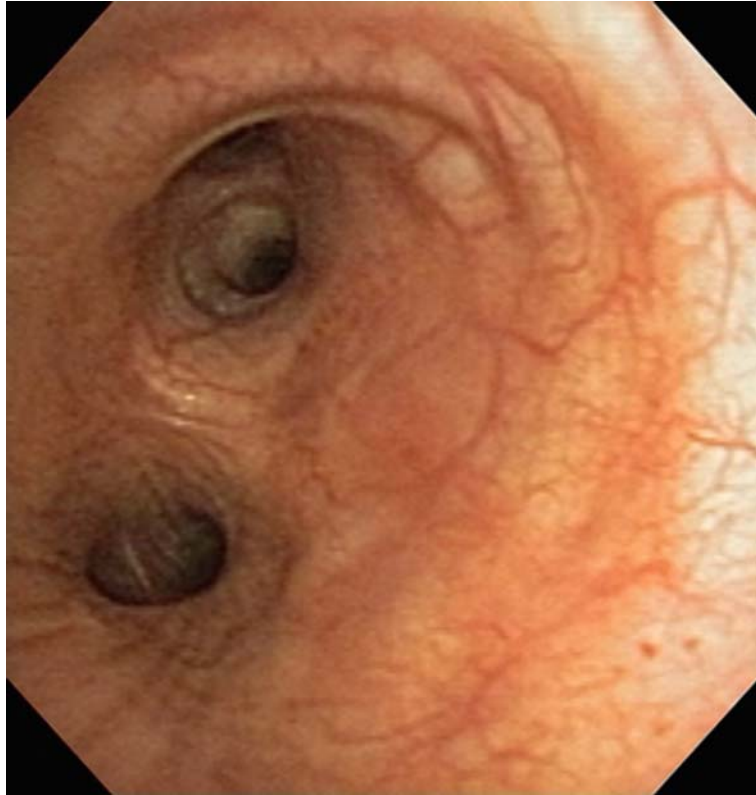

Fig. 2.10. Bronchoscopy performed from the head of the bed with the patient supine. The bronchoscope is positioned in the distal left main stem bronchus. The left upper lobe and lingual are at 12 o'clock with the first orifice at this position being the lingual, and the superior segment of the lower lobes and distal lower lobes are at 6 o'clock.

The lingula is the first orifice to appear and is found in the medial position. The lingula further subdivides into the superior and inferior lingular divisions.

The left upper lobe divides into the apicoposterior and anterior subdivisions.
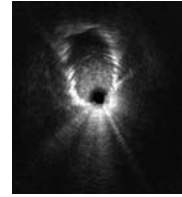
6.3. Left Lower Lobe

The left lower lobes divide off the posterior wall of the left main stem carina. The lower lobes divide into the superior segment across from the upper lobe takeoff and the anterior medial, lateral and posterior segments. Similar to the right bronchial tree, there is frequent variation to the remaining basilar subsegments.

7. Summary

A comprehensive understanding of airway anatomy is critical to effective bronchoscopy and good communication with colleagues. Developing a pattern for away inspection that methodically inspects each anatomic landmark in order is good practice. With knowledge of airway landmarks the bronchoscopist should be able to withdraw to the last recognized anatomic land in order to regain anatomic orientation.

References

1. Wang KP, Mehta AC, Turner JF (eds.). Flexible Bronchoscopy. 2nd Edition. Blackwell Publishing, 2004.
2. Fraser RS, Muller NL, Colman N, Pare PD (eds.). Diagnosis of Diseases of the Chest. 4th Edition. W.B. Saunders Company, 1999.
3. Pearson GF, Cooper JD, Deslauriers J, et al. (eds.). Thoracic Surgery. Second Edition. Churchill Livingstone, 2002.
4. Griscom NT, Wohl ME. Dimensions of the growing trachea related to Age and Gender. AJR Am J Roentgenol 1986; 146(2): 233–237.
5. Cleveland RH. Symmetry of bronchial Angles in Children. Radiology 1979; 133(1): 89–93.

Basic Principles of TBNA

Gaetane C. Michaud

Transbronchial needle aspiration (TBNA) is a bronchoscopic technique popularized in the 1980s to obtain histologic or cytologic specimens. A needle is passed either through the barrel of the rigid bronchoscope or alternatively via the working channel of a flexible bronchoscope (**Fig. 3.1**). TBNA can be used to obtain tissue from endoluminal abnormalities, lymph nodes or tissue adjacent to the airway, as well as peripheral lung tissue.

The technique was first described by Schieppati in 1949 using both a rigid needle and bronchoscope *(1)*. Its use in North America evolved in the late 1970s and early 1980s. With the more widespread use of flexible bronchoscopy, newer needles were developed, the first description of this innovative technology being in 1979 *(2)*. Since then, both TBNA's use and its technology have expanded.

Fig. 3.1. TBNA via Rigid Bronchoscope.

1. Indications

TBNA is primarily used to diagnose and stage bronchogenic malignancy. TBNA may be used to sample tissue from endobronchial tumors, submucosal lesions and tumors adjacent to the central airways, particularly when resulting in extrinsic compression of the airway. Peripheral lung tissue may be sampled using this technique; for example, peripheral lung nodules or masses. It may also be used to evaluate mediastinal adenopathy for presence of malignancy.

1.1. Mediastinal Staging

Cancer stage is a factor of tumor extension, lymph node involvement and metastatic spread. This is particularly true in the case of non-small cell lung cancer (NSCLC) (3). With few exceptions, prognosis and subsequent therapeutic options are in turn dependent on the stage of disease at clinical presentation (4, 5). Recently published guidelines by the European Society of Thoracic Surgery and American College of Chest Physicians for the staging of NSCLC recognize the importance of correct staging of the mediastinum when considering surgery for curative intent (4, 5). Stage III NSCLC has been found to be a heterogeneous group; therefore, multi-station sampling may be of benefit. Both computed tomography (CT) and positron emission tomography (PET) play a role in defining the anatomy and screening for lymphatic and metastatic involvement; however, tissue is still required for pathologic confirmation of abnormal findings (6). Mediastinoscopy is considered the gold standard; however, it does require a general anesthesia and has an associated 2 percent morbidity and 0.08 percent mortality rate in experienced hands (5). Multimodality treatment protocols for stage III NSCLC often include restaging following induction chemotherapy and radiation. Remediastinoscopy may be a technically challenging procedure due to the development of adhesions and scar tissue in the prior surgical bed. TBNA with or without guidance has the advantage over other techniques for mediastinal staging as it can be performed at the time of the diagnostic bronchoscopy with minimal sedation. Lymph nodes in the right paratracheal (4R), left paratracheal (4L), subcarinal (7) and right and left interlobar (11R, 11L, respectively) by Mountain's lymph node map are all readily accessible without significant morbidity or mortality (7, 8) (**Fig. 3.2**). Due to the minimally invasive nature of TBNA, there should be no deleterious impact on restaging if necessary.

A recent systematic review of the literature and a meta-analysis to assess the diagnostic yield of TBNA for mediastinal adenopathy in NSCLC varied between 14 percent and 100 percent (5, 8). Detterbeck's review of the literature included 1,339 patients with pooled TBNA sensitivity and specificity of 78 percent and
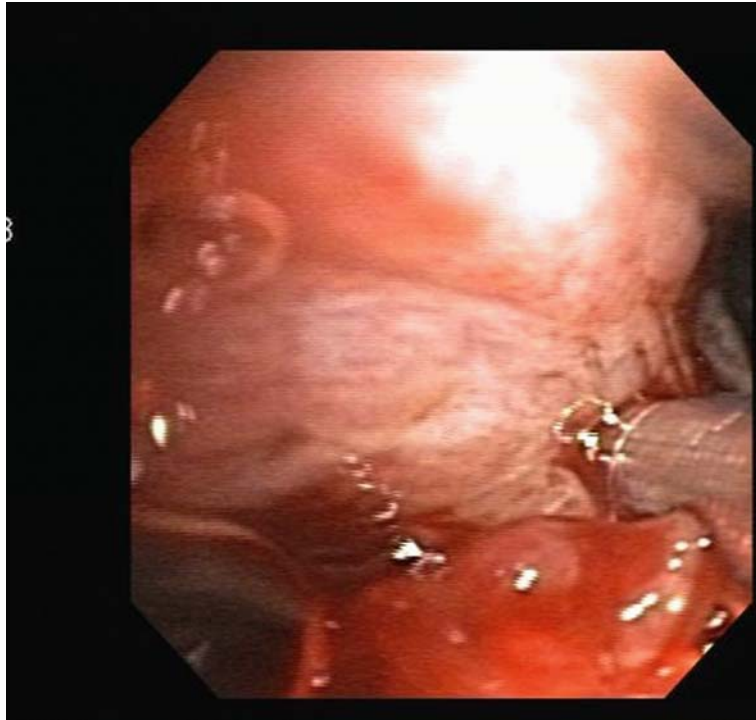
Fig. 3.2. TBNA for mediastinal staging in non-small cell lung cancer.

99 percent, respectively. There was only a 1 percent false positive rate; however, there was a 28 percent false negative rate. The prevalence of disease in this pooled analysis was 75 percent *(5)*. Holty's meta-analysis included many of the studies included in Detterbeck's systematic review; however, classified studies into two tiers. Non-tier 1 was more liberal and included studies designed to prospectively sample mediastinal lymph nodes in patients with NSCLC. Sufficient information had to be included to determine TBNA's sensitivity and specificity and must include at least 10 patients. Tier 1 was more rigorous and included studies in which TBNA findings were surgically confirmed and there were at least 10 subjects with and without metastatic lymph node involvement from NSCLC *(8)*. There was marked heterogeneity amongst the studies; therefore, a pooled sensitivity of all studies was not reported. The sensitivity and specificity for the tier 1 studies were 36 and 98 percent, respectively. The sensitivity is much lower than in Detterbeck's analysis; however, the prevalence of disease in the tier 1 studies was only 34 percent. This was more in keeping with the pooled prevalence in a recent meta-analysis of mediastinoscopy for mediastinal staging in NSCLC *(5)*. A higher prevalence of disease will positively influence the sensitivity and likely at least partially explains the marked variability in the diagnostic yield of TBNA for mediastinal staging.

Small cell lung cancer is staged differently from NSCLC. It is classified as either limited to a single radiation port (limited stage), or extending beyond a single radiation field (extensive). In small cell lung cancer, TBNA is often performed as a primary diagnostic test rather than for mediastinal staging. The results of TBNA for small cell lung cancer will be discussed in detail later in this chapter.

1.2. Endobronchial Tumors

The conventional approaches to presumed malignant endoscopically visible malignancy is a combination of bronchoalveolar lavage, bronchial cytology brush and endobronchial biopsy. TBNA has been shown to improve the yield when combined with the conventional diagnostic tests in endoscopically visible disease, whether exophytic, submucosal or resulting from extrinsic compression *(9–12)* (**Fig. 3.3**). The yield of TBNA alone for endobronchial tumor involvement ranges between 69 percent and 96 percent. The incremental benefit of TBNA over conventional diagnostic tests differs depending on whether the malignant involvement manifests as an exophytic tumor or submucosal/extrinsic compression. The yield from endobronchial biopsy in the case of exophytic tumors is quite high and approximately 80 percent, increasing to 90–95 percent *(9–11)*. With respect to extrinsic or submucosal disease, the yield without TBNA is 30–70 percent and increases to 85–95 percent *(9–11)*. In addition, in 20 percent of cases it was the only positive diagnostic test *(10)*.
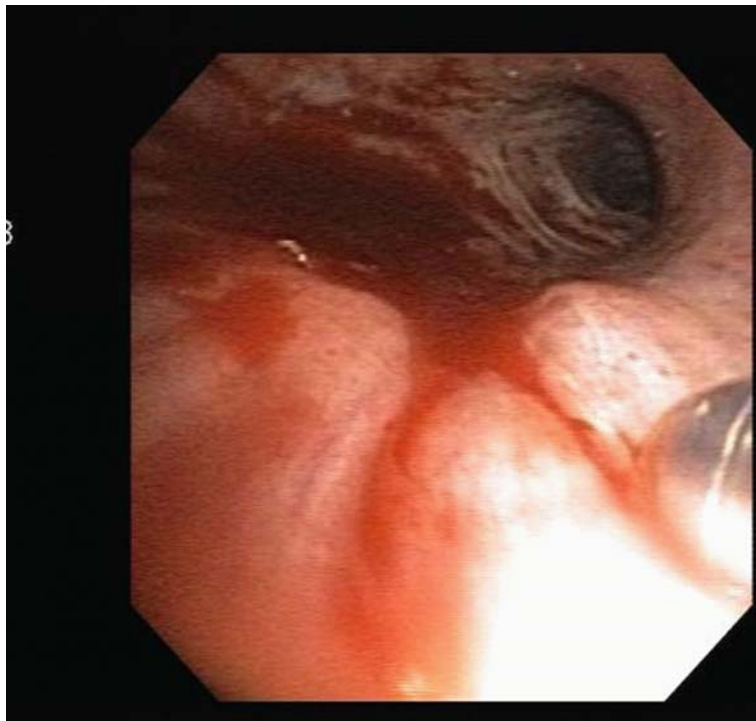

Fig. 3.3. TBNA of submucosal lesion in small cell lung cancer.

1.3. Peripheral Tumor

TBNA with or without imaging guidance has been used to sample tissue in the periphery of the lungs of patients suspected of bronchogenic malignancy. As is the case with other sampling techniques, the yield of TNBA for peripheral tumors is directly dependent on the size of the lesion, being 30–50 percent and 65–80 percent for lesions less and greater than 3 cm, respectively *(13, 14)*. Overall, the yield in the absence of image guidance is 50–55 percent, with TBNA being the only positive diagnostic test in approximately 20 percent *(13–16)*. This improved yield of TBNA over forceps biopsy or cytology brushing can at least partially be explained by the relationship between the airway and peripheral tissue target. Tsuboi and his colleagues described four discreet relationships between peripheral tumors and the peripheral airways *(17)* (**Fig. 3.4**). In both the first and second situations, the airway leads directly into the center of the tumor. The difference between these two situations is that in the second case the tumor infiltration completely surrounds and invades the distal airway. TBNA is unlikely to add to the yield over brush or biopsy in either of these settings. However, in the third type, the tumor extrinsically compresses the airway lumen, rendering it impossible for the brush or the biopsy forceps to access the tumor. The needle is able to penetrate through the airway wall and into the tumor mass. The final situation occurs when there is malignant obstruction of the airway proximal to the target. Again, access to the tumor by either the brush or biopsy forceps is limited, but the needle is able to pierce through the obstruction penetrating the tumor mass. Types 3 and 4 may be responsible for the increased yield of TBNA in peripheral tumors *(13)*.
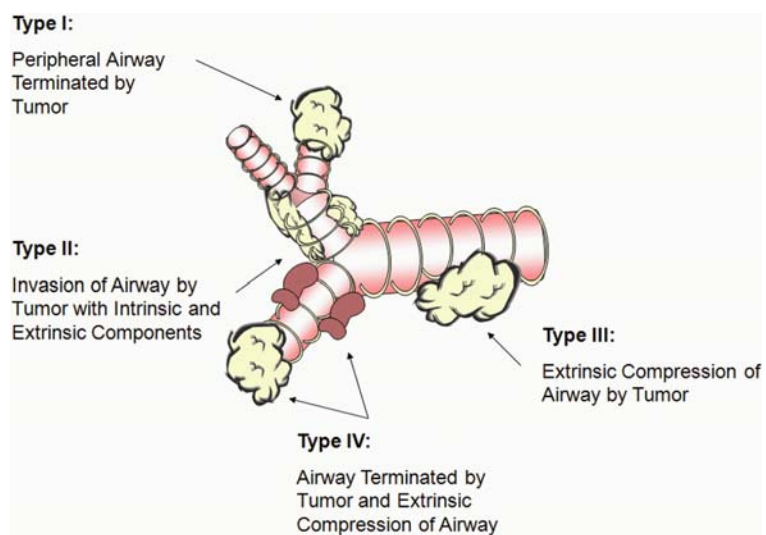

Fig. 3.4. Relationship between tumors and the airway adapted from Tsuboi.

The largest TBNA study for peripheral tumors was a step-wise diagnostic approach of airway examination with flexible bronchoscopy, followed by fluoroscopic guided TBNA with on-site cytology. If no diagnosis was obtained after two consecutive aspirations, a minimum of three transbronchial biopsies were performed and, finally, a TTNA. The overall diagnostic sensitivity with this combined modality approach was 95 percent in cases of malignancy, and 60 percent for benign disease. Four-hundred-eighty-three transbronchial aspirations were performed without complication. TBNA was positive in 75 percent of malignant cases. Interestingly, in 13 percent of cases, unexpected endoscopically visible disease was present. This important finding has the potential to change the patient's management, particularly if he/she was previously being considered for curative surgery *(18)*.

Transthoracic needle aspiration (TTNA) is the alternate minimally invasive technique to obtain tissue for diagnosis in peripheral tumors. Although little has been published concerning the risk of pneumothorax using TBNA to biopsy peripheral tumors, it is certainly less than the 25 percent risk cited with a transthoracic approach *(19)*. This is an important consideration as many patients will have comorbidities limiting both their pulmonary reserve and, in turn, their ability to tolerate even a small pneumothorax. TTNA has been associated with a slightly higher diagnostic yield; however, this should be balanced against the procedure-related risks and additional information that may be acquired from the endoscopic approach *(18)*. In a randomized trial comparing TTNA to TBNA with fluoroscopic guidance, there was no statistically significant difference in the yields (78% and 69%, respectively). The pneumothorax rate did differ with no complications in the TBNA group, and two asymptomatic pneumothoraces in the TTNA patients *(20)*.

To date no studies have examined the impact of the radial ultrasound probe or electromagnetic guidance on the yield of TBNA of peripheral lesions *(21)*. These modalities have improved the yield of transbronchial biopsy. As TBNA yield is superior to forceps biopsy for peripheral lesions, it may be suggested that adding one of these guidance modalities could further improve the yield of TBNA, particularly in the setting of type 3 or 4 lesions.

1.4. TBNA for Benign Disease

TBNA not only plays a role in the diagnosis of suspected malignant adenopathy, but also in benign disease. Worldwide its most common benign uses include sarcoidosis and mycobacterial disease. Other less common utilities have also been described.

1.4.1. Sarcoidosis

By definition, stages I and II sarcoidosis present with mediastinal adenopathy, stage I being only adenopathy and stage II adenopathy and interstitial changes. Traditionally, sarcoidosis has been diagnosed on the basis of a compatible clinical presentation and radiographic abnormalities with supportive ancillary testing.

Bronchoscopy has become the mainstay to diagnose pulmonary sarcoidosis. Transbronchial biopsies, endobronchial biopsies, bronchoalveolar lavage and TBNA are all employed as part of the diagnostic workup. Comparative studies aimed at assessing the diagnostic yield of these various bronchoscopy adjuncts in stage I, II and III sarcoidosis have been performed. As would be expected the yield for TBNA is the greatest in stage I sarcoidosis (50–80 percent) *(22–24)*, and is the sole positive result demonstrating noncaseating granulomas in approximately 20 percent *(22, 24)*. This compares favorably to transbronchial biopsies and endobronchial biopsies reported to have yields in the range of 55–45 percent, respectively. for stage I sarcoidosis *(22, 23)*. TBNA results for stage II sarcoidosis are less impressive and in the order of 45 percent, compared to 65 percent with transbronchial biopsies and 50 percent with endobronchial biopsies *(24)*. In this setting, TBNA has been found to be the only positive diagnostic test in 10 percent *(22, 23)*. It important to note that there is indeed an additive effect on the yield by combining these modalities, increasing the diagnosis of up to 90 percent of cases with stage I and II sarcoidosis *(22–24)*. It has been suggested that the use of a histology rather than cytology needle may improve the yield in benign diseases such as sarcoidosis *(25)*. More recent data using small bore needles with imaging guidance challenges this theory *(26)*. Early data from the only study randomizing patients suspected of sarcoidosis to either blind TBNA using a 19G histology needle and endobronchial ultrasound using a 22G needle showed equivalence *(27)*.

1.4.2. Mycobacterial Disease

Both tuberculous mycobacteria and nontuberculous mycobacteria can present with mediastinal adenopathy, particularly in the HIV population. A bronchoscopic diagnosis is not the first choice in patients with adenopathy and question of tuberculosis considering the risk of aerosolization of the infected droplets. It has, however, been used in patients who have three negative sputum samples for acid-fast bacilli and no firm diagnosis of their adenopathy. In a small study of patients with lymphadenopathy, HIV-1 infection and negative sputum, a diagnosis of mycobacterial disease was made in 87 percent by a combination of smear, histology and culture *(28)*. In the non-HIV population with three negative smears the yield was approximately 80 percent in a tuberculosis endemic country *(29, 30)*.

2. TBNA Technique

2.1. Equipment

Transbronchial needles are available in varying gauges ranging from 18–gauge to 22–gauge, with needle lengths ranging between 13 mm and 15 mm. A longer needle is preferable in the central

airways in order to ensure penetration through the airway and into the target lymph node or mass. A slightly shorter needle can be used for peripheral nodules due to the risk of pneumothorax. Selecting the most appropriate needle gauge will be discussed in detail later in the chapter. All transbronchial needles consist of a beveled needle that may be fully retracted into a plastic protective sheath. A locking mechanism prevents the needle from being accidentally deployed or retracted. Finally, there is a Luer Lock system such that suction can be applied.

Transbronchial needle aspiration is performed either through the working channel of a flexible bronchoscope or, alternatively, via the barrel of a rigid bronchoscope. It is essential to ensure proper functioning of the needle prior to aspiration attempts. Therefore, it is recommended that the assistant or endoscopist perform a trial deployment of the needle prior to each use. In cases where the needle is bent or filled with residue from prior aspirations, the needle may fail to deploy within the airway, or a satisfactory specimen may not be obtained. Malfunction or damage to the needle during prior attempts may also lead to the needle passing through a false passage in the catheter. This risks inadvert damage to the bronchoscope working channel by the needle protruding through the false channel and shearing the working channel. On the same note, the needle should be thoroughly flushed with saline following each use to minimize residue that may result in a poor quality specimen.

Once proper needle function is demonstrated, the bronchoscope is advanced to the site of interest based on information derived from the imaging (either CT or PET-CT). The scope should be positioned in a large central airway, either the trachea or main stem bronchus, to facilitate manipulation of the needle. Also, it is important to ensure the bronchoscope is in a neutral position whenever the needle is passed through the working channel to avoid damage to the working channel. The needle is advanced through the working channel until such time as the hub of the catheter is seen just barely protruding from the end of the bronchoscope. There are multiple techniques to penetrate the lesion or the airway wall with the TBNA needle. These will each be described and may actually be used in combination.

2.2. Jabbing Method **(31)** *(Fig. 3.5)*

Once the catheter hub is visualized protruding from the end of the bronchoscope, the needle is then advanced such that the bevel is clearly seen in the central airway. The entire needle (catheter and actual needle) are carefully retracted into the working channel of the bronchoscope to the point where only the beveled portion of the needle is seen protruding from the end of the bronchoscope. The entire apparatus is advanced en bloc to the site of interest, and the tip of the bronchoscope is used to position the needle perpendicular to the airway wall. This usually requires rotation at the wrist
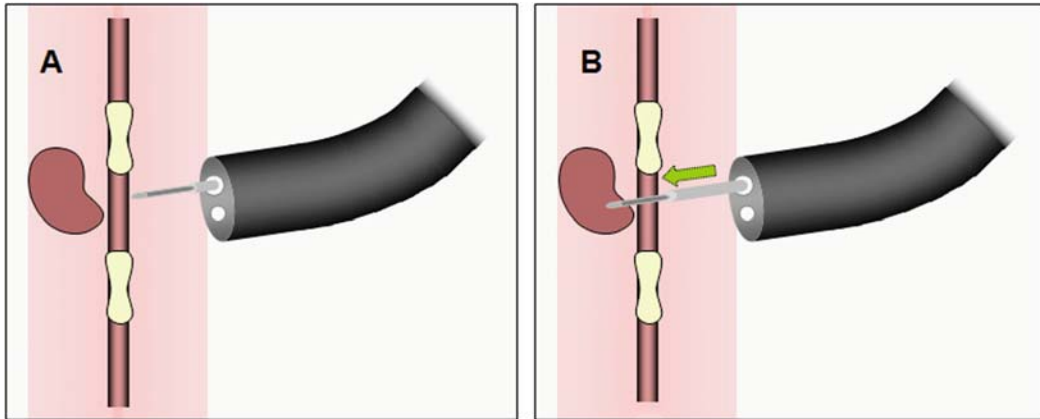
Fig. 3.5. The catheter is advanced out of the end of the bronchoscope such that the hub is visible. (**A**) The needle is then advanced out of the catheter and the bevel of the needle is positioned against the airway wall. (**B**) The bronchoscope is stabilized and the both catheter and needle are advanced such that the needle penetrates the airway wall.

and flexion of the bronchoscope tip. With the bevel gently abutting the airway wall at 90°, the bronchoscope is held in position by the assistant either at the mouth or nose while the endoscopist pushes the needle forcefully through the airway wall. The entire length of the needle should penetrate the airway. A Luer Lock syringe is then used to apply suction on the needle. Twenty milliliters of suction usually suffice. The catheter is slowly advanced and withdrawn within the target, with care being taken to avoid fully withdrawing the needle from the target. It is our practice to perform approximately 10 passes of the target to maximize the yield, particularly when attempting to obtain a histology specimen. The suction is released, the needle withdrawn into the catheter under direct visualization and finally the catheter is completely removed from the working channel with the endoscope again in neutral position.

2.3. Hub Against the Airway Method (31) (Fig. 3.6)

This technique involves approximating the hub of the needle catheter to the airway wall. It is essential that the catheter be perpendicular to the airway to avoid mucosal laceration or creating a false submucosal channel, as is the case with all TBNA techniques. The bronchoscope is secured in position by the assistant and then the needle is advanced through the airway wall and into the target. Again, the needle is passed several times through the target while suction is applied, and then the apparatus is removed from the airway and bronchoscope as described above.

2.4. Piggy Back Method (31) (Fig. 3.7)

In the Piggy Back Method, the bronchoscope is positioned in proximity of the site of interest. The catheter is advanced until the hub is seen on the endoscopic image and then the needle is deployed and locked into place. The entire apparatus is positioned
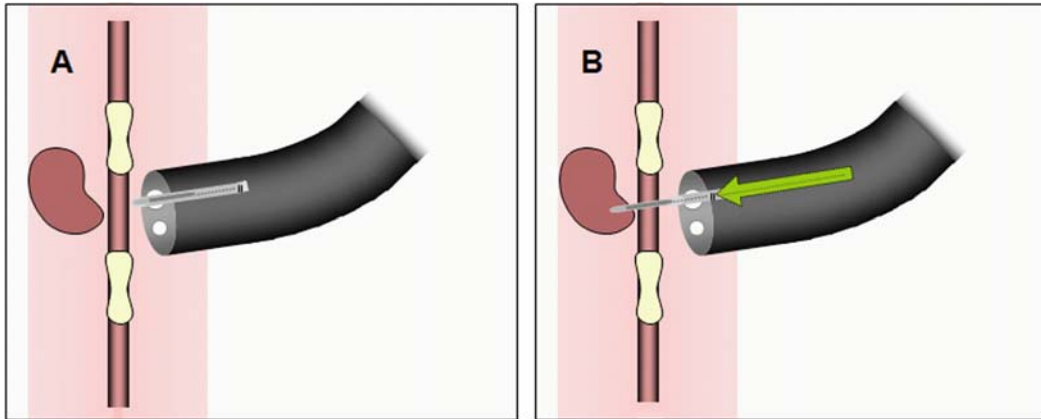
Fig. 3.6. Hub Against Wall Method. The catheter is advanced out of the end of the bronchoscope such that the hub is visible. (**A**) The catheter is positioned against the airway wall. (**B**) The bronchoscope is stabilized and the needle is advanced such that the needle penetrates the airway wall.

perpendicular to the airway wall and advanced en bloc, the needle penetrating the mucosa. Care is taken to ensure that the needle does not migrate proximally or distally when advancing the bronchoscope. The needle can be secured by stabilizing the catheter at the port of the working channel by wrapping the endoscopist's 5th digit around the catheter. It is essential to minimize the length of the catheter/needle beyond the distal end of the bronchoscope as the complex lacks integrity and becomes difficult to manipulate into the desired position to optimize the yield and minimize airway trauma.
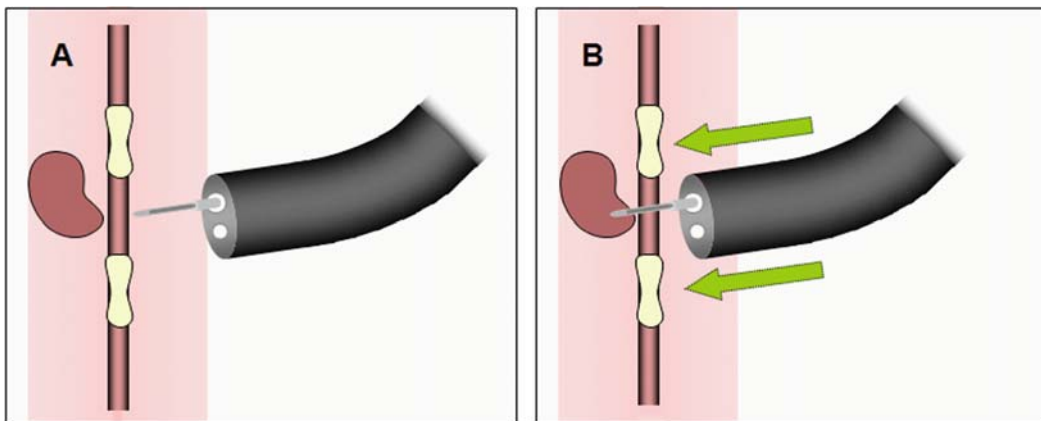

Fig. 3.7. Piggy Back Method. The catheter is advanced out of the end of the bronchoscope such that the hub is visible. (**A**) The needle is then advanced out of the catheter and the bevel of the needle is positioned against the airway wall. (**B**) The bronchoscope, catheter and needle are advanced en bloc such that the needle penetrates the airway wall.

2.5. Cough Method (31)
(Fig. 3.8)

The patient's coughing can facilitate the penetration of the needle through the airway wall. Cough assist can be used in combination with either the Piggy Back or Jabbing Method. Once the needle is in a satisfactory position, the patient is requested to cough while the needle is deployed. It is recommended that 3–5 needle aspirates of each target be performed to optimize the yield.
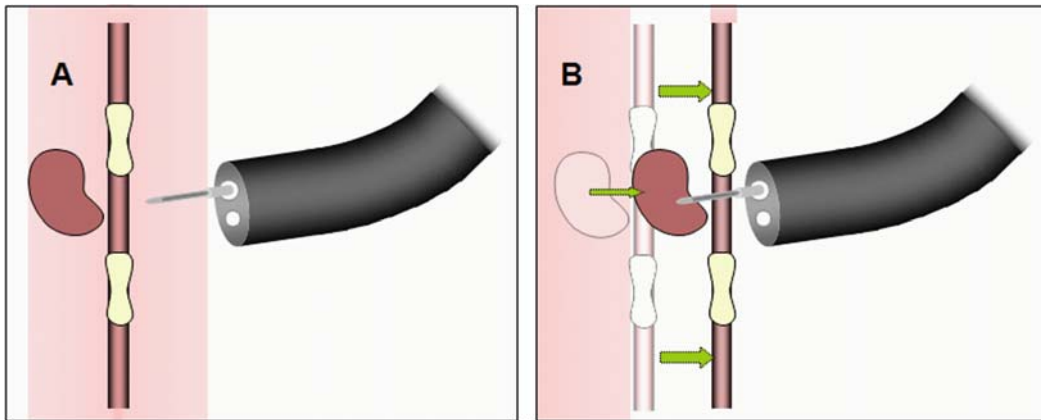

Fig. 3.8. Cough Method. The catheter is advanced out of the end of the bronchoscope such that the hub is visible. (**A**) The needle is then advanced out of the catheter and the bevel of the needle is positioned against the airway wall. (**B**) The patient is then asked to cough as the needle is advanced by jabbing or piggy back method and needle penetrates the airway wall.

As stated above, it is important to accurately stage the patient with non-small cell lung cancer. The risk when performing TBNA for mediastinal staging is to aspirate cells from the central airways and attribute their origin to be from a higher stage lesion, either from a lymph node or a secondary endobronchial source. This could result in the false belief that a patient who may benefit from a surgical cure is not a candidate for such therapeutic modalities. The risk of upstaging a potentially curable patient is the reason it is suggested that, when performing TBNA for mediastinal staging, the first aspiration attempt should be of the potentially highest stage accessible lesion (i.e., N3>N2>N1>primary tumor). Other lymph nodes and the primary tumor can then be sampled in a systematic fashion. Secretions that are aspirated from the central airways while the bronchoscope is advanced to the area of interest also have the potential to contaminate future specimens; therefore, this practice should be avoided. After an aspirate has been performed, it is also important to interrupt the suction prior to removing the needle from the airway wall as superficial cells and secretions from the wall can be pulled into the needle and contaminate the specimen.

3. Training/ Competency Requirements

According to the American College of Chest Physicians consensus statement on training and competency for interventional pulmonary procedure, it is recommended that physicians receive supervised training for 25 procedures to be considered competent. Ten procedures should be performed on an annual basis to maintain competency in this technique *(32)*.

Recent surveys of both pulmonary trainees and program directors in the United States and Canada revealed that, despite over 90 percent of training programs offering the opportunity to perform TBNA, less than 60 percent and 25 percent of U.S. and Canadian trainees, respectively, said they had actually performed the requisite number of procedures for competency *(33–35)*. This is particularly disappointing considering that the majority of these same trainees also stated that the opportunity to perform procedures had attracted them to pulmonology and, in addition, it was their opinion that the minimum competency number was feasible *(36)*. The program directors poled stated that on average fellows were offered the opportunity to perform 30 TBNAs during their training (range 0–100) *(35)*.

The low numbers of pulmonary trainees meeting competency numbers for TBNA is disappointing, but not surprising. In 1997, a survey of pulmonary fellows revealed that only 10 percent performed TBNA on a routine basis for the diagnosis and staging of lung cancer. The yield of TBNA was estimated to be ≤25 percent *(36)*. By 2000, the number of fellows stating that they performed TBNA had increased to >70 percent; however, no mention was made of frequency of use *(37)*.

Surveys of practicing pulmonologists have clearly shown that TBNA is underutilized *(38)*. Of the U.S. physicians surveyed, 12 percent routinely performed TBNA in malignant disease, and 2 percent for sampling suspected benign adenopathy. Perceived limitations to the routine use of TBNA include: concern regarding bronchoscope damage, poor diagnostic yield, lack of formal training, cost of disposable needles and inability to obtain support of the cytopathologist *(36–38)*.

The lack of physicians routinely using this technology due to low yield is concerning as there is a direct correlation between experience and yield. Raveglia and his colleagues published their experience/yield over an 18-month training period with TBNA. Yield increased from 19 percent to 88 percent, and inadequate specimens dropped from 44 percent to 12 percent *(39)*. TBNA is an underutilized adjunct to flexible bronchoscopy that has the potential to provide valuable diagnostic and staging information. Increasing experience with this easily learned technique is rewarded by improved yields and less risk to the bronchoscope.

4. Predictors of Positive TBNA

4.1. Patient-Related Factors

Published yields for TBNA vary widely in the medical literature related to differences in patient populations, clinician experience with TBNA as well as technical differences. As shown above, there is a direct correlation between experience and yield. This further supports the importance of increasing experience and procedure-specific training.

There are several tumor-specific factors that impact TBNA results. A high disease prevalence in the study population correlates with higher yields *(8)*. As stated above, the yield of TBNA for malignant disease is superior to that for benign disorders. In cancers, the cell type of the primary tumor can impact the diagnostic yield of TBNA. The exact yield of TBNA for metastatic disease is difficult to determine due to the small numbers of patients included in various studies; however, it is thought to be less than with bronchogenic malignancies. The greatest yields have been reported in small cell lung cancer followed by non-small cell lung cancer (odds ratio 28.5 versus 6.5, sensitivities in the range of 70 percent versus 50 percent for small cell and non-small cell lung cancers, respectively) *(40, 41)*. Many studies have also stratified their yields based on nodal station and have found the greatest yield for right paratracheal-4R (70–90 percent) and subcarinal lymph nodes-7 (65–80%). *(40, 41)* The greater the size of a lymph node, the greater the likelihood not only of malignancy, but also of obtaining a positive TBNA result *(8)*.

4.2. Technical Factors

Beyond the direct patient-related factors, there are also differences in technique that contribute to the variability in the yield documented in the medical literature. These include use of image guidance, needle size, number of needle passes, sample preparation and whether or not there the cytopathologist was on-site during the procedure.

5. Image Guidance

The addition of image guidance in an attempt to sample either central or peripheral lesions has led to an improved diagnostic yield. Several authors have documented greater diagnostic yields for peripheral TBNA with the addition of fluoroscopic guidance. The benefit of ultrasound guidance for both peripheral and central lesions including mediastinal lymph nodes has been well established. The use of integrated positron-emission tomography and CT scanning has become commonplace in many centers,

particularly when there is a high likelihood of malignancy. Data suggests that the addition of PET scanning to TBNA in mediastinal staging for malignancy results in improved sensitivity, specificity, negative predictive value and diagnostic accuracy. More importantly, the authors suggest that 57 percent of their study patients could have avoided mediastinoscopy as they had both a negative PET scan and a negative TBNA *(42)*. This data is quite provocative although PET in combination with TBNA is not yet considered standard of care in many institutions.

6. Needle Specifications

Transbronchial needles have been developed to obtain either cytology or histology specimens. Histology and cytology needles are 18–19- and 20–22-gauge, respectively. Studies comparing histology and cytology needles show that specimens considered adequate to make a diagnosis are obtained less frequently with histology needles. However, when an adequate specimen is obtained, the diagnostic yield is higher. There is marked variability in the overall yield of TBNA in these studies; however, the diagnostic yield for specimens obtained using a histology needle ranges between 40 percent and 87 percent *(25, 42–43)*. All studies have shown the highest yield when both cytology and histology are obtained, rather than either technique alone. The concern that the larger needle may be associated with increased bleeding may at least partially explain the increased frequency of inadequate specimens. Physicians may sample less aggressively due to these concerns despite there being no evidence to support the association between the use of histology needles and increased bleeding. The only TBNA study to correlate the actual size and quality of specimens demonstrated that smaller samples were more likely to contain nondiagnostic, nonspecific tissue *(44)*.

6.1. Number of Needle Passes and Onsite Cytology

6.1.1. Rapid On-Site Cytology Evaluation (ROSE)

A specimen that is considered satisfactory for analysis is essential in order to make a diagnosis with TBNA. As previously discussed the false negative rate is directly correlated with the quality of the specimen *(44)*. Unfortunately, the adequacy of the specimen can only be determined once it has been reviewed by the pathologist or the cytology technician. The desire to ensure an adequate specimen and establish a preliminary diagnosis while minimizing the number of aspirates necessary to achieve a diagnosis has spurred the interest of bronchoscopists to have a member of the cytology team on-site during the procedure (Rapid on-site cytology evaluation, ROSE). The cytopathologist's immediate technical feedback can potentially to guide the bronchoscopist to consider alternate

approaches to the acquisition of a specimen, for example selecting an alternate angle or orientation. The limitations to this approach are the availability of the cytologist or cytology technician, and the expense. Studies have, therefore, been performed to determine whether there is indeed an improvement in the diagnostic yield when ROSE was employed and if it is cost-effective *(45)*. Diacon found the use of on-site cytology to be cost-effective as the immediate feedback resulted in decreased procedure time, reduced sampling and a decreased need for other diagnostic modalities *(45)*. Davenport showed that the rate of inadequate specimens dropped from 56 percent to 31 percent *(46)*. Davenport found the addition of ROSE led to an incremental increase in the diagnostic yield from 50 percent to 80 percent. As ROSE has been shown to be a cost-effective means to reduce inadequate specimens and improve the diagnostic yield, it is recommended that this technique be used if a cytopathologist or cytology technician is available.

6.1.2. Number of Needle Aspirates per Site

The number of aspirations per nodal station is one of the variables that has the potential to impact on the yield and varies markedly amongst TBNA studies. It has been suggested that up to seven needle passes are required to optimize the yield *(47–49)*. Two prospective studies were performed with the specific goal of determining the optimal number of needle passes. Both studies showed the highest yield for the first pass, which was positive in approximately 50 percent *(47, 48)*. Diacon and his group found a plateau in the diagnostic yield after three aspirates with a diagnosis in ≥ 94 percent. Chin demonstrated a plateau after seven aspirates, with 77 percent being diagnosed within first four aspirates and a further 7 percent incremental benefit by the seventh aspirate. The study protocols differed between these two studies, the most important difference being the use of rapid on-site cytology (ROSE). ROSE was used in all of Diacon's cases, but only in 70 percent of Chin's. Also, sampling was stopped once a positive sample was obtained in Diacon's study. Interestingly, Chin found that when ROSE was used, there was a tendency to perform more aspirates (6.2 ± 2.5 versus 4.5 ± 1.7); however, the mean number of passes prior to obtaining a diagnosis was 2.5 ± 2.0 with ROSE, compared to 3.7 ± 1.6 without it. Fewer passes were required for lymph nodes measuring greater than 2 cm in short axis with nearly 90 percent being positive with 2–3 aspirates.

7. Specimen Preparation

Specimen preparation is dependent on the institution. No studies have directly compared various preparation techniques of TBNA specimens. Many centers prefer that a slide for cytology be

prepared at the time of bronchoscopy. This technique consists of flushing the needle with a small amount of air using a syringe directly onto a slide. A thin preparation is then made by smearing the specimen across the slide using a second slide. The slide is then immediately fixed with 95 percent ethanol. The needle is then flushed with sterile saline into cytology preparation. Other laboratories prefer that the cytology specimen be expelled from the needle directly into the cytology preparation using a small amount of air. Core specimens can readily be obtained using histology needles, as shown above. As there has been shown to be an incremental increase in the yield when specimens are sent for both cytology and histology, a specimen should be sent for histology. Patel and colleagues evaluated their diagnostic yield following a change in preparation *(50)*. In this before/after study, they switched from simply sending TBNA specimens in cytology preservative, to also sending core biopsies fixed in formalin and embedded in paraffin to surgical pathology. The failure rate (i.e., inability to make a diagnosis based on TBNA specimen) decreased from 47 percent to only 9 percent. It is recommended that physicians performing TBNA discuss a priori the preferred specimen preparation technique with their cytopathologist.

8. Complications

TBNA is a very safe procedure, particularly when performed properly by physicians experienced in bronchoscopy. The most commonly described complications include bleeding, pneumothorax, pneumomediastinum and post-procedure fevers. In a meta-analysis of 13 TBNA studies, the overall major complication rate, including bleeding, pneumothorax and pneumomediastinum, was 0.26 percent. This included two major bleeds and one pneumothorax requiring intervention *(8)*. Although no study has systematically evaluated the effect of anticoagulants on the bleeding risk with TBNA, it seems prudent to extrapolate from the experience with transbronchial biopsy. As such, it is likely that aspirin has little impact on bleeding risk; however, irreversible anti-platelet agents such as clopidogrel should be discontinued 7–10 days prior to the procedure *(51)*. The rate of febrile illness is likely underreported in most articles as it is not usually clinically relevant, resolves spontaneously after 24–48 h and is readily treated with anti-pyrexials. Other complications are extremely rare.

Probably the most costly and preventable complication of TBNA is bronchoscope trauma. Improper use of the TBNA needle can result in damage to the working channel *(52, 53)*. The working channel is protected from the sharp beveled end of the needle as

long as it is within the outer catheter. To minimize the risk of shearing the working channel with the needle, it is essential to ensure the bronchoscope is in a neutral position while the outer catheter is being extended. In addition, the bronchoscope should also be in a neutral position when the catheter is being retracted.
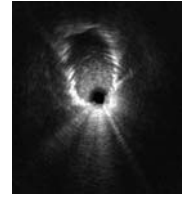
Conclusion

In summary, there a large number of TBNA studies with varying sensitivities depending on the patient population studied, size and location of the lymph node or nodule, as well as experience of the operator. It is minimally invasive and can easily be performed at the same time as the diagnostic bronchoscopy. Although there are not an insignificant number of false negatives, the false positive rate is acceptable. As TBNA incurs virtually no risk above that of a routine diagnostic bronchoscopy, it should be used routinely by pulmonologists caring for patients with mediastinal adenopathy.

References

1. Schieppati E. La punction mediastinal traves del espolon traquel. Rev As Med Argent 1949; 663: 497–499.

2. Oho K, Kato H, Ogawa I, et al., A new needle for transfiberoptic bronchoscope use. Chest 1979; 76: 492.

3. Goldstraw P, Crowley J, Chansky K, et al., The IASLC lung cancer staging project: proposals for the revision of the TNM stage groups in the forthcoming (seventh) edition of the TMN classification of malignant tumours. J Thorac Oncol 2007; 2: 706–714.

4. DeLeyn P, Lardinois D, VanSChil P, et al., ESTS guidelines for preoperative lymph node staging for non-small cell lung cancer. Eur J Cardiothorac Surg 2007; 32: 1–8.

5. Detterbeck F, Jantz M, Wallace M, et al., Invasive mediastinal staging of lung cancer: ACCP evidence-based clinical practice guidelines (2nd edition). Chest 2007; 132: 202S–220S.

6. Silvestri G, Gould M, Margolis M, et al., Noninvasive staging of non-small cell lung cancer: ACCP evidence-based clinical practice guidelines (2nd edition). Chest 2007; 132: 178S–201S.

7. Mountain C, Dresler C. Regional lymph node classification for lung cancer staging. Chest 1997; 111: 1718–1723.

8. Holty J-E, Kuschner W, Gould M. Accuracy of transbronchial needle aspiration for mediastinal staging of non-small cell lung cancer: a meta-analysis. Thorax 2005; 60: 949–955.

9. Caglayan B, Akturk U, Fidan A, et al., Transbroncial needle aspiration in the diagnosis of endobronchial malignant lesions: A 3-year experience. Chest 2005; 128: 704–708.

10. Dasgupta A, Jain P, Minai O, et al., Utility of transbronchial needle aspiration in the diagnosis of endobronchial lesions. Chest 1999; 115: 1237–1241.

11. Gullon J, Fernandez R, Medina A, et al., Transbronchial needle aspiration in bronchogenic carcinoma with visible lesions: diagnostic yield and cost. Archivos de Bronconeumologia 2003; 39: 496–500.

12. Karahalli E, Yilmaz A, Turker H, et al., Usefulness of various diagnostic techniques during fiberoptic bronchoscopy for endoscopically visible lung cancer: should examinations be performed routinely? Respiration 2001; 68: 611–614.

13. Wang KP, Haponik E, Britt J, et al., Transbronchial needle aspiration of peripheral pulmonary nodules. Chest 1984; 86: 819–823.

14. Reichenberger F, Weber J, Tamm M, et al., The value of transbronchial biopsy needle

aspiration in the diagnosis of peripheral pulmonary lesions. Chest 1999; 116: 704–708.

15. Shure D, Fedullo F. Transbronchial needle aspiration of peripheral masses. American Review of Respiratory Disease 1983; 128: 1090–1092.

16. Lundren R, Bergman F, Angstrom T. Comparison of transbronchial fine needle aspiration biopsy, aspiration of bronchial secretions, bronchial washing, brush biopsy and forceps in the diagnosis of lung cancer. Eur J Respir Dis 1983; 64: 378–385.

17. Tsuboi E, Ikeda S, Tajima M, et al., Transbronchial biopsy smear for diagnosis of peripheral pulmonary carcinomas. Cancer 1967; 20: 687–698.

18. Gaspirini S, Ferretti M, Secchi E, et al., Integration of transbronchial and percutaneous approach in the diagnosis of peripheral pulmonary nodules or masses. Experience with 1,027 consecutive cases. Chest 1995; 108: 131–137.

19. Geraghty P, Kee S, McFarlane G., et al., CT-guided transthoracic needle aspiration biopsy of pulmonary nodules: needle size and pneumothorax rate. Radiology 2003; 229: 475–481.

20. Shankar S, Gulati M, Gupta D, et al., CT-guided transthoracic fine-needle aspiration versus transbronchial fluoroscopy-guided needle aspiration in pulmonary nodules. Acta Radiologica 1998; 39: 395–399.

21. Eberhardt R, Anantham D, Ernst A, et al., Multimodality bronchoscopic diagnosis of peripheral lung lesions: a randomized controlled trial. Am J Respir Crit Care Med 2007; 176: 36–41.

22. Trisolini R, Lazzari A, Cancelleri A, et al., Transbronchial needle aspiration improves the diagnostic yield of bronchoscopy in sarcoidosis. Sarcoidosis Vasc Diffuse Lung Dis 2004; 21: 147–151.

23. Bilacerolu S, Perim K, Gunel O, et al., Combining transbronchial aspiration with endobronchial and transbronchial biopsy in sarcoidosis. Monaldi Arch Chest Dis 1999; 54: 217–223.

24. Leonard C, Tormey V, O'Keane C, et al., Bronchoscopic diagnosis of sarcoidosis. Eur Respir J 1997; 10: 2722–2724.

25. Metha A, Kavaru M, Meeker D, et al., Transbronchial needle aspiration for histology specimens. Chest 1989; 96: 1228–1232.

26. Garwood S, Judson M, Silvestri G, et al., Endobronchial ultrasound for the diagnosis of pulmonary sarcoidosis. Chest 2007; 132: 1298–1304.

27. Stather D, Field S, Khalil M, et al., Endobronchial ultrasonography in the diagnosis of sarcoidosis: preliminary results of a randomized trial. Chest 2007; 132: 465.

28. Harkin T, Ciotoli C, Addrizzo-Harris D, et al., Transbronchial needle aspiration (TBNA) in patients infected with HIV. Am J Respir Crit Care Med 1998; 157: 1913–1918.

29. Bilacerolu S, Gunel O, Eri N, et al., Transbronchial needle aspiration in diagnosing intrathoracic tuberculous lymphadenitis. Chest 2004; 126: 259–267.

30. Centinkaya E, Yildiz P, Kadakal F, et al., Transbronchial needle aspiration in the diagnosis of intrathoracic lymphadenopathy. Respiration 2002; 69: 335–338.

31. Dasgupta A, Metha A. Transbronchial needle aspiration: an underused diagnostic technique. Clin Chest Med 1999; 20: 39–51.

32. Ernst A, Silvestri G, Johnstone D. Interventional pulmonary procedures: guidelines from the American College of Chest Physicians. Chest 2003; 123: 1693–1717.

33. Pastis N, Nietert P, Silvestri G. Fellows' perspective of their training in interventional pulmonary procedures. J Bronchol 2005; 12: 88–95.

34. Pastis N, Nietert P, Silvestri G. Variation in training for interventional pulmonary procedures among US pulmonary/critical care fellowships: A survey of fellowship directors. Chest 2005; 127: 1614–1621.

35. Jarand J, Michaud G, Silvestri G, et al., Evaluation of pulmonary procedural training in Canadian pulmonary fellowship programs – Program directors and fellows' perspective. Am J Respir Crit Care Med 2007; 175 (Abstracts Issue).

36. Haponik E, Shure D. Underutilization of transbronchial needle aspiration: Experiences of current pulmonary fellows. Chest 1997; 112: 251–253.

37. Haponik E, Russell G, Beamis J, et al., Bronchoscopy training: Current fellows experiences and some concerns for the future. Chest 2000; 118: 625–630.

38. Prakash U, Offord K, Stubbs S. Bronchoscopy in North America: The ACCP survey. Chest 1991; 100: 1668–1675.

39. Raveglia F, Meda S, Conforti S, et al., Diagnostic value and learning curve of transbronchial needle aspiration in thoracic surgery. Minerva Chir 2006; 61: 459–466.

40. LeJeune I, Baldwin D. Measuring the success of transbronchial needle aspiration in

everyday clinical practice. Respir Med 2007; 101: 670–675.

41. Sharafkhaneh A, Baaklini W, Gorin A, et al., Yield of transbronchial needle aspiration in the diagnosis of mediastinal lesions. Chest 2003; 124: 2131–2135.

42. Bernasconi M, Chhajed P, Gambazzi F, et al., Combined transbronchial needle aspiration and positron emission tomography for mediastinal staging of NSCLC. European Respiratory Journal 2006; 27: 889–894.

43. Hermens F, Van Engelenburg T, Visser F, et al., Diagnostic yield of transbronchial histology needle aspiration in patients with mediastinal lymph node enlargement. Respiration 2003; 70: 631–635.

44. Oki M, Saka H, Kitagawa C, et al., The size and quality of the histology specimens obtained with transbronchial needle aspiration. J Bronchol 2005; 12: 71–75.

45. Diacon A, Schuurmans M, Theron J, et al., Utility of rapid on-site evaluation of transbronchial needle aspirates. Respiration 2005; 72: 182–188.

46. Davenport R. Rapid on-site evaluation of transbronchial aspirates. Chest 1990; 98: 59–61.

47. Chin R, McCain T, Lucia M, et al., Transbronchial needle aspiration in diagnosing and staging lung cancer. Am J Respir Crit Care Med 2002; 166: 377–381.

48. Diacon A, Schuurmans M, Theron J, et al., Transbronchial needle aspirates: how many passes per target site? Eur Respir J 2007; 29: 112–116.

49. Harrow E, Halbert M, Hardy S, et al., Bronchoscopic and roentgenographic correlates of a positive transbronchial needle aspiration in the staging of lung cancer. Chest 1991; 100: 1592–1596.

50. Patel N, Pohlman A, Husain A, et al., Conventional transbronchial needle aspiration decreases the rate of surgical sampling of intrathoracic lymphadenopathy. Chest 2007; 131: 773–778.

51. Trosini-Desert V, Vergnon JM, Collet JP, et al., Fiberoptic bronchoscopy and anti-platelet agents : a risk benefit analysis. Rev Mal Respir 2007; 24: 48–56.

52. Metha A, Curtis P, Scalzitti M, et al., The high price of bronchoscopy: maintenance and repair of the flexible fiberoptic bronchoscope. Chest 1990; 98: 448–454.

53. Kirkpatrick M, Smith J, Hoffman P, et al., Bronchoscope damage and repair costs: results of a regional postal survey. Respir Care 1992; 37: 1256–1259.

Chapter 4

Staging Principles in Lung Cancer

Sidhu P. Gangadharan

Lung cancer remains the most common cancer worldwide, with an incidence of 1.35 million new cases in 2002 *(1)*. It also is the leading cause of cancer mortality globally, with 1.18 million deaths. This represents over 12 percent of all newly diagnosed cancers, and nearly 18 percent of all cancer deaths in the world *(1)*. In the United States, it is estimated that 215,000 new cases of lung cancer will be diagnosed in 2008, and nearly 162,000 people will die from the disease. Though the trend in new lung cancer cases appears to be declining in men and plateauing in women, the overall five-year survival rate for lung cancer in the United States still remains around 15 percent *(2)*.

The importance of accurate staging in lung cancer is based on the intertwined principles of treatment and prognosis. Without establishing a precise stage, it is unclear which treatment modalities should be offered, which clinical trials the patient would be eligible to participate in, or how to assess the outcomes of any treatment. Moreover, given the wide range of potential survival based on how localized or advanced the disease is, the clinician cannot counsel the patient adequately without this knowledge.

In this chapter, the staging system for non-small cell lung cancer will be discussed. The goals of the chapter are:

- To define the TNM staging system for lung cancer
- To review the data that support the TNM staging system, including the proposed revisions
- To review the noninvasive and invasive modalities used to establish accurate staging

- To explore the effect of stage on the effectiveness and appropriateness of various treatment modalities for lung cancer

1. History

In the mid-1900s, Denoix defined the tumor, node, metastasis (TNM) system for classifying cancers which is the underpinning of the staging scheme used today *(3)*. This system was subsequently adopted by the International Union Against Cancer (UICC) and published in 1968 as a TNM classification scheme which included a rudimentary description of lung cancer. There was no stage grouping associated with this system. The T stage was based on level of involvement of the lung (segment, lobe, multilobe, extrapulmonary), and the nodal stage was either N0 for no nodal involvement or N1 for any nodal involvement.

In 1974, Mountain and colleagues published a clinical staging system utilizing modified TNM descriptors *(4)*. The five-year survival curves justifying stage groupings were derived from a database of over 2,100 cases of lung cancer treated at the M.D. Anderson Cancer Center. The UICC adopted this system in the 2nd edition of the staging guide in 1975, and revised to a 3rd edition in 1978. Mountain subsequently published a revised staging system in 1986, based on the outcomes of over 3,700 treated cases, which became the foundation of the UICC 4th edition staging system *(5)*. Finally, in 1997, Mountain proposed further revisions to the staging system based on the database which had increased to over 5,300 cases *(6)*. It was adopted for the UICC 5th edition and remained unchanged in its revision to the 6th edition, which is its most recent iteration, published in 2002. (**Table** 4.1)

The prognosis based on stage in Mountain's 1997 revision to the staging system revealed five-year survivals of pathological stage IA at 67 percent, IB at 57 percent, IIA at 55 percent, IIB at 39 percent, and IIIA at 23 percent. Clinical staging revealed five-year survivals of stage IA at 61 percent, IB at 38 percent, IIA at 34 percent, IIB at 24 percent, and IIIA at 13 percent. Clinical staging also included stage IIIB at 5 percent and IV at 1 percent *(6)*. (**Table** 4.2) This relative improvement in survival in pathologically staged patients reflects a purification of stage–culling out the inferior prognosis of clinically unsuspected, but actually pathologically higher staged patients.

Table 4.1
TNM stage classification (UICC 6th edition). Adapted
with permission from Mountain CF *(4)*

Stage	T	N	M
0		Carcinoma in situ	
IA	T1	N0	M0
IB	T2	N0	M0
IIA	T1	N1	M0
IIB	T2	N1	M0
	T3	N0	M0
IIIA	T1-2	N2	M0
	T3	N1-2	M0
IIIB	T1-3	N3	M0
	T4	N0-3	M0
IV	T1-4	N0-3	M1

Table 4.2
Prognosis by TNM stage. Adapted with permission
from Mountain CF *(6)*

		5-year survival (%)
Clinical stage	cIA	61
	cIB	38
	cIIA	34
	cIIB	24
	cIIIA	13
	cIIIB	5
	cIV	1
Pathological stage	pIA	67
	pIB	57
	pIIA	55
	pIIB	39
	pIIIA	23

1.1. T Descriptor (UICC 6th Edition TNM Classification)

T1 tumors are <3 cm in diameter. They are wholly contained within the lung parenchyma. T2 tumors are ≥3 cm, or invade the visceral pleura. T2 status may also be conveyed if the tumor (of any size) is invading a main bronchus, but still remains ≥2 cm from the carina. Atelectasis or obstructive pneumonitis may be present, but must involve less than the whole lung in order to remain T2. T3 tumors invade the parietal pleura/chest wall, diaphragm, mediastinal pleura, parietal pericardium, or invade the main bronchus <2 cm from the carina. Additionally, T3 status may result if there is atelectasis or obstructive pneumonitis of the whole lung. Finally, T4 includes tumors which invade the mediastinum (not just mediastinal pleura), heart, great vessels, trachea, carina, esophagus, or vertebral body. Malignant pleural effusion is classified as T4, as are satellite nodules found within the primary tumor-bearing lobe.

The pathologist may encounter dilemmas in T staging. For example, the surgical resection specimen will almost never include the carina; thus distance from the carina and differentiation of T2 or T3 status may not be ascertained without a discussion with the operating surgeon *(7)*. Also, it is unclear what the correct T stage would be for a tumor which crosses an interlobar fissure and invades the adjacent lobe. T2 status would be conferred based on the involvement of the visceral pleura of the fissure, though invasion into another structure usually conveys at least T3 status in most cases *(7)*.

1.2. N Descriptor (UICC 6th Edition TNM Classification)

A thoracic lymph node map based on a modification by Mountain and Dresler of the American Thoracic Society's map was agreed upon by the American Joint Committee on Cancer (AJCC) and the UICC in 1997 *(8)* (**Fig.** 4.1). N0 denotes no nodal spread. N1 represents metastatic cancer to the ipsilateral intrapulmonary, hilar, or peribronchial lymph nodes (double-digit numbered lymph nodes). N2 lymph nodes are involved ipsilateral or subcarinal mediastinal nodes (single-digit numbered lymph nodes). N3 status is conferred by positive contralateral mediastinal lymph nodes, or supraclavicular lymph nodes, or either side.

1.3. M Descriptor (UICC 6th Edition TNM Classification)

Metastatic staging is reported as M0 if there are no metastases or M1 if metastasis is present. A distinction is made in the UICC 6th edition about tumor foci in different lobes. Unlike the designation of T4 based on satellite tumor nodules within the same lobe, an M1 stage is conferred if the separate tumor focus is in a different lobe, whether in the ipsi- or contralateral lung. Whereas the verification of different tumor histologies in nodules in different lobes may be a straightforward way to establish synchronous primary lung cancers, if the tumors found in different lobes happen to be the same histology, there can be controversy about whether it is truly M1 stage, as opposed to synchronous primaries of similar histology.
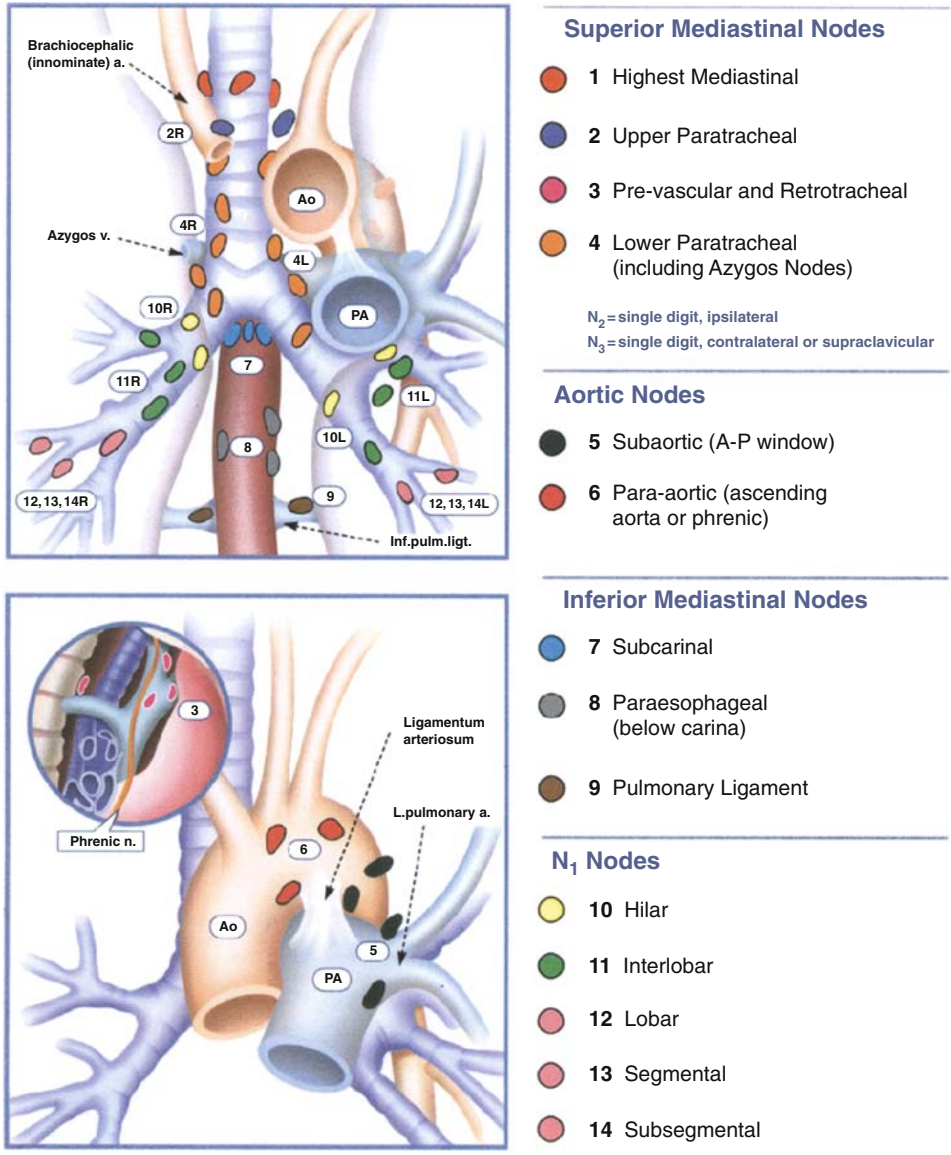
Fig. 4.1. Regional lymph node staging system. From Mountain CF, et al. *(8)*. Reprinted with permission.

2. Proposed Revisions to the 7th Edition of the TNM Classification for Lung Cancer

The International Association for the Study of Lung Cancer (IASLC) established the Lung Cancer Staging Project in 1998 in order to address some of the shortcomings which were carried unchanged from the 5th to the 6th edition of the UICC staging system *(3)*. Chief among its aims was to amplify the database's size

on which the descriptors and stage groupings were based, to expand to a multi-institutional and multinational database, and to more adequately represent non-surgical treatment modalities in the outcomes. Based on the creation of a database far more comprehensive than that used for the 1997 revision to the TNM staging system, the proposed IASLC TNM descriptors and stage groupings were then validated internally and externally, by applying them to the Surveillance, Epidemiology, and End Results (SEER) registry database.

By 2005, over 100,000 cases had been submitted to the IASLC Lung Cancer Staging Project database, of which 81,015 had adequate information to be included in the analysis *(3, 9)*. These represented patients from 46 institutions treated in 19 countries worldwide. The treatment modalities included surgery alone in 41 percent, radiotherapy alone in 11 percent and chemotherapy alone in 23 percent, with the remainder being treated with combined modality therapy.

2.1. Proposed Revisions for the T Descriptor

From the total database of over 100,000 cases, 18,198 contained sufficient information to be included in the T stage analysis *(10)*. Previous reports had suggested that tumor size needed to be stratified further within the existing T descriptor definitions. Survival was found to be higher with <2 cm tumor size within T1 stage *(11, 12)*. Similarly, T2 tumors of increasing size correlate with a worsening prognosis *(13, 14)*. In fact, the SEER database previously had been analyzed for the effect of increasing tumor size within stage I (i.e., node negative) and supported further clarification of the T descriptor based on differential survival of tumors which measured <2 cm, ≥2 to <4 cm, and ≥4 cm *(15)*. Based on cutpoints established in N0 R0 cases, the IASLC Lung Cancer Staging Project T descriptors subcommittee found that there were significant survival differences in tumor size groupings ≤2 cm, >2 cm to ≤3 cm, >3 cm to ≤5 cm, >5 cm to ≤7 cm, and >7 cm *(10)* (**Fig.** 4.2a). This was internally validated by assessing the survival between global regions within the database and also between data sources (i.e., clinical trials, surgical series, etc.) *(16)*. Thus, the *proposed revisions to the T descriptor based on size* are as follows:

- Subclassify T1 as **T1a** (≤2 cm) and **T1b** (>2 cm to ≤3 cm)
- Subclassify T2 as **T2a** (>3 cm to ≤5 cm or T2 by other factor and ≤5 cm) and **T2b** (>5 cm to ≤7 cm)
- Reclassify T2 tumors >7 cm as **T3**

The external validation of these recommendations utilizing the SEER database cases of NSCLC in 1998–2000 supports these changes, though there was some overlap in the T2b and reclassified T3 (previously T2c; >7 cm) group (**Fig.** 4.2b).
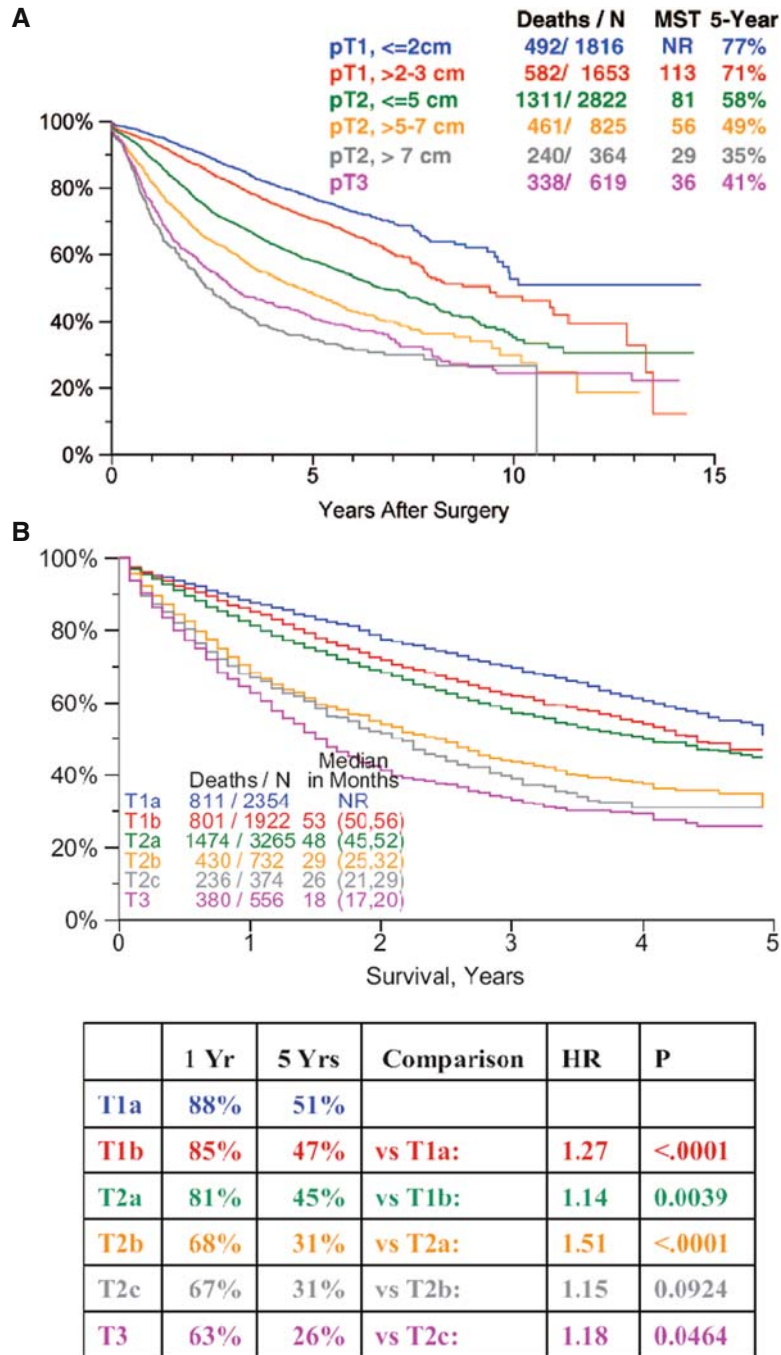
Fig. 4.2. (**a**) Overall survival by pathologic tumor size (using UICC 6th edition classification). From Rami-Porta R, et al. *(10)*. Reprinted with permission. (**b**) Overall survival of T1-3 N0 by tumor size (applying IASLC proposed T descriptor revision to SEER database). From Groome PA, et al. *(16)*. Reprinted with permission.

The T descriptor subcommittee also reviewed multifocal tumors, either T4 based on the presence of satellite nodule(s) within the primary tumor-bearing lobe, or M1 if the additional nodule was found in a lobe other than the one in which the primary tumor was located. Previous studies have shown that stage IIIB by virtue of T4 satellite nodules have found that the prognosis after resection for such patients may be higher than expected for similarly staged patients based on other criteria *(17, 18)*. Others have shown that the multifocal T4 may be no better than other resected T4 lesions, or perhaps even similar to the poor prognosis seen in stage IV disease *(18, 19)*.

After analyzing over 2,300 cases within the database, the IASLC group showed that multifocal T4 exhibited survival more similar to T3 patients, and they had significantly better survival when compared against T4 patients based on other criteria *(10)*. Similarly, M1 tumors by virtue of additional nodule(s) within an ipsilateral but separate lobe from the primary tumor exhibited survival characteristics more similar to T4 patients. Thus, the *proposals for revisions of the T descriptor based on multifocality* are:

- Reclassify T4 tumors by virtue of satellite nodule(s) within the primary tumor-bearing lobe as **T3**

- Reclassify M1 additional nodules within an ipsilateral but different lobe than that in which the primary tumor is located as **T4**

Finally, the T4 status of pleural dissemination (effusion or nodules) was examined. The reported five-year survival was 2 percent, far below that of other T4 tumors *(10)*. Thus, the final *proposal for revision in the T descriptor based on malignant pleural effusion* is:

- Reclassify T4 pleural dissemination (pleural or pericardial effusion or pleural nodules) as **M1**

Validating proposed revisions based on both multifocal and pleural dissemination descriptors was consistent both internally and externally (**Fig.** 4.3b).

2.2. No Proposed Revision for the N Descriptor

The IASLC Lung Cancer Staging Project subcommittee on N descriptors analyzed over 38,000 patients who had clinical N staging, and over 28,000 patients with pathological N staging *(20)*. The clinical (non-surgical) N staging and clinical and pathological (surgical) N staging revealed that the current UICC 6th edition classification system of N0-3 yields statistically significant differences between each N category. (**Fig.** 4.4a,b) When applied to the SEER data, these prognostically significant differences were maintained.

The possibility that survival could be influenced by several nodal characteristics – anatomic location, skip metastasis (N2 disease with negative N1 nodes), or number of involved nodal stations – was explored. These possibilities were not borne out

Fig. 4.3. (**a**) Overall survival for T3 and T4 tumors (based on UICC 6th edition classification). From Rami-Porta R, et al. *(10)*. Reprinted with permission. (**b**) Overall survival for T3 and T4 (and M1) tumors including multifocal tumors and pleural dissemination (applying IASLC proposed T descriptor revision to SEER database). From Groome PA, et al. *(16)*. Reprinted with permission.

by the analysis, though there was a suggestion that nodal involvement might be grouped by single station N1 positivity, multiple N1 or single N2 positivity, or multiple N2 positivity. However, limited numbers precluded meaningful application of statistics to
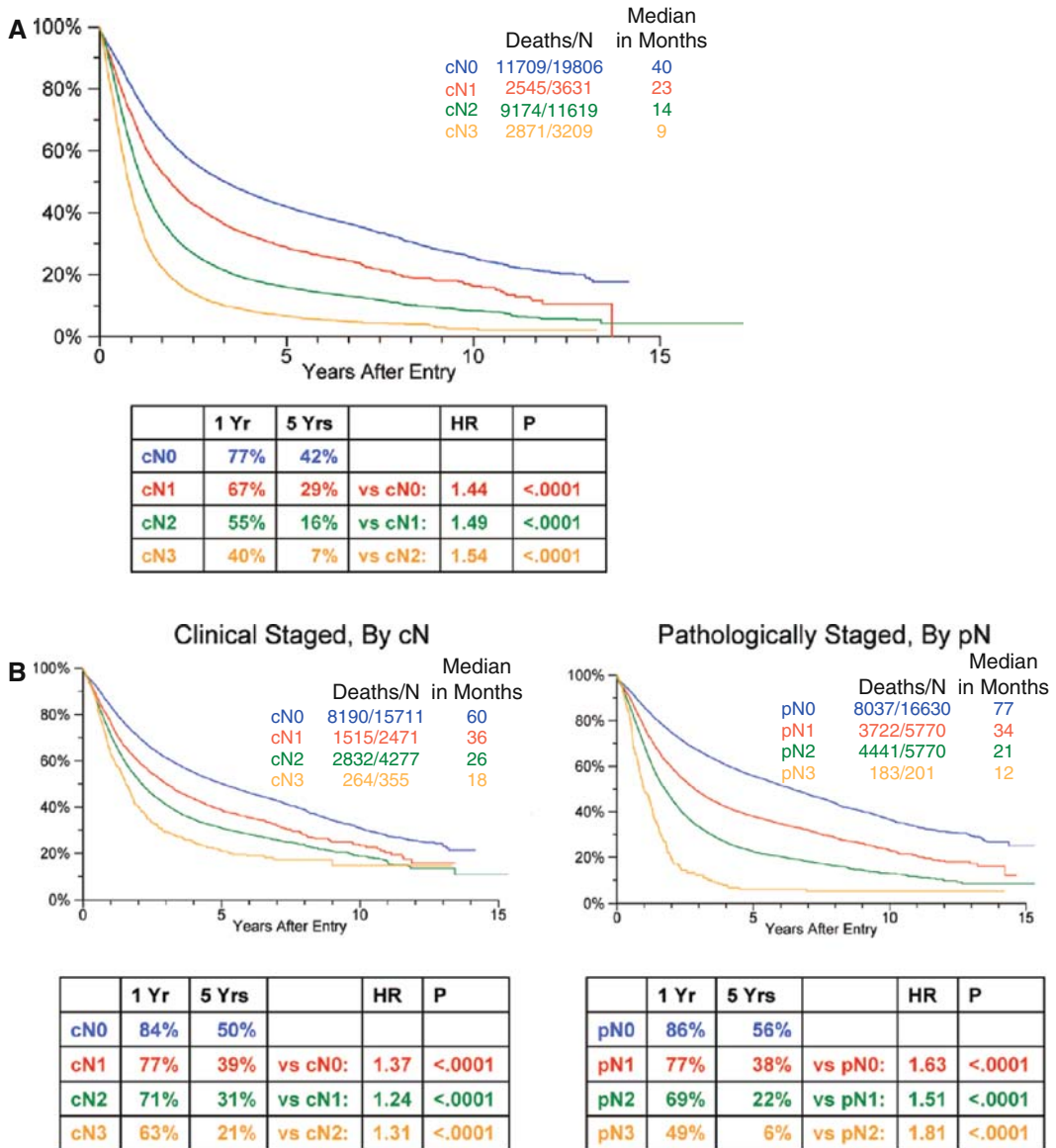
Fig. 4.4. (**a**) Survival by clinical N stage in non-surgical patients (cM0). (**b**) Survival by clinical stage and pathological stage in surgical patients (cM0). From Rusch VW, et al. *(20)*. Reprinted with permission.

these groups in conjunction with each T stage, so no conclusion could be drawn from this analysis. Thus, no recommendation for revising the existing N descriptor was made.

2.3. Proposed Revisions for the M Descriptor

The subcommittee on M descriptors analyzed 6,596 cases with either T4 or M1 stage by clinical or pathological staging *(21)*. As noted in the section on T descriptors above, pleural dissemination was determined to convey a survival similar to metastatic disease

and, thus, the recommendation was made to reclassify these as M1. Also, additional nodule(s) in an ipsilateral non-primary tumor-bearing lobe were proposed to be reclassified as T4; satellite nodules within the primary tumor-bearing lobe would be reclassified as T3.

This subcommittee addressed the presentation of an additional nodule detected in a contralateral lobe *(21)*. These resulted in a median survival of 10 months, closer to that resulting from pleural dissemination than that associated with distant metastasis, which was worse. Unfortunately, the database did not allow analysis of single versus multiple contralateral nodules, which could have implications on the likelihood of metastatic spread versus synchronous primary tumor, as most of this M1 subgroup was staged clinically, not pathologically. Finally, it was noted that a single metastatic site led to modest, but statistically significant improved median survival compared with multiple sites (6 months vs. 5 months, p = 0.0006). Within a single locus of metastasis (e.g., brain), the data did not permit analysis of single versus multiple metastatic lesions. The proposed revisions for the M descriptor are:

Table 4.3a
Changes to the proposed stage groupings resulting from revisions of the TNM descriptors. From Goldstraw P, et al. *(9)*. Reprinted with permission

Sixth Edition T/M Descriptor	Proposed T/M	N0	N1	N2	N3
T1(≤2 cm)	T1a	IA	IIA	IIIA	IIIB
T1(>2–3 cm)	T1b	IA	IIA	IIIA	IIIB
T2(≤5 cm)	T2a	IB	**IIA**	IIIA	IIIB
T2(>5–7 cm)	T2b	**IIA**	IIB	IIIA	IIIB
T2(>7 cm)	T3	**IIB**	**IIIA**	IIIA	IIIB
T3 invasion		IIB	IIIA	IIIA	IIIB
T4 (same lobe nodules)		**IIB**	**IIIA**	**IIIA**	IIIB
T4 (extension)	T4	**IIIA**	IIIA	IIIB	IIIB
M1 (ipsilateral lung)		**IIIA**	**IIIA**	**IIIB**	**IIIB**
T4 (pleural effusion)	M1a	**IV**	**IV**	**IV**	**IV**
M1 (contralateral lung)		IV	IV	IV	IV
M1 (distant)	M1b	IV	IV	IV	IV
Cells in bold indicate a change from the sixth edition for a particular TNM category.					

- Reclassify pleural dissemination from T4 to **M1a**
- Subclassify M1 by additional nodules in the contralateral lung as **M1a**
- Subclassify M1 by virtue of distant metastasis as **M1b**

As with the other descriptors, these recommendations were validated internally and externally, utilizing the SEER data.

2.4. Proposed Revision of Stage Groupings

As a result of the proposed revisions to the descriptors detailed above, the stage groupings will be comprised differently in the 7th edition of the UICC TNM staging system *(9)*. (**Table** 4.3a,b) The resultant survival curves for both clinical staging and pathological staging are seen in **Figs.** 4.5 and 4.6, respectively. These stage groupings were also validated with the SEER database, and generated similar curves. Overall, the five-year survival by pathologic stage is similar to that generated in the 1997 revision: stage IA at 73 percent, IB at 58 percent, IIA at 46 percent, IIB at 36 percent,

Table 4.3b
Proposed stage groupings for the 7th edition of the UICC TNM staging system. From Goldstraw P, et al. *(9)*. Reprinted with permission

Occult Carcinoma	TX	N0	M0
Stage 0	Tis	N0	M0
Stage IA	T1a, b	N0	M0
Stage IB	T2a	N0	M0
Stage IIA	T1a,b	N1	M0
	T2a	N1	M0
	T2b	N0	M0
Stage IIB	T2b	N1	M0
	T3	N0	M0
Stage IIIA	T1, T2	N2	M0
	T3	N1, N2	M0
	T4	N0, N1	M0
Stage IIIB	T4	N2	M0
	Any T	N3	M0
Stage IV	Any T	Any N	M1a, b
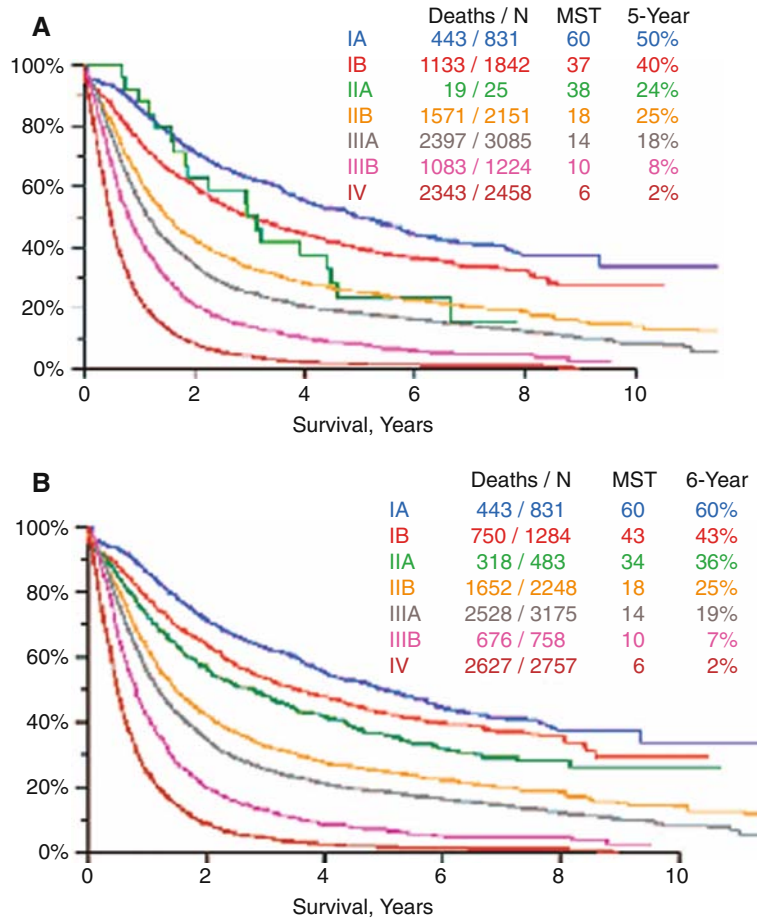
Fig. 4.5. Overall survival, comparing clinical stage groupings from the 6th edition TNM staging system (**A**) and the proposed IASLC revisions to the staging system (**B**). From Goldstraw P, et al. *(9)*. Reprinted with permission.

IIIA at 24 percent, IIIB at 9 percent, and IV at 13 percent. A major difference which is readily apparent in the survival curves is avoidance of overlap. Most notably in early stage groupings (IB, IIA, and IIB), there is improved separation. In addition, the distribution of cases throughout the stage groupings is more even, as a greater proportion of cases are assigned to stage IIA. Overall, the proposed revisions of the TNM staging system will allow more powerful application of stage groupings, based on increased hazard ratios for a stage modeled as an ordered variable. The advantages of a more international database of significantly increased size, compared with those used for previous staging system revision, are also clear.
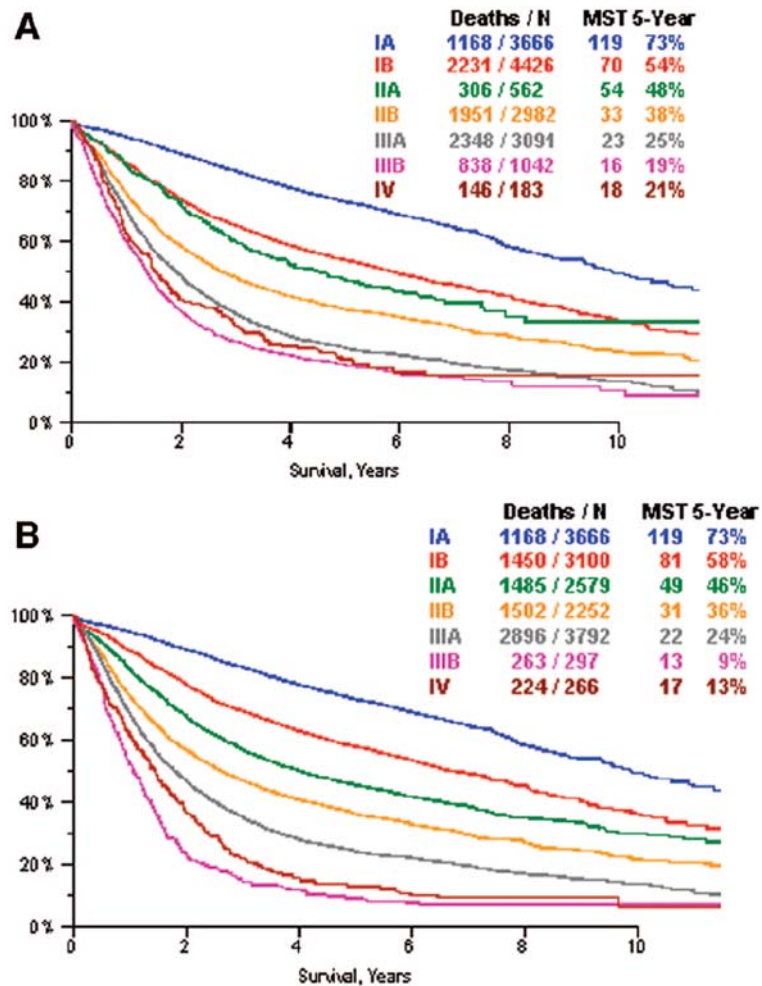
Fig. 4.6. Overall survival, comparing pathologic stage groupings from the 6th edition TNM staging system (**A**) and the proposed IASLC revisions to the staging system (**B**) From Goldstraw P, et al. *(9)*. Reprinted with permission.

References

1. Parkin DM, Bray F, Ferlay J, Pisani P. Global cancer statistics, 2002. CA Cancer J Clin. 2005 Mar–Apr;55(2):74–108.

2. Jemal A, Siegel R, Ward E, Hao Y, Xu J, Murray T, et al. Cancer statistics, 2008. CA Cancer J Clin. 2008 Mar–Apr;58(2):71–96.

3. Goldstraw P, Crowley J. The International Association for the Study of Lung Cancer international staging project on lung cancer. J Thorac Oncol. 2006;1(4):281–286.

4. Mountain CF, Carr DT, Anderson WA. A system for the clinical staging of lung cancer. Am J Roentgenol Radium Ther Nucl Med. 1974 Jan;120(1):130–138.

5. Mountain CF. A new international staging system for lung cancer. Chest. 1986 Apr;89(4 Suppl):225S–233S.

6. Mountain CF. Revisions in the International System for Staging Lung Cancer. Chest. 1997 Jun;111(6):1710–1717.

7. Flieder DB. Commonly encountered difficulties in pathologic staging of lung cancer. Arch Pathol Lab Med. 2007 Jul;131(7):1016–1026.

8. Mountain CF, Dresler CM. Regional lymph node classification for lung cancer staging. Chest. 1997 Jun;111(6):1718–1723.

9. Goldstraw P, Crowley J, Chansky K, Giroux DJ, Groome PA, Rami-Porta R, et al. The IASLC Lung Cancer Staging Project: proposals for the revision of the TNM stage groupings in the forthcoming (seventh) edition of the TNM Classification of malignant tumours. J Thorac Oncol. 2007 Aug;2(8):706–714.

10. Rami-Porta R, Ball D, Crowley J, Giroux DJ, Jett J, Travis WD, et al. The IASLC Lung Cancer Staging Project: proposals for the revision of the T descriptors in the forthcoming (seventh) edition of the TNM classification for lung cancer. J Thorac Oncol. 2007 Jul;2(7):593–602.

11. Mulligan CR, Meram AD, Proctor CD, Wu H, Zhu K, Marrogi AJ. Lung cancer staging: a case for a new T definition. Ann Thorac Surg. 2006 Jul;82(1):220–226.

12. Padilla J, Calvo V, Penalver JC, Sales G, Morcillo A. Surgical results and prognostic factors in early non-small cell lung cancer. Ann Thorac Surg. 1997 Feb;63(2):324–326.

13. Carbone E, Asamura H, Takei H, Kondo H, Suzuki K, Miyaoka E, et al. T2 tumors larger than five centimeters in diameter can be upgraded to T3 in non-small cell lung cancer. J Thorac Cardiovasc Surg. 2001 Nov;122(5):907–912.

14. Takeda S, Fukai S, Komatsu H, Nemoto E, Nakamura K, Murakami M. Impact of large tumor size on survival after resection of pathologically node negative (pN0) non-small cell lung cancer. Ann Thorac Surg. 2005 Apr;79(4):1142–1146.

15. Mery CM, Pappas AN, Burt BM, Bueno R, Linden PA, Sugarbaker DJ, et al. Diameter of non-small cell lung cancer correlates with long-term survival: implications for T stage. Chest. 2005 Nov;128(5):3255–3260.

16. Groome PA, Bolejack V, Crowley JJ, Kennedy C, Krasnik M, Sobin LH, et al. The IASLC Lung Cancer Staging Project: validation of the proposals for revision of the T, N, and M descriptors and consequent stage groupings in the forthcoming (seventh) edition of the TNM classification of malignant tumours. J Thorac Oncol. 2007 Aug;2(8):694-705.

17. Battafarano RJ, Meyers BF, Guthrie TJ, Cooper JD, Patterson GA. Surgical resection of multifocal non-small cell lung cancer is associated with prolonged survival. Ann Thorac Surg. 2002 Oct;74(4):988–93; discussion 93–94.

18. Miyazawa M, Shiina T, Kurai M, Makiuchi A, Numanami H, Kondo R, et al. [Assessment of the new TNM classification for resected lung cancer]. Kyobu Geka. 2000 Oct;53(11):915–918.

19. Hosokawa Y, Matsuge S, Murakami Y, Satoh K, Yamazaki S, Kan T, et al. [Validity and controversies in the new postoperative pathologic TNM classification based on the results of surgical treatment of non-small cell lung cancer]. Kyobu Geka. 2000 Oct;53(11):910–914.

20. Rusch VW, Crowley J, Giroux DJ, Goldstraw P, Im JG, Tsuboi M, et al. The IASLC Lung Cancer Staging Project: proposals for the revision of the N descriptors in the forthcoming seventh edition of the TNM classification for lung cancer. J Thorac Oncol. 2007 Jul;2(7):603–612.

21. Postmus PE, Brambilla E, Chansky K, Crowley J, Goldstraw P, Patz EF, Jr., et al. The IASLC Lung Cancer Staging Project: proposals for revision of the M descriptors in the forthcoming (seventh) edition of the TNM classification of lung cancer. J Thorac Oncol. 2007 Aug;2(8):686–693.

Technique, Anatomy and Application of Radial Ultrasound

Heinrich D. Becker

Within the central airways, the endoscopist's view is restricted to the lumen and to the internal surface. Intramural processes and those adjacent to the airways, as well as mediastinal structures, can only be assessed from indirect signs, including discoloration, displacement and destruction of anatomical structures. In the 1980s, despite early enthusiasm with the broader application of computed tomography (CT), clinical staging of lung cancer was correct only 60 percent of cases, leading clinicians to consider endoscopic ultrasound as a potentially useful technology for the airways. External mediastinal ultrasound and transesophageal endosonography proved insufficient for exploration of the mediastinal structures. In 1989 this led to the beginning of the development of endobronchial ultrasound *(1)*, first using miniaturized radial scanning probes that were applied in the gastrointestinal tract (EUS) *(2)* and cardiovascular endosonography, preliminary experience of which had been reported in endovascular sonography of the pulmonary artery to exclude tumor invasion *(3)*.

1. Development of Miniprobe Systems

In the early 1990s miniaturized probes with mechanical transducers of 7.5 MHz were used. Later probes with 12 and 20 MHz became available. The first probes had a diameter of 3 mm, a mechanical single-element transducer at the tip, which rotated at 400 rpm and provided a 360° image of the airways and the

surrounding structures, perpendicular to its axis. As it could not be inserted via the biopsy channel of regular flexible bronchoscopes, we applied it in rigid bronchoscopy using metallic tubes as a guide. As contact with the naked probe proved insufficient we fixed latex balloons, filled with sterile water from a proximal side port to the tip of the tubes to provide circular contact. Later probes with 2.5 mm became available, that could be inserted via bronchoscopes with biopsy channels of at least 2.8 mm and those systems are commercially available. The system is complete with balloon catheters that are attached to the probe and to the driving unit (Olympus UM-BS20-26R) (**Fig. 5.1**).
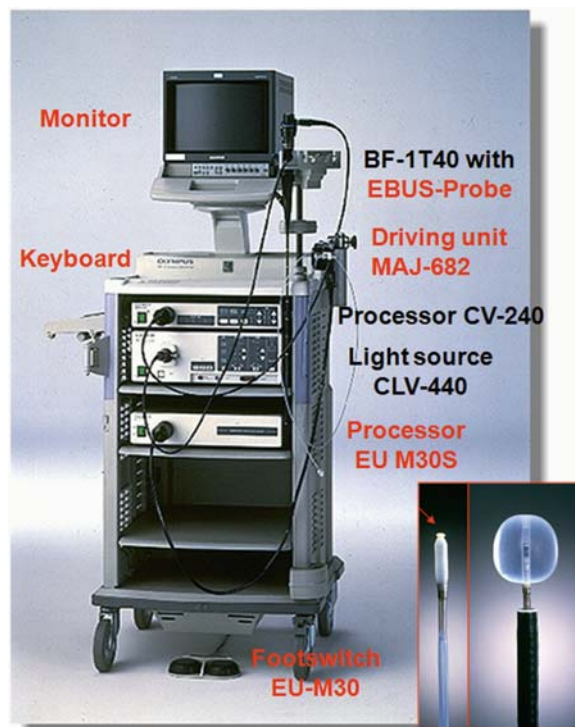
Fig. 5.1. Radial Probe with balloon catheter (evacuated and inflated), light source for videoscope and processors for endoscope and ultrasound.

The balloon is fixed at the tip of the probe by an O-ring that slips into a notch at the tip of the probe. If over-inflation or excessive pressure occurs the balloon slips from the tip and the small amount of water is released into the airways, preventing the balloon from rupturing and latex particles dislodging into the lung (**Fig. 5.2**). The development of the balloon provided three essential features for imaging within the airways. First, it provided circular contact, giving a 360° view for exact anatomical orientation; second, the 20 MHz frequency allows detailed analysis of the
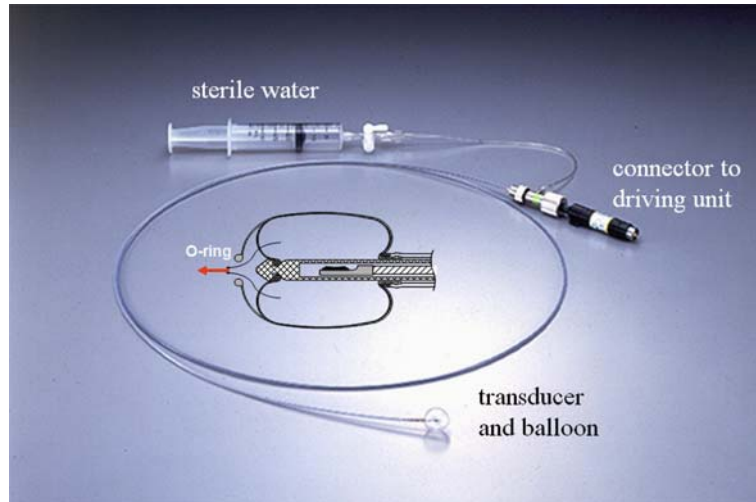
Fig. 5.2. Radial ultrasound probe with balloon catheter and illustration of safety function of the balloon.

tracheobronchial wall in high resolution, and third, the water shifts the focus towards the periphery, thus the parabronchial mediastinal structures that frequently are the grey zone in CT can also be analyzed, *(4)*.

2. Handling of Miniprobes

2.1. Storage and Preparation

Miniprobes are delicate, fragile devices that must be handled with care. The transducer and the connecting driving wire are protected from friction inside the plastic sheath by a gel solution. The catheter might not be completely air sealed and small air bubbles can collect in front of the transducer and interfere with the image. Therefore, the devices should be stored in a hanging position with the connector upwards and the tip of the probe downward. If a bubble has collected at the tip of the catheter, it can be cleared by holding the probe approximately 40 cm proximally from the tip and rotating it like a lasso to drive the gel peripherally and the bubble proximally. After inserting the probe into the balloon catheter and connecting the proximal end to the connector with the driving unit, the catheter – including the balloon – should be filled completely with sterile water to clear the system from air and make slipping the O-ring over the notch easier. We advise not to use saline solutions as the salt can crystallize on the probe and interfere with imaging. After filling, the O-ring can be slipped onto the tip of the probe with the fingertip or a special rubber device. This should be done gently without bending or kinking the tip.

Then, the balloon is filled to expand. If some air bubbles remain, the balloon is kept with its tip pointing down and the air is removed by suctioning the water from the balloon with the syringe. The syringe should always be held in an upright position so that the air collects above the fluid and is not flushed back into the catheter.

2.2. Application for Examination

When applied with the balloon sheath, bronchoscopes with a biopsy channel of at least 2.8 mm should be used. To enhance passage we apply a little medical silicone and the assistant should apply suction to completely evacuate the balloon, preventing it from slipping off the probe and from damage by friction inside the biopsy channel. The probe should never be advanced inside the biopsy channel with the tip of the bronchoscope in a sharply bent position. It should also not be activated then as the transducer might be fixed while the wire is still rotating and could then shear off. Never use force while advancing the probe, neither advancing the tip, nor pressing the probe sideways against the wall. This applies also for passing stenoses or into the periphery as the tip easily kinks. The balloon should not be over-inflated, especially while advancing the probe inside conical airways and when a patient is coughing; otherwise the special mechanism is not functioning and the balloon might break, since the O-ring cannot slip off. But even then, mostly the fragments will adhere to the tip of the probe and to the catheter and not dislodge into the lung.

3. Technique of EBUS with the Miniature Probe

After insertion via the biopsy channel of the flexible endoscope precise placement of the probe inside the central airways is carried out under visual control. Once the transducer is positioned the balloon is filled with water until firm contact with the wall is established. Adequate contact is confirmed by a complete circular image of the bronchial wall and the surrounding structures. The development of the image is similar to sunrise, when all the structures gradually become visible. After sufficient preoxygenation with the patient under local anaesthesia inflation of the balloon is possible in bilateral ventilated lungs up to the main bronchi and even inside the trachea. Complete obstruction of a remaining main bronchus after contralateral resection or occlusion of the trachea can be tolerated for up to two minutes with sufficient sedation. If necessary the bronchoscope can be introduced via a laryngeal mask. In these cases, general anaesthesia might be preferable, as it can provide additional time for imaging of the mediastinal structures. According to our experience, this procedure is well

justified in relation to the valuable information that can be obtained. We have never observed barotrauma during complete obstruction since, according to our measurements, even with high frequency jet ventilation, the pressure distal to the balloon rapidly drops to zero during inflation. If the patient cannot tolerate complete obstruction at all, the balloon can be partially filled and applied with semicircular contact. For passing via stenoses or introduction into the periphery no balloon catheter is necessary. However, since the naked probe is so fragile we prefer to insert it via a plastic catheter sheath. This can also serve as an extended working channel to insert biopsy or therapeutic tools after removing the miniature probe once the lesion is reached.

4. Imaging Artifacts

The image construction begins in a radial way at the nine o'clock position and the rotation is slow enough to create a motion artifact since the wall can change its position during one revolution due to pulsation or respiration. This creates an artificial interruption in the continuity of the bronchial wall and a motion of the wall can be suggested. As the artifacts are not synchronous with respiration and pulsation they can easily be recognized as such. The strong echo of the balloon occasionally causes multiple ring reflections (**Fig. 5.3**). Strong reflections of surrounding structures can create multiple reflex echoes, mirror or comet artifacts. This applies especially to the adjacent surface of the lung, the vertebral column, calcified cartilages or lymph nodes. Triangular distortions of lymph nodes and attenuation of the outer contours of echogenic structures is also very common with the 20 MHz probes. Air bubbles in the balloon can cause shadows or image distortion, resembling a "rabbit's ear."

4.1. Sonographic Anatomy

The complex structure of the airway wall as described in anatomy textbooks can be clearly seen with the 20 MHz probe. The number of layers visible with 20 MHz EBUS is still being debated. The descriptions range from three to five and seven layers *(5, 6, 7)*. By in vitro experiments on resected human specimens we found a complex seven layer structure for which a high resolution setting is necessary. The first innermost hyperechoic layer is composed of a combination of the reflections from the balloon and the mucosa. The next hypoechoic layer is the submucosa. Under normal conditions it can be easily differentiated from the mucosa and from the third layer, the hyperechoic internal surface of the cartilage, which anatomically can be described as tabula interna or endochondrium, as I used to call it. This borderline structure is important
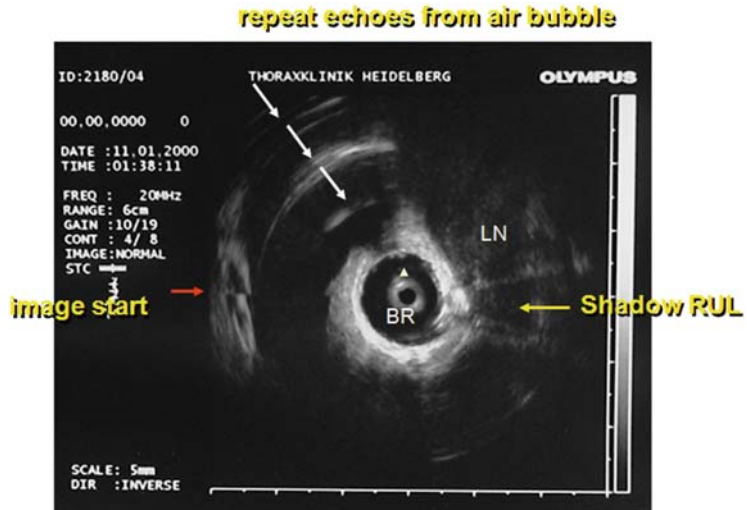
Fig. 5.3. Imaging artifacts in bronchus (BR). *Rotation artifact:* At the 9 o'clock position the edge with displacement of the wall and the pulmonary artery can be seen (*red arrow*). This is the location from which after one cycle of the transducer the image is constructed, again. If the bronchial wall has moved by ventilation, pulsation or motion of the bronchoscope a fracture in the image is created. *Repeat echoes:* At 11 h the balloon has insufficient contact with the bronchial wall. The strong echo of the balloon is repeatedly reflected and the image shows three concentric segments of a *circle* (*three arrows*). *Shadow due to air:* At the same position small air bubbles have collected in the balloon (*small arrow*). They are producing a conical shadow by which the structures of the wall are hidden. However, the strong reflexes of the balloon are persistent. At the right side there is another shadow, which is caused by the branching of the right upper lobe (RUL). The air produces a bright strong echo with a shadow distally. *Attenuation:* Above this shadow a lymph node can be seen (LN). Due to the comparably low energy of the 20 MHz the proximal parts can be clearly seen, while the distal contours are fading because the energy is absorbed by the tissue.

as tumors that do not transgress it, by histopathological definition, are early cancers and can be efficiently treated by bronchoscopic means such as photodynamic therapy (PDT) or endobronchial high dose radiation (HDR or brachytherapy) as has been demonstrated by Miyazu, et al. *(8)*. The internal spongiform structure of the cartilage appears as hypoechoic in EBUS, whereas the outer surface (tabula externa or perichondrium) is hyperechoic, again. The central airways are surrounded by a double layer of loose and dense connective tissue *(9)*, representing the sixth (hypoechoic) and seventh (hyperechoic) layer. This seven layer structure has been confirmed in another prospective experimental study *(10)* (**Fig. 5.4**).

In vivo this complex structure can only be seen under high magnification, whereas at medium and low magnification especially the delicate hypoechoic layers condense with the strong echoes of the supporting cartilages. With the Linear 7.5 MHZ and 12 MHz transducers of the ultrasonic bronchoscope these
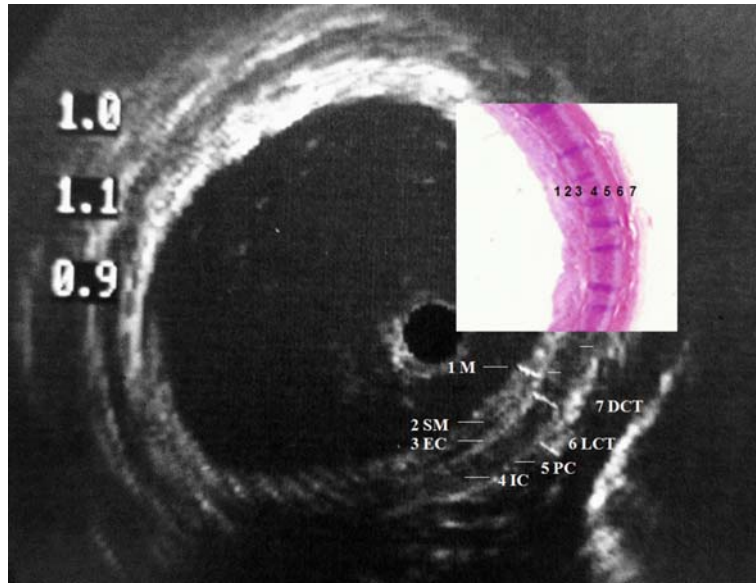
Fig. 5.4. Layer structure of the bronchial wall. In the central airways by high magnification of the 20 MHz image the seven layers can be clearly differentiated. The three layer structure of the cartilage with endochondrium (EC), Perichondrium (PC) and spongiform internal structure (IC) is lined by mucosa (MC) and submucosa (SM) internally and by loose (LCT) and dense connective tissue on the outside (DCT). The HE-stain of the inserted tissue specimen shows the corresponding structures.

layers are invisible. The multilayer structure progressively comes down to five and three layers with passage towards the peripheral bronchi as the cartilages become scarce and finally disappear altogether.

Spatial orientation within the mediastinum is not easy. This is due to the complex anatomy as well as to motion artifacts, pulsation and in addition to the uncommon planes of the images. The plane of the circumferential image of the miniprobe is perpendicular to the axis of the probe. Whereas the horizontal planes inside the trachea are comparable to those in computed tomography (CT), following the oblique course of the airways down from the bifurcation the images are tilting more and more with passage through the left main bronchus until an almost coronary plane is reached at the distal left main bronchus. Entering the apical segments of the upper lobes the horizontal images become almost inverse.

In order to enhance orientation, it is useful to recognize key anatomical landmarks, their relationship to the airways and to each other, rather than to observe the position of the probe. Familiarity with the mediastinal anatomy is essential for orientation *(11)*. The image must be set accordingly, so that landmark structures that are found only ventrally or dorsally to the bronchi, such as the esophagus or the pulmonary artery, are in the correct position. It is

helpful to place the tip of the bronchoscope in direct contact with the balloon to look inside and follow the direction of the transducer when the tip of the bronchoscope is flexed sideways or up and down, and adjust the ultrasonic image accordingly with the scroll ball or the reverse button on the keyboard. Vessels can be easily recognized due to their low echogenicity and pulsations; arteries show a pulsation that is congruent with the pulse oximetry signals, whereas veins show the typical double motion as can be observed on the large peripheral veins. A Doppler function is not currently available for the miniprobes. However, lymph nodes can be easily differentiated from vessels due to their higher echogenicity.

As the water in the balloon shifts the focus more distally, with the 20 MHz probe the depth of penetration into the mediastinum can be well up to 5 cm. Thus, from the distal left main bronchus the left atrium and the mitral valve can frequently be seen. Near the bifurcation, from the left main bronchus, the main pulmonary artery and its left and right branches are visualized ventrally. Dorsally the descending aorta, the multilayer structure of the esophagus and the vertebral column appear from left to the right behind the proximal left main bronchus as clear landmarks for orientation (**Fig. 5.5**). Ventrally to the right main bronchus appear the right pulmonary artery, which is accompanied by the ascending aorta to
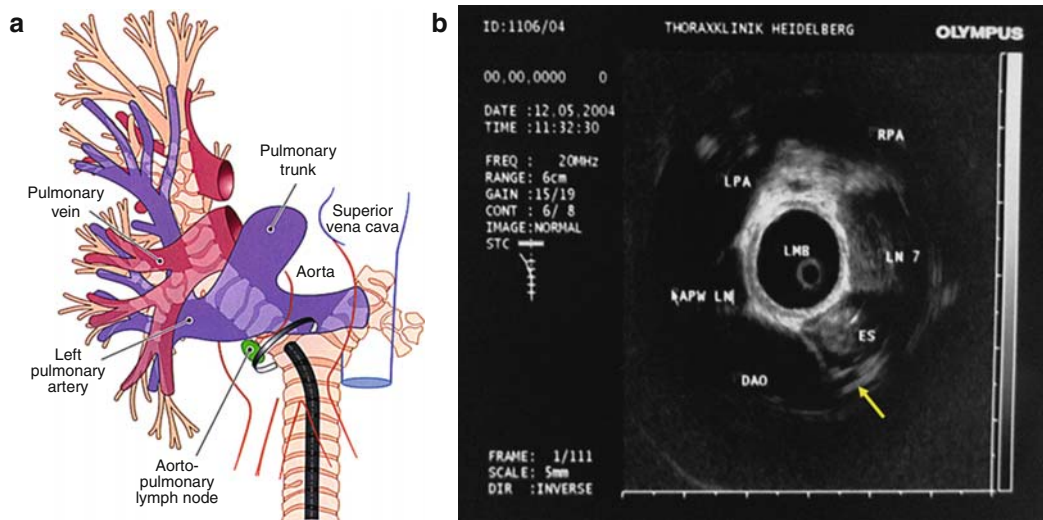
Fig. 5.5. Ultrasonic mediastinal anatomy at the level of the proximal left main bronchus. (**a**) On the left is a situational sketch with approximately the plain of the radial ultrasonic depicted. (**b**) On the right is the corresponding ultrasonic image with the probe inside the left main bronchus (LMB). Anterior the left (LPA) and right main pulmonary (RPA) artery are seen. Dorsally, more to the left the descending aorta is passing behind the left main bronchus and medially the multilayer structure of the esophagus is seen (ES) with some air and fluid inside. Anterolateral to it a paraesophageal/subcarinal lymph node is located in position 7 (LN 7). Another lymph node can be found between the aorta and left pulmonary artery, the medial compartment of the aorto-pulmonary window (APW LN). Behind the esophagus and in front of the vertebral column an intercostal artery crosses from the descending aorta to the right (arrow). (Courtesy of Atul Mehta)

the left and by the cava vein to the right. Somewhat more proximally in the distal trachea, at the level of the right tracheobronchial angle, the azygos vein is located dorsally to the right besides the esophagus, where it circumflexes the trachea to the anterior and joins the cava vein. Further distally, at the level of the intermediate bronchus pulmonary artery and vein are crossing ventrally. Close to the middle lobe the artery for the apical segment of the lower lobe is crossing laterally backwards. This is important to know as it is easily punctured during TBNA of lymph node No. 10 on the right side. Dorsally the bright reflection corresponds to the adjacent pleura of the apical segment of the lower lobe, and medially the pulmonary vein is entering the atrium. The branching of the vessels at the segmental levels of the bronchi is less consistent and shows a lot of variations. Localization of the vessels, however, can be important to avoid contamination of TBNA specimens by blood and perforation during laser treatment of tumors, especially in both upper lobes. The lung tissue itself is highly reflective and shows a "snowstorm" like feature with the alveoli and capillary vessels. Some authors described alterations in the pattern by interstitial lung diseases *(12)* and benign infiltrates can be easily differentiated from malignant nodular lesions and cystic structures. Using computer assisted analysis of the structures in the form of a histogram in a prospective study we were able to accurately diagnose malignancies in over 90 percent of cases.

4.2. Clinical Application

EBUS with the radial scanning miniature probe is easily applied, has a negligible complication rate and usually adds 6.3 minutes to regular bronchoscopy, as was shown in a prospective study, with a total of 19.9 minutes for the whole procedure *(13)*. Complications were rare and of only minor nature: 5 percent of patients required additional oxygen. Transient minor arrhythmias were observed in 18 out of 103 patients (17%) who underwent complete blockage of the left main bronchus by the balloon. Rarely, minor self limiting bleeding occurred during placement of the probe in the periphery of the lung. We could prove the cost effectiveness of the procedure by re-sterilization and reusing the probes as long as they resisted the stress and strain, which was several hundred procedures in our hands, but at least for up to 100. We have performed several prospective studies to validate EBUS for various indications *(14–18)*. Meantime the results have been confirmed by other authors and it has been shown that EBUS is comparable and, in many instances, even superior to other procedures. Although the dedicated ultrasonic bronchoscope with electronic linear transducer drew the main attention of the physicians after its introduction, there are a number of indications for endobronchial ultrasound that are only met by the radial probe. Both instruments are complementary, not competitive.

4.3. Indications for Clinical Application of the Radial Ultrasound Probe

According to its specific properties, namely the high resolution of the image with 20 MHz and the small diameter, there are several indications for applying the radial scanning ultrasound probe that are not met by the other devices.

4.3.1. Staging of Lung Cancer

The purpose of staging is to provide a precise classification in accordance with the current TNM system as a rational basis for treatment. Bronchoscopic criteria are documented in the UICC classification *(19)*. Radiologically invisible endobronchial tumors must be located in persons who are at high risk or who have positive sputum cytology. Once they are detected, a decision on the appropriate therapy is made based on the histological differentiation and local tumor spread and depth of penetration into the wall. Lymph node involvement is diagnosed by CT, EBUS and transbronchial needle aspiration (TBNA). In addition to their extent and size, the relationship of tumors to parabronchial mediastinal structures, central airways, lung and pleura is important. Here EBUS can provide additional information, especially in regions that are not easily accessible by the bronchoscope or other diagnostic procedures.

4.4. Primary Lung Cancer: Endobronchial Extent

Early cancer. By pathological definition, in situ lung cancer is limited to the mucosa, not transgressing the lamina propria, and early lung cancer is limited within the confines of the inner layers of the bronchial wall and does not infiltrate or transgress the cartilage. Until recently it was assumed that this equals radiological invisibility by high resolution CT. However, earlier radiographic studies have shown that only 75 percent of bronchoscopically visible tumors are detected by radiology *(20)*. Radiographically invisible tumors included lesions that had penetrated into the wall and from the beginning of its application in our institution, we frequently found radiologically invisible lesions that had even penetrated transmurally by EBUS and also showed local lymph node metastasis that had escaped all previous diagnostic procedures.

In all malignant lesions that were detected by videobronchoscopy, autofluorescence (AF) and narrow band imaging (NBI), we found sonographic alterations in the texture of the bronchial wall using the 20 MHz radial probe, either by thickening of specific layers or by destruction of the architecture (**Fig. 5.6**). As AF is unspecific and also positive in benign lesions such as scars, granulomas and inflammation, EBUS can improve specificity significantly and reliably clarify the nature of the lesion *(21)*. In our experience, correlation with the histology was improved from 58 percent to 92 percent. Even in macroscopically intact mucosa, submucosal and intramural tumor spread can be detected by EBUS. Tumors that do not show any signs of infiltration of the deeper layers or involvement of lymph nodes can be classified as
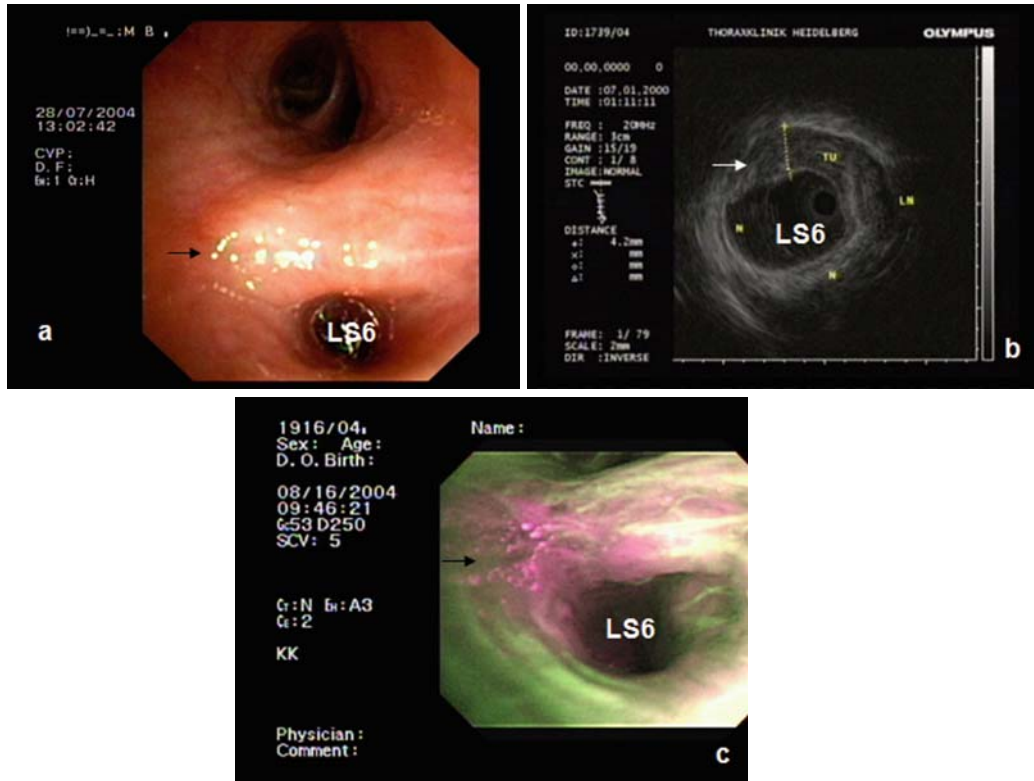
Fig. 5.6. Early lung cancer. On the left side the carina at entrance to B6 (LS 6) is somewhat widened and shows an irregular surface with scattering of the light reflection (**a**). In autofluorescence (AFI system, Olympus Co.) the area becomes clearly visible by its magenta color as compared to the normal green fluorescence (**b**). Endobronchial ultrasound shows a thickening of the mucosa/submucosa of 4 mm as compared to the normal walls (N) (**c**). If the radiologically invisible lymph node (LN) adjacent to B6 has been proved to be negative by transbronchial needle aspiration (TBNA), in the case of inoperability local destruction by endoscopic means (Nd-YAG laser, APC) could be considered. Otherwise high dose radiation by Ir192 brachytherapy would be preferable as it can also cover the lymph node.

early cancers and treated successfully with curative intent using endoscopic methods such as photodynamic therapy (PDT), endo-luminal high dose radiotherapy (HDR, brachytherapy) or even laser and argon plasma coagulation (APC) *(22)*. This is in contrast to former studies on treatment by electrocautery and PDT that reported recurrence rates of up to 50 percent *(23)*. A prospective study by Miyazu, et al. *(8)* could show that this is not due to inefficient treatment, but to insufficient local staging with conventional imaging technologies. All tumors that they staged by EBUS as limited within the internal layers of the bronchial wall were associated with complete remission in long-term follow-up. This proves that EBUS is currently the only reliable technique for staging of early lung cancer. Thus, we assume that in future cancer detection by molecular biological markers in sputum, blood or mouth swab, localization by autofluorescence and NBI and local

staging by EBUS with the miniature radial scanning probe will be the three pillars of early detection and local minimally invasive treatment for central early lung cancer *(24)*.

Local staging of more advanced cancer. CT is still the gold standard for diagnosing local tumor spread. However, clinical staging corresponds with postoperative staging in only 60–70 percent *(25)*. In locally advanced bronchial carcinoma EBUS also provides useful information. In patients with complete obstruction of the airway we can localize the base and the surface of the occluding tumor, diagnose the extent to which the tumor has penetrated into the wall and into the mediastinum and, by passing the stenosis with the probe, we can assess whether the airways distally to the stenosis are patent. Not infrequently the airways are plugged with sticky proteinaceous secretions that cannot be differentiated from tumor on CT. Particularly with regard to surgical strategy it is important to know the exact extent with regard to prospective resection lines. Involvement of the main bronchi, the carina and the trachea requires elaborate techniques for resection and not infrequently precludes operability. The combination of autofluorescence and EBUS proved useful in detecting submucosal tumor spread. In particular diagnosing involvement of the pulmonary vessels has great influence on decisions for interventions *(18)* (**Fig. 5.7**). Perfusion of the lung can be shut down completely by the Euler-Liljestrand reflex, even if the pulmonary artery is patent, and in former times one had to resort to angio-CT to exclude obstruction. With the radial probe one is able to see minor infiltrations of the wall and pulsations of the wall as well as fluid inside the vessel. However, with this respect the Doppler function of the linear scanning probe is an additional advantage, provided the stenosis can be passed with the endoscope.

Mediastinal infiltration: trachea, pulmonary vessels, esophagus, large vessels. Diagnosing infiltration of the large mediastinal vessels – the aorta, vena cava, main pulmonary artery and vein – is crucial and can be difficult by radiographic methods. Tumors located in the trachea, main bronchus and left hilum are in close vicinity to the esophagus and we have been able to detect direct infiltration by EBUS in several cases.

In addition, tumor invasion of the aortic arch, the descending aorta and the main pulmonary artery can be seen from both main bronchi and the trachea. Infiltration of these structures usually excludes surgical procedures. However, if one can see a distinct sonographic interface between the tumor and these structures, operability is possible, as has been shown in many of our patients. Only with the high resolution of the radial probes can infiltration of the external layers of the trachea and main bronchi be reliably diagnosed and distinguished from impression without infiltration. In our prospective study, CT had a sensitivity of only 25 percent and specificity of 80 percent (accuracy 51%), compared to EBUS
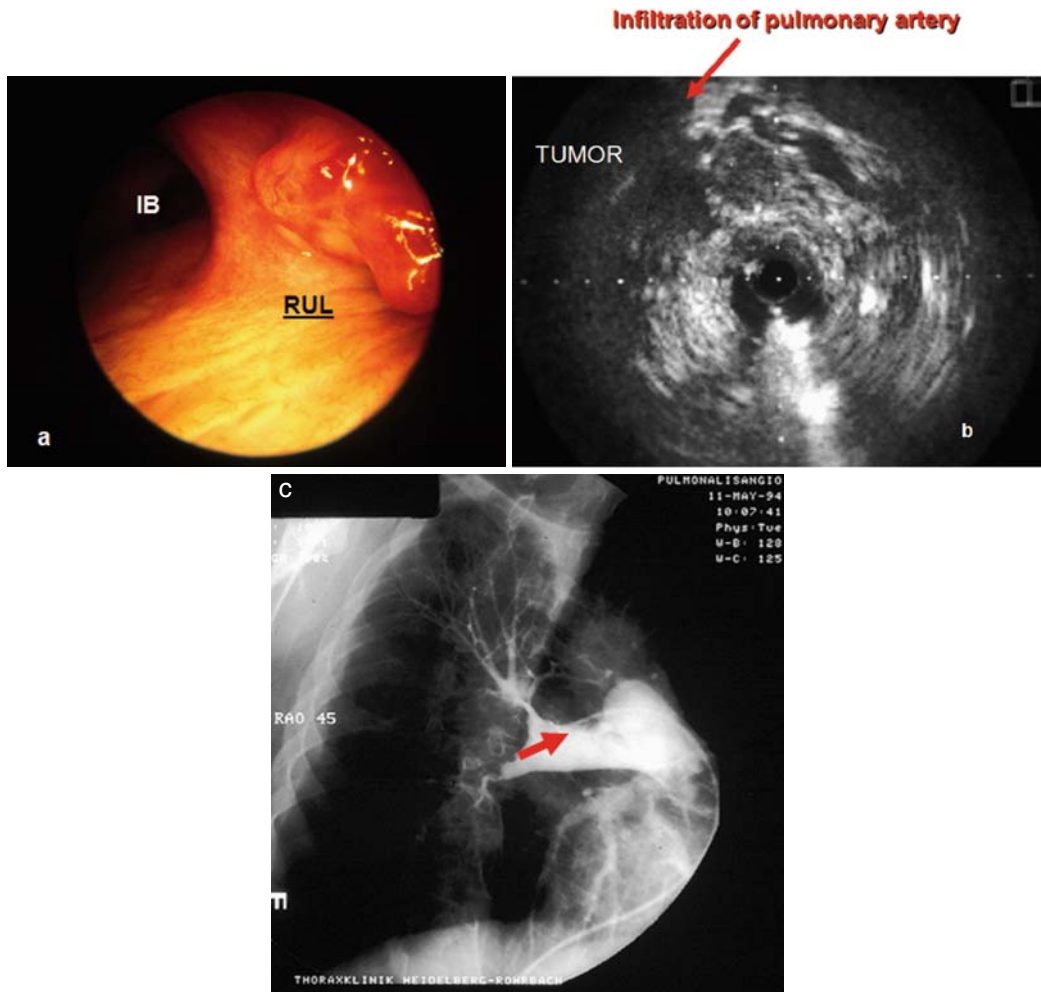
Fig. 5.7. Involvement of the pulmonary artery. A tumor is occluding the right upper lobe bronchus (RUL). The intermediate bronchus (IB) is not involved (**a**). Ultrasound shows extensive infiltration of the pulmonary artery by the tumor (**b**). In the beginning we confirmed our findings by conventional angiography (*arrow in* **c**). The images were documented in 1994.

with an accuracy of 94 percent, sensitivity of 89 percent and specificity of 100 percent *(15)*. For this purpose the resolution of the EBUS linear scope is insufficient.

Lymph nodes: Location, size, structure, infiltration and biopsy. Detection, localization, structure analysis, and especially real time *ultrasound-controlled* transbronchial needle biopsy or aspiration (TBNA) is the one indication for which the radial scanning probe has been replaced by the linear electronic scanning ultrasonic bronchoscope (EBUS-scope or so called "puncture scope") and is described extensively elsewhere in this book. In contrast to the esophagus, which is mobile within the mediastinal structures and can change its position in relation to the lymph nodes, the airways always remain in stable contact with their

vicinity and have distinct landmarks. This is why lymph nodes can be localized by CT guidance and especially with the radial scanning probe, and after withdrawal of the probe from the biopsy channel the biopsy needle is inserted according to the anatomical landmarks. Even with this *ultrasound-guided* technique we had a success rate of more than 80 percent. *(16)*

4.4.1. Mediastinal Lesions   If lesions within the mediastinum are in contact with the central airways they can also be explored with the radial probe and approached by TBNA. If the wall is infiltrated deep transmural biopsies (so called buttonhole biopsies) can be performed without risk (**Fig. 5.8**). However, as the depth of penetration with 20 MHz is limited, exploration with the linear probe is superior in many instances. We have been able to diagnose infiltration of the lateral wall of the traches and the anterior wall of the esophagus. If in
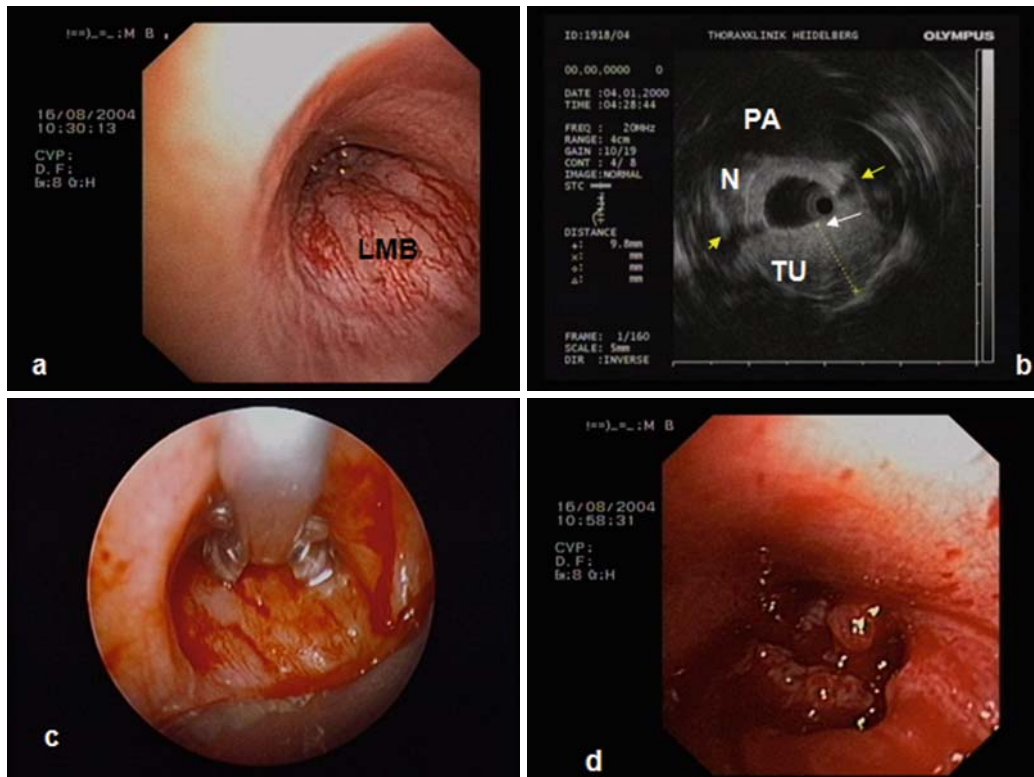
Fig. 5.8. External infiltration of the bronchial wall. The left main bronchus (LMB) is subtotally occluded by a lymph node compression from dorsally. The mucosa is intact and only shows some vascular engorgement. By ultrasonography the intact mucosa can be seen as uninterrupted white line (*arrow*), whereas the deeper layers are completely invaded by tumor as compared to the normal wall (N) and to the pulmonary artery (PA). Due to the oval deformation the balloon is lacking contact at the dorsolateral walls (*yellow arrows*) (**b**). In these cases the tumor can be biopsied by the rigid forceps (**c**) right through the intact muscosa without any risk, a so-called buttonhole biopsy. After biopsy the tumor is protruding through the defect, which is lined by the thinned mucosa (**d**).

doubt whether an esophageal lesion is a primary cancer, lymph node invasion or leiomyoma, the radial probe can be inserted into the esophagus and, after reaching the cardia, the balloon is inflated and the esophagus is explored during retraction. Whereas malignant lesions show a destruction of the wall, leiomyomas expand within the layer structures of the wall in a spiral arrangement without destroying the architecture and can be very reliably differentiated (**Fig. 5.9**). Bronchogenic or other mediastinal cysts are easily seen by their low echogenic structure. Sometimes they are septated and, in case of bleeding, infection or more solid content, they show irregular echoes inside. In contrast to reports after transesophageal puncture we did not observe severe complications after transbronchial needle aspiration by infections so far. This might be due to the less contaminated environment within the airways.
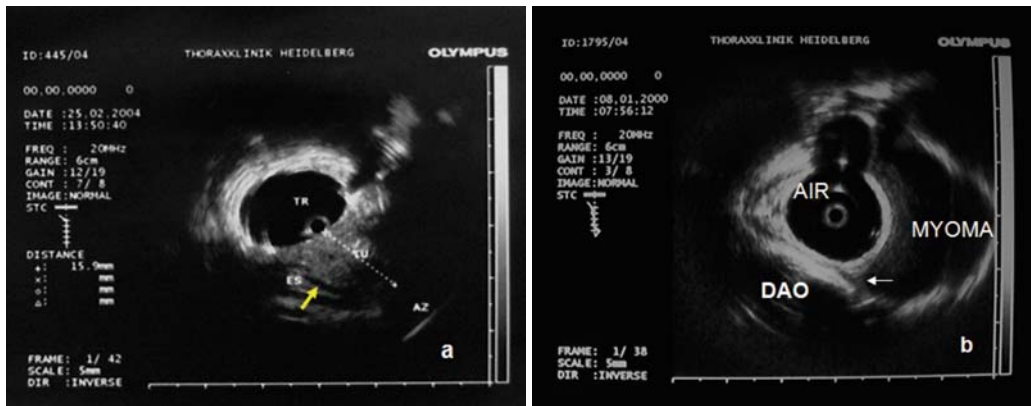
Fig. 5.9. In this patient the trachea (TR) is compressed and infiltrated from dorsally by an extensive paraesophageal tumor (TU), that does not infiltrate the esophageal wall (*arrow*) (**a**). This esophageal tumor is evolving from the muscular layers of the esophageal wall and by passing downwards with the probe inside the esophagus shows a spiral extension, which is both typical for leimyomas. Dorsolateral to the esophagus the descending aorta can be seen (DAO), ventrally a large air bubble inside the balloon is creating artifacts by repeat echoes and the "rabbit ear" effect (**b**).

4.4.2. Intrapulmonary Lesions

Ultrasound is strongly reflected by air. Therefore, in the beginning we were skeptical about its application within the lung. However, in their early publications Hürther and Hanrath reported that EBUS is useful for detecting peripheral lesions *(5, 6)* and it even appeared to be possible to analyze the lung tissue *(12)*. Later we have also been able to localize solid and cystic lesions within the periphery of the lung with the radial probe. Localization for biopsy was successful in up to 80 percent of cases, and particularly superior to fluoroscopy in lesions of less than 3 cm and those that were hidden behind the heart or other anatomical structures and pleural effusion *(17)* (**Fig. 5.10**).
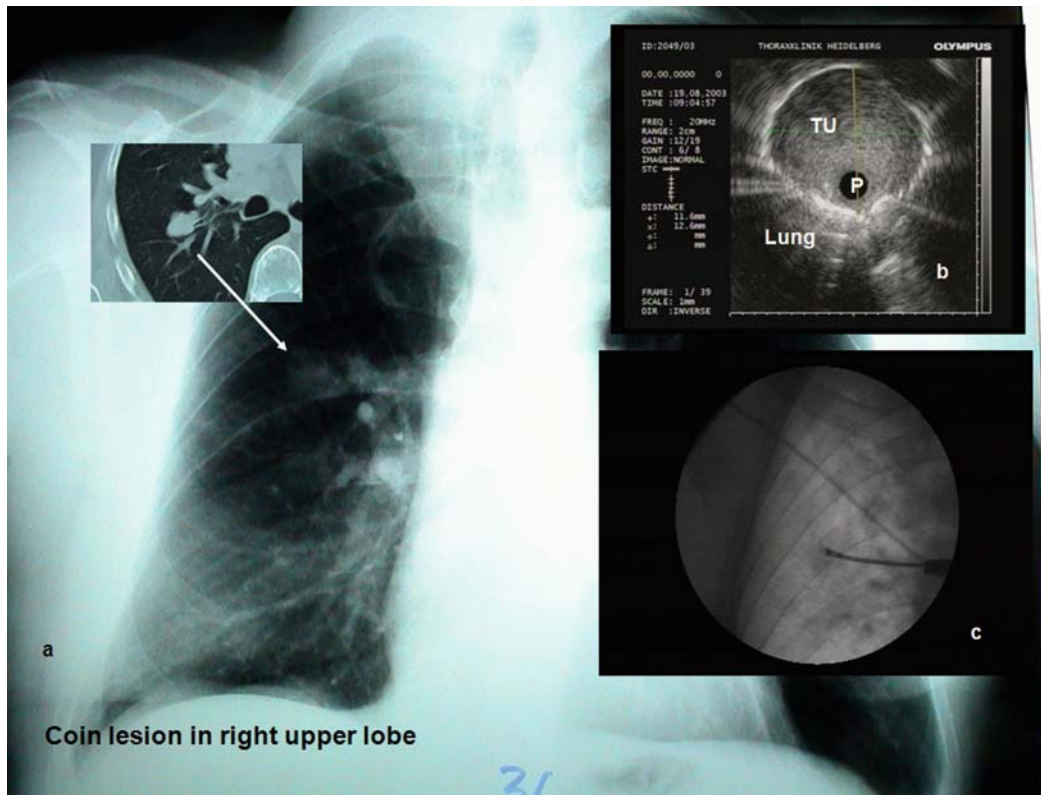
Fig. 5.10. Ultrasound-guided biopsy of a peripheral lung lesion. A small lesion that is clearly visible on CT is not easily seen on plain X-ray and especially under fluoroscopy in supine position with elevated diaphragm (**a**). The radial probe (P) has been introduced into the lesion (TU) of 11 × 12 mm, which has a significantly different ultrasonic structure as compared to the lung (LUNG), which is highly suggestive of malignancy (**b**). The biopsy forceps can be introduced into the lesion via a catheter that has been placed into the lesion with help of the radial probe as extended working channel (EWC) (**c**). Histological examination revealed squamous cell carcinoma.

If the probe is introduced via a catheter as extended working channel and can be placed exactly inside the lesion, biopsies are positive in up to 100 percent. When used in combination with electromagnetic navigation placement, EBUS has become so reliable that we currently use it to place Ir192 probes to treat inoperable peripheral lesions by brachytherapy. The high resolution provided by 20 MHz allows detailed imaging of the anatomic infrastructure of these lesions, which correlate significantly to the histological diagnosis *(26)*. By applying computer-assisted analysis of the EBUS images we were able to predict the nature of such lesions in 92 percent of cases *(27)* (**Fig. 5.11**).

In patients with infiltrations or atelectasis EBUS is useful in exploring the cause, such as bronchial compression by lymph nodes, benign strictures, tumor infiltration or compression of the

Adenocarcinoma

Round atelectasis
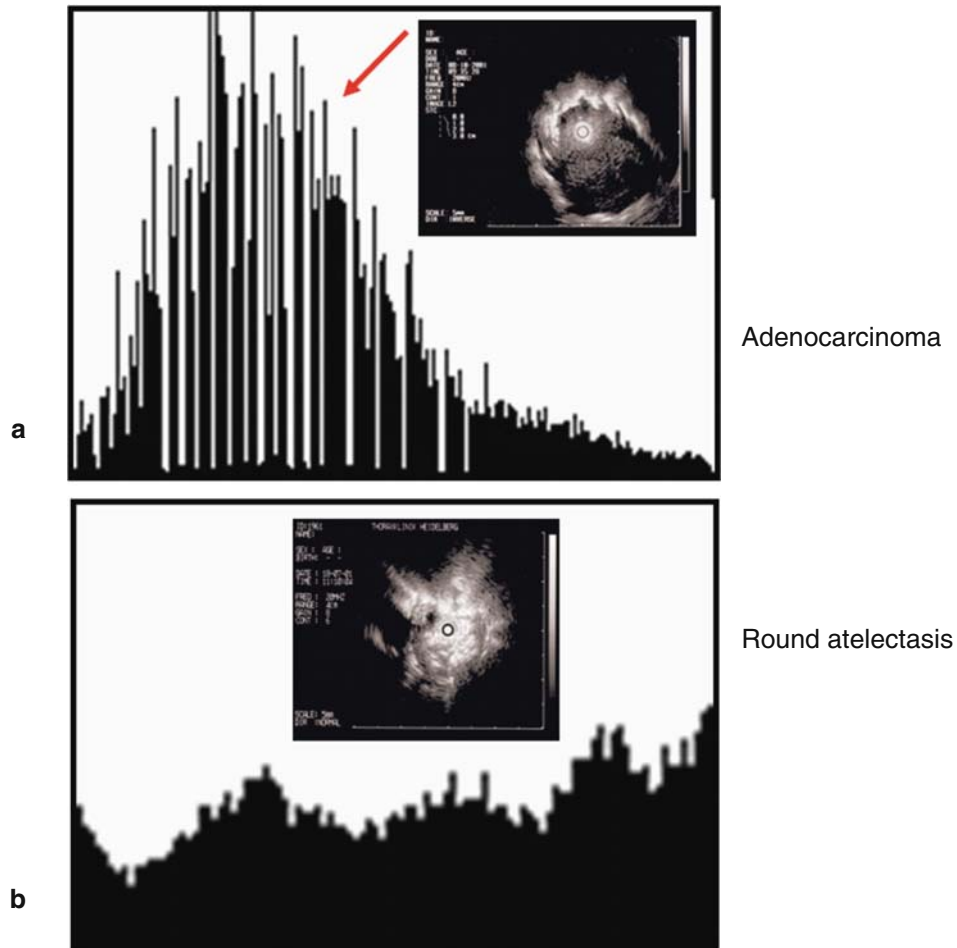
Fig. 5.11. Histogram of two lesions. The comparatively homogenous lesion (**a**) shows a peak on the dark side of the histogram, when all pixels are counted, which is highly suggestive for malignancy, in this case an adenocarcinoma. In contrast the benign lesion, a round atelectasis, shows an even distribution of the echo signals (**b**). Probably, the dark peak corresponds to the neovascularization of malignant lesions.

lung by pleural effusion or solid formations. The diagnosis and localization of cavitating lesions due to tuberculosis, necrotizing tumors and mycetomas is helpful in guiding placement of pigtail catheters for drainage and instilling drugs (**Fig. 5.12**).

4.4.3. Pleura and Neighboring Organs

If there is an acoustic window due to atelectasis, pleural fluid or a solid lesion, the pleura and neighboring structures, such as solid structures on the visceral and parietal pleura or on the pericardium, can be visualized. In case that pleural effusion reaches the central airways we successfully performed transbronchial thoracocentesis for diagnostic purposes by needle aspiration (**Fig. 5.13**).
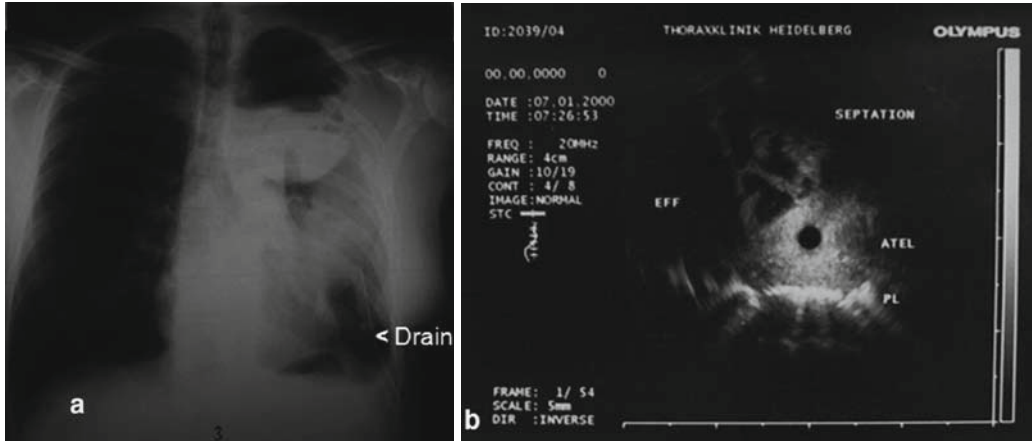
Fig. 5.12. Septated pleural effusion. In the left upper thorax a cavitation with fluid level can be seen on the X-ray. A drain has been inserted into the left lower chest (**a**). Ultrasound demonstrates atelectasis (ATEL) of the left upper lobe with strong reflection of the pleural surface (PL) (**b**). On the opposite site the echo free structure of the pleural effusion (EFF) is crossed by strands of connective tissue.
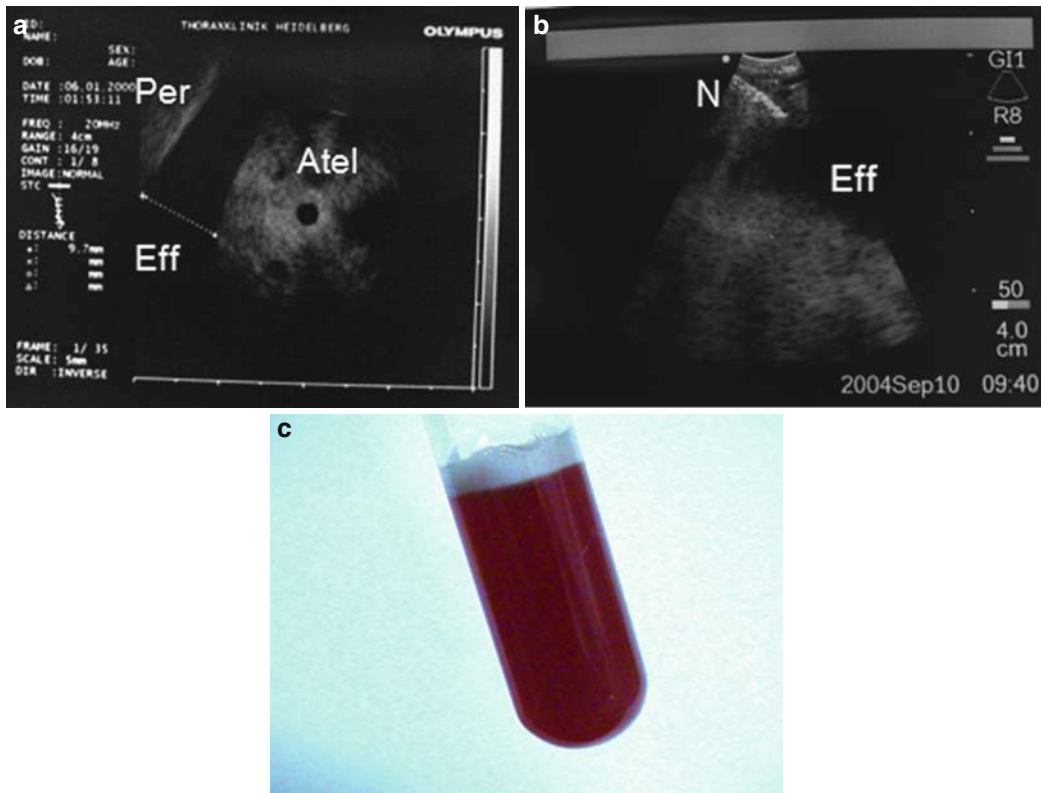
Fig. 5.13. Pleural effusion and transbronchial thoracocentesis. On the radial ultrasound image the atelectatic lung is surrounded by pleural effusion (**a**). If the pleural fluid is surrounding the central airways it can be tapped by transbronchial needle aspiration, which is best performed by the ultrasonic endoscope (**b**). The sanguinolent fluid contained cells of adenocarcinoma (**c**).

5. EBUS in Therapeutic Bronchoscopy

In our institution approximately 20 percent of all procedures are performed for therapeutic interventions. In 48 percent of these ultrasound provides useful additional information, which has strategic importance for planning the procedure in 43 percent of cases *(18)*. Exploration of central airway stenoses with EBUS in order to assess the cause and extent of a lesion and its relation to surrounding structures is helpful in making a decision on the appropriate technique – e.g., mechanical dilation, laser or argon plasma coagulation and stenting – and for controlling the effect during follow-up (**Figs. 5.14, 5.15, 5.16, 5.17**). Before resecting granulomas and scars, evaluation of the wall and vascularization is important to avoid perforation and bleeding.

As described before, local staging of small cancers in preparation for bronchoscopic therapy has become essential. Complications in healing of anastomoses after bronchoplastic procedures can be difficult to diagnose by bronchoscopy alone. Edema, superficial necrosis and beginning dehiscence can be differentiated by EBUS and it is especially useful to detect involvement of the adjacent pulmonary artery by localized abscess formation in order to indicate prophylactic surgical repair, before hemoptysis signals a fatal hemorrhage.

6. EBUS in Pediatric Bronchoscopy

EBUS is also useful in pediatric bronchoscopy since conventional radiological imaging in these patients can be even less reliable due to the smaller organs, motion artifacts and restrictions with regard to radiation exposure. In 412 children (3% of our population) with a median age of 4.2 years that we examined in an observation period between January 1998 and December 2001, EBUS was applied in 140 cases (34%), with almost equivalent frequency as in adults (**Fig. 5.18**). The indications were analysis of structures in stridor and intermittent dyspnea which, particularly in this age, can be caused by vascular malformations, especially pulmonary sling syndrome. We diagnosed 11 of these cases by EBUS, some even after radiological diagnosis failed. Solid lesions, perforating lymph nodes, atelectasis and pneumonia were other indications. Children tolerated the procedure as well as adults and it did not take any longer *(28)*.
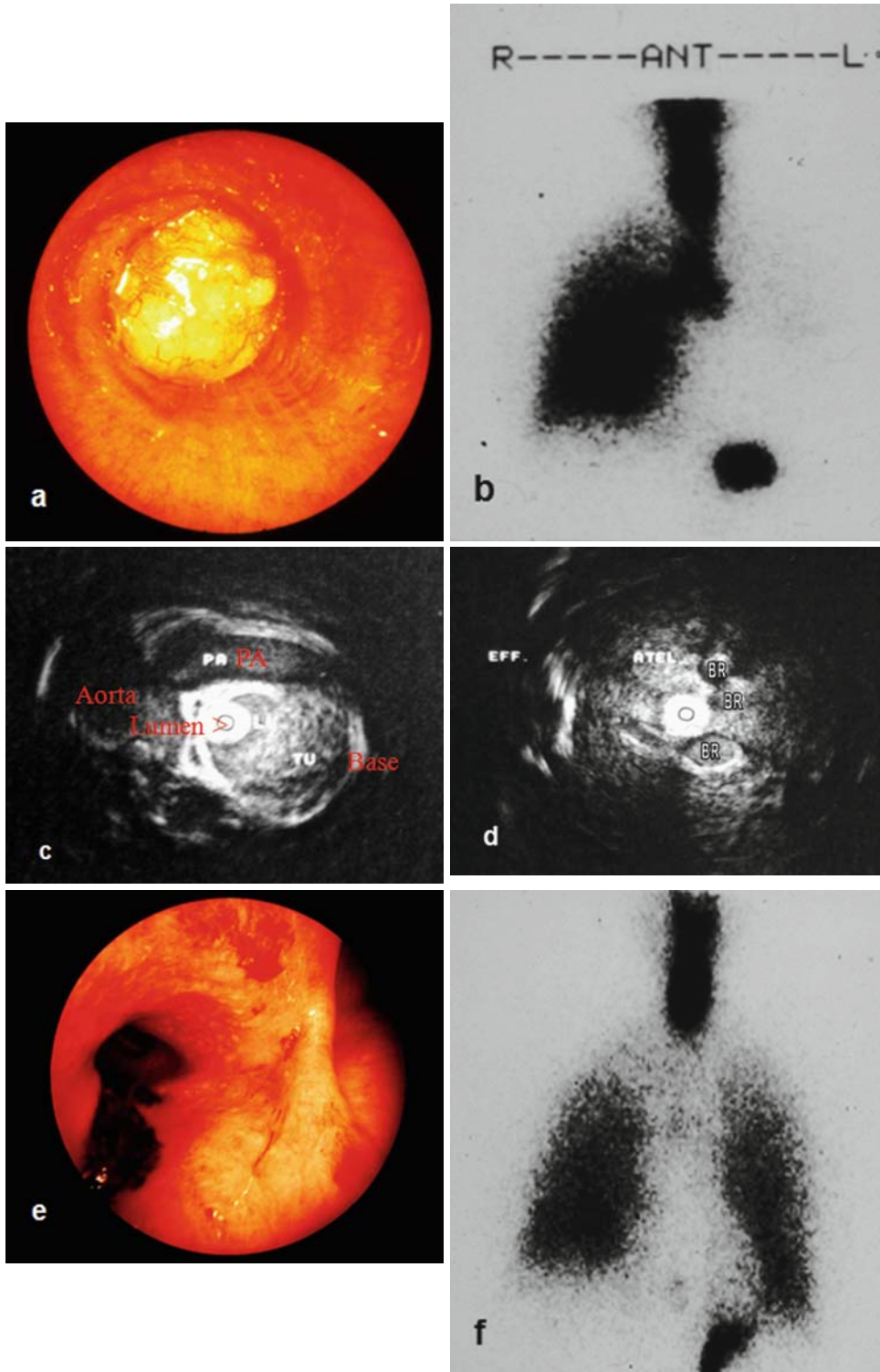
Fig. 5.14. Endobronchial ultrasound for intervention. A patient with complete tumor obstruction of the left main bronchus (**a**) has a loss of perfusion and ventilation on his left lung (**b**). Radial ultrasound shows a polypiod tumor with the base
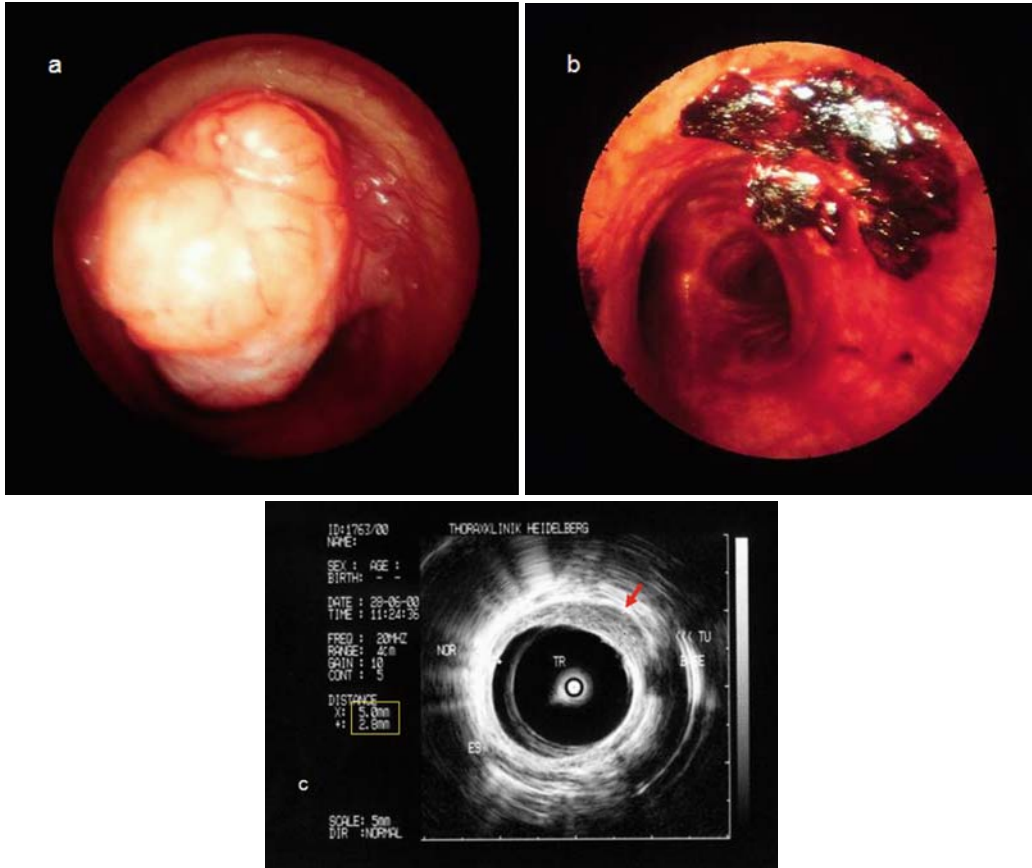
Fig. 5.15. Adenoid cystic carcinoma of the trachea. The pedunculated tumor is attached to the right lateral wall of the trachea (**a**). After combined mechanical and laser resection only flat carbonized residuals remain (**b**). However, ultrasound shows extensive tumor residuals within the wall. The thickness is 5 mm as compared to the normal contralateral side with 2.8 mm (**c**).

7. Training and Learning Curve for EBUS

Compared to other bronchoscopic techniques, EBUS takes considerably longer to learn and apply. This is primarily due to the fact that pulmonologists are becoming exposed to ultrasound technology and interpretation of images only very recently. Secondly, considerable skill is needed to handle the fragile radial scanning

Fig 5.14. (continued) medially and the surface laterally. The probe is inserted via the stenosis through the remaining lumen. The pulmonary artery (PA) is reduced in diameter and the flow is sluggish, but it is not obstructed (**c**). Thus after resection the lung will be perfused. Further passage of the stenosis shows fluid filled, but otherwise patent bronchi (BR) in the lower lobe atelectasis, surrounded by pleural effusion (EFF) (**d**). After laser resection the ventilation is restored (**e**) and perfusion and ventilation are restored (**f**).
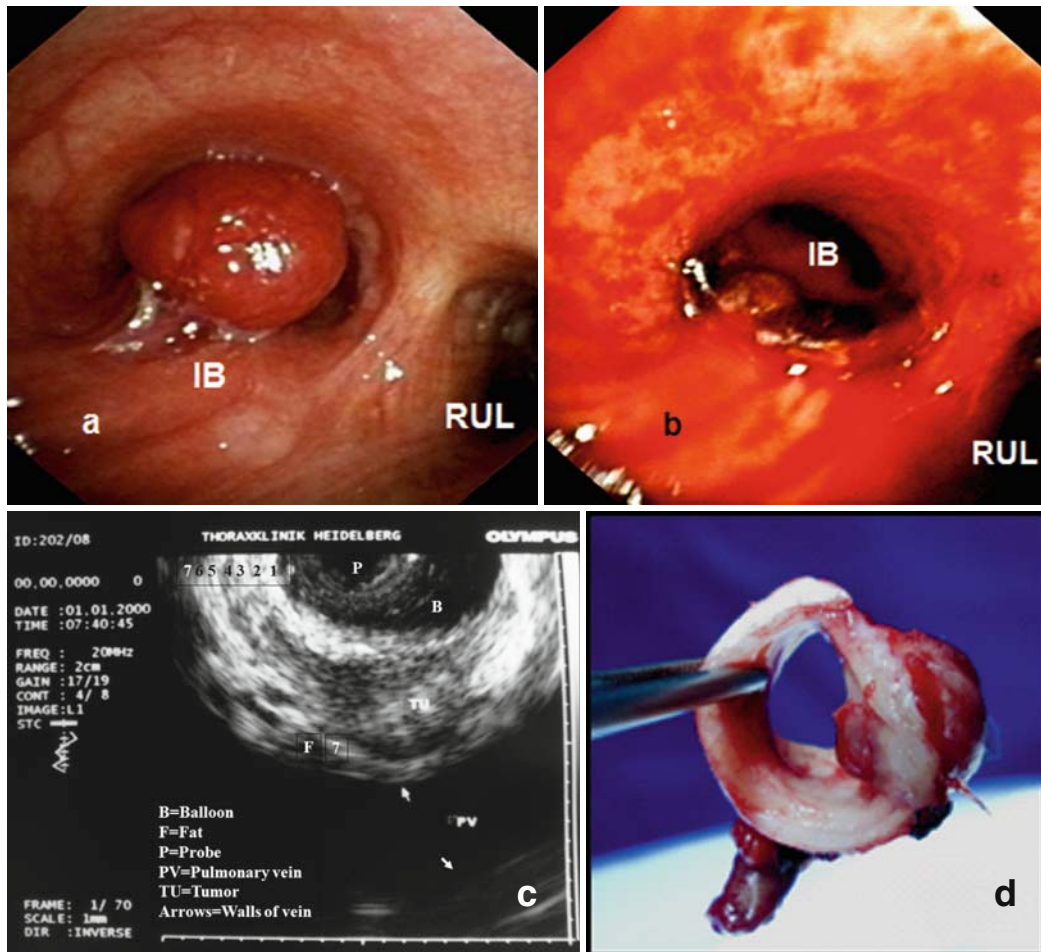
Fig. 5.16. Carcinoid tumor. A pedunculated tumor is located on the dorsal wall of the intermediate bronchus (**a**). Laser resection looks radical (**b**), but ultrasound reveals intramural residuals that are covered by connective tissue on the outside (**c**), which is demonstrated on the resection specimen (**d**, courtesy of Dr. Michael Klopp).

miniprobe. This is all the more demanding as for imaging the time that the airways can be occluded by the balloon probe is usually restricted and, especially when performed under local anesthesia, the procedure may be repeatedly interrupted for re-oxygenation. And lastly, as was described dealing with the anatomy, orientation within the complex mediastinal structures is difficult. These are the reasons why it has been some time before EBUS became accepted and more widely distributed. It was only with the introduction of the linear ultrasonic bronchoscope, a more familiar instrument than the radial probe, that use of EBUS is now spreading with increasing speed worldwide and has become "...the highest impact technology in 2007". *(29)*

In our experience, after instruction through reading, lectures and digital media, hands-on training is essential. This initial exposure can be achieved in training courses that usually last one or two
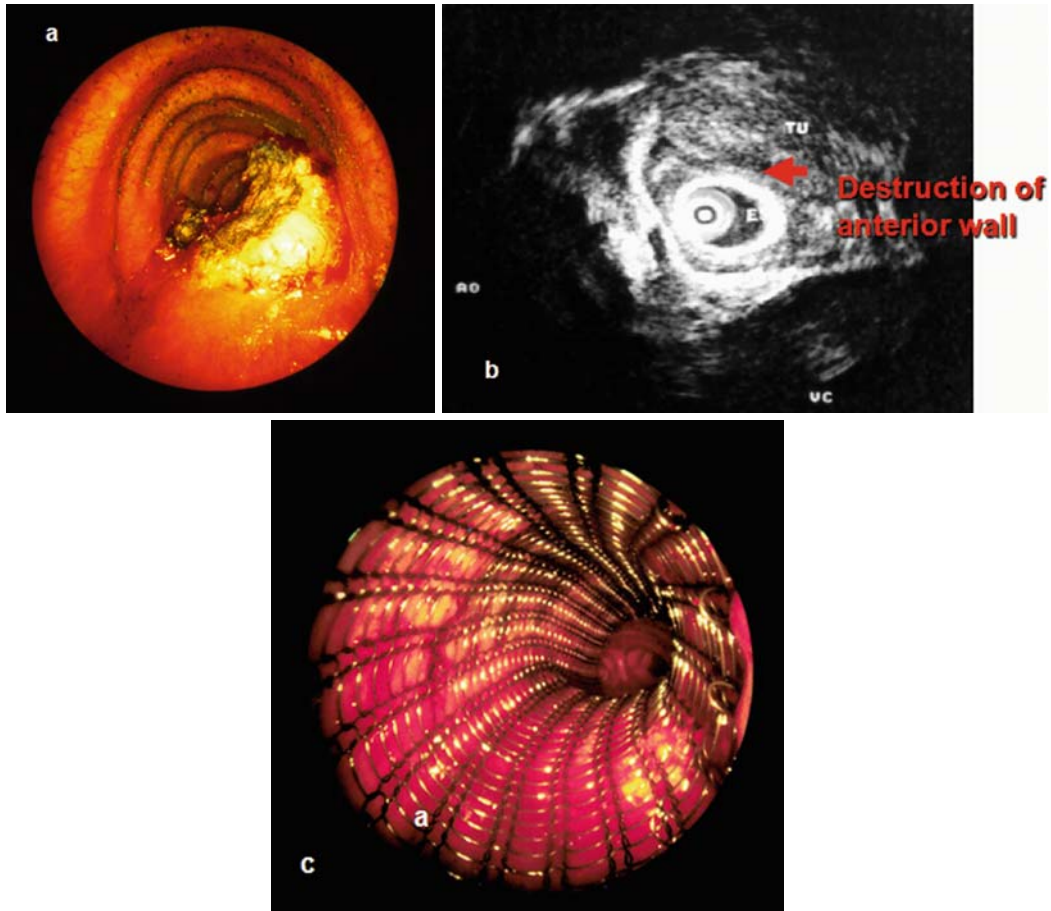
Fig. 5.17. Primary squamous cell cancer of the trachea. After partial resection for restoration of the lumen (**a**) endobronchial ultrasound shows deep infiltration of the dorsal wall and infiltration of the anterior wall of the esophagus (**b**). Because of risk of creating an esophago-tracheal fistula by further resection a stent is placed before radiotherapy (**c**).

days. However, after this more extensive experience, more detailed insight is necessary. Depending on the primary experience, usually at least one week of observation in a dedicated training center is useful to gain anatomical orientation and become familiar with image interpretation. Posters illustrating the mediastinal anatomy and the corresponding ultrasound images, including the location of lymph nodes, are available for this purpose, and digital media (CDs and DVDs) are available for interactive learning. This must be intensified through personal practical experience with patients, for which approximately 50 procedures are necessary. According to Falcone, et al. *(30)*, 20 procedures are necessary for image interpretation, and sufficient experience was gained after 6–24 months, depending on the frequency of examinations, illustrating the difficulty of this method as compared to other techniques.
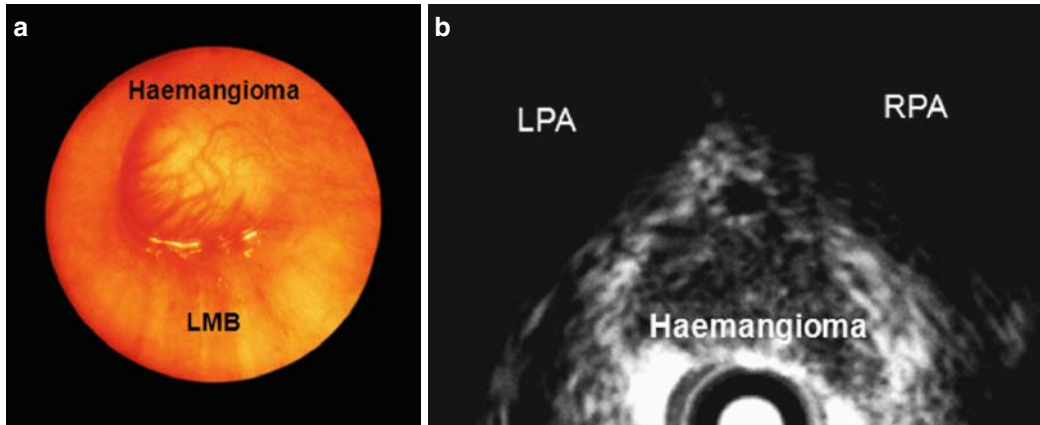
Fig. 5.18. Hemangioma of left main bronchus. In this 4 year old girl the left main bronchus is obstructed by a moderately vascularized mass (**a**). Ultrasound shows a highly vascularized mass limited within the bronchial without contact to the pulmonary arteries (**b**). The lesion was removed by isolated segmental resection of the left main bronchus and reanastomosis without loss of lung tissue.

Developing interactive virtual training models could be very efficient in shortening the learning curve, since currently neither training on phantom models nor in animal models is capable of replacing experience in real patients.

8. Future Prospects

As EBUS spreads worldwide it is beginning to replace other methods. These include staging of early lung cancer and TBNA. Currently the ultrasonic endoscope is attracting wide attention, as the technique is more similar to what bronchoscopists are accustomed to handling. However, it should be borne in mind that both methods are complementary rather than competitive. Exploration by 30 MHz probes might become useful in viewing the small mucosal vessels in bronchoplastic procedures, inflammation and neoplasia. Special processing algorithms and elastography could be useful for tissue characterization. Combination with electromagnetic navigation (**Fig. 5.19**) is improving our means for diagnosis and treatment of peripheral lesions, including radio frequency ablation and injection of chemotherapeutic agents besides brachytherapy, and tumor response can be assessed by computer analysis of images. The role of EBUS in local staging of early cancers that will be detected by screening programs has been described. Also in screening programs for peripheral lesions by low dose spiral CT EBUS will play an important role as a large number of these lesions are benign and
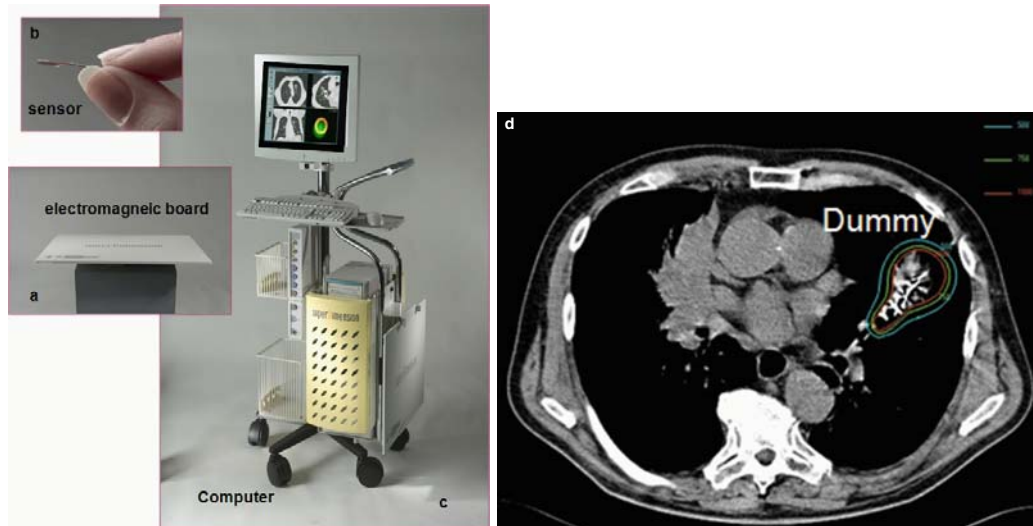
Fig. 5.19. Combination with electromagnetic navigation. The superDimension system consists of a electromagnetic board (**a**), a sensor that is introduced via a catheter as extended working channel (EWC) and can be located within the magnetic field (**b**), and a processor that displays the sensor's position inside the patient in projection on the patient's CT on the monitor (**c**). Afterwards a brachytherapy catheter can be inserted and left in place for potentially curative treatment if the lesion's diameter is well within range of a curative dosage as calculated from the isodose lines by insertion of a dummy probe (**d**).

do not need interventions. Ultrasound might also be applied for tissue destruction as its inherent energy can be focused in high intensity focused ultrasound (HIFU) and transformed into heat. As the EBUS image changes with water content of the tissue, computed analysis of changes in impendence could serve as a control for treatment effectiveness. The same could be applied to transmural treatment of mediastinal lesions after localization by the radial probe or under direct vision via the channel of the ultrasonic bronchoscope.

In conclusion, EBUS is currently complementing and, in some respects, begins to replace other technologies. By applying EBUS, diagnostic and therapeutic decisions can be made immediately during bronchoscopy without further time consuming and costly procedures. As has been shown by the introduction of the ultrasonic bronchoscope, interest in this new technique has increased significantly, and we are currently observing the beginning, rather than the end, of a development that will provide an ever-increasing range of instruments and applications.

References

1. Becker, HD. EBUS – A New Dimension in Bronchoscopy. Editorial. Respiration 2006; 73:583–586.

2. Koga T, Ogata K, Hayashida R, Hattori R. Usefulness of transluminal ultrasonography in the evaluation of bronchial stenosis

secondary to tuberculosis. J Jpn Soc 1994; 16:477–482.

3. Frank N, Holzapfel P, Wenk A. Neue Endoschall Minisonde in der täglichen Praxis. Endosk Heute 1994;3:238–244.

4. Becker HD. Endobronchial Ultrasound with Miniprobe Radial Scanning. in: CF Dietrich (ed). Endoscopic Ultrasound – an Introductory Manual and Atlas. Thieme, Stuttgart-New York, 2006, 334–351.

5. Hürther T, Hanrath P. Endobronchial sonography in the diagnosis of pulmonary and mediastinal tumors. Dtsch Med Wochenschr 1990;115:1899–1905.

6. Hürther T, Hanrath P. Endobronchial sonography: feasibility and preliminary results. Thorax 1992;47:565–567.

7. Kurimoto N, Murayama M, Yoshioka S, et al. Assessment of usefulness of endobronchial ultrasonography in determination of depth of tracheobronchial tumor invasion. Chest 1999;115:1500–1506.

8. Miyazu Y, Miyazawa T, Kurimoto N, Iwamoto Y, Kanoh, K Kohno N. Endobronchial ultrasonography in the assessment of centrally located early-stage lung cancer before photodynamic therapy. Am J respir Crit Care Med 2002;165:832–837.

9. Netter FH. The Ciba collection of medical illustrations. Respiratory system. CIBA-GEIGY Corporation, Ardsley, N.Y. 1979, 23.

10. Shirakawa T, Miyazawa T, Becker HD. The Layer Structure of Central Airways as Described by Endobronchial Ultrasonography (EBUS). J Bronchol 2008;in press.

11. Becker HD. Bronchoscopy for Airway Lesions in: Wang K.P. and A.C.Mehta (eds.) Flexible Bronchoscopy. Blackwell Scientific Publications, 1995, S.136-159.

12. Omori S, Takiguchi Y, Hiroshima K, Tanabe N, Tatsumi K, Kimura H et al. Peripheral pulmonary diseases: evaluation with endobronchial US; initial experience. Radiology 2002;24:603–608.

13. Herth F, Becker HD, Manegold C, Drings P. Endobronchial ultrasound (EBUS): assessment of a new diagnostic tool in bronchoscopy for staging of lung cancer. Onkologie 2001;24:151–154.

14. Becker HD. Options and results in endobronchial treatment of lung cancer. Minim Invasive Ther Allied Technol 1996;5:165–178.

15. Herth F, Ernst A, Schulz M, Becker HD. Endobronchial ultrasound reliably differentiates between airway infiltration and compression by tumor. Chest 2003;123: 458–462.

16. Herth FJ, Becker HD, Ernst A. Ultrasound – guided transbronchial needle aspiration: an experience in 242 patients. Chest 2003; 123:604–607.

17. Herth FJ, Ernst A, Becker HD. Endobronchial ultrasound-guided transbronchial lung biopsy in solitary pulmonary nodules and peripheral lesions. Eur Respir J 2002;20: 972–974.

18. Herth FJ, Becker HD, LoCocero J III, Ernst A. Endobronchial ultrasound in therapeutic bronchoscopy. Eur Respir J 2002;20: 118–121.

19. Mountain CF. Revisions in the international system for staging lung cancer. Chest 1997; 111:1710–1717.

20. Naidich DP. Staging of lung cancer. Controversy: computed tomography versus bronchoscopic needle aspiration: pro computed tomography. J Bronchol 1996;3:73.

21. Herth F, Becker HD, LoCicero J, Ernst A. Endobronchioal ultrasound improves classification of suspicious lesions detected by autofluorescence bronchoscopy. J Bronchol 2003;10:249–252.

22. Becker HD. Endobronchial ultrasound: a new perspective in bronchology. J Ultraschall Med 1996;17:106–112.

23. Becker HD. The role of endobronchial ultrasound (EBUS) in: diagnosis and treatment of centrally located early lung cancer. In: Hirsch FR, Bunn Jr PA, Kato H, Mulshine L (eds). Textboook of Prevention and detection of Early Lung cancer. Taylor and Francis, London and NewYork, 2006, 161–175.

24. Lam S, Becker HD. Future diagnostic procedures. Chest Surg Clin N Am 1996;6: 363–380.

25. Becker HD, KayserK, Schulz V, Tuengerthal S, Vollhaber H-H. Atlas of Bronchoscopy. Technique, Diagnosis, Differential Diagnosis, Therapy. B.C. Decker, Inc., Philadelphia – Hamilton, 1991.

26. Kurimoto N, Murayama M, Yoshioka S, Nishisaka T. Analysis of the internal structure of peripheral pulmonary lesions using

endobronchial ultrasonography. Chest 2002; 122:1887–1894.

27. Becker HD, Herth F, Shirakawa T. Computer assisted analysis of endosonographic images of solitary pulmonary nodules (SPN). Eur Respr J 2001;20:462.

28. Link B, Liman YST, Becker HD, Dienemann H. Endobronchial juvenile hemangioma in infancy: removal by main bronchus cuff resection. Chirurg 2001; 72:584–587.

29. Kovitz K. Literature Review. Lecture at the Meeting of the American Association for Bronchology, Chicago, Oct. 2007.

30. Falcone F, Fois F, Grosso D. Endobronchial ultrasound. Respiration 2003;70:179–194.
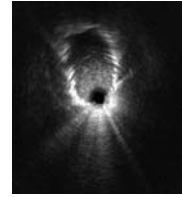
Endobronchial Ultrasound in Therapeutic Bronchoscopy

Felix J.F. Herth

Many abnormalities that require bronchoscopy arise from the airway wall and parabronchial structures *(1)*. There was a need to expand the view of the endoscopist beyond the confines of the mucosal wall *(2)*.

There is evidence that radial endobronchial ultrasound (EBUS) is superior to a conventional computed tomography scan of the lung in evaluating the tracheal and bronchial wall structures, and the parabronchial space *(3)*. It could serve as an ideal tool for evaluating airway wall anatomy and related tumor pathology *(4, 5)* (**Fig. 6.1a,b**).

Also the assessment of preoperative tracheobronchial invasion in case of cancer is important to select the best treatment, including surgery, chemo- and radiochemotherapy, and to predict prognosis. It is important to establish the extent of tumor spread to determine whether cancer has invaded beyond the airways adventitia *(6)*.

However, as for example in case of early lung cancer, the general imaging procedure, chest computed tomography (CT), is often not helpful since it cannot delineate the layers of the airway wall *(7)*. Therefore, it is important to correctly assess the absence/presence and depth and extent of invasion, as well as the attached length of cancer with tracheobronchial invasion pretherapeutically.

Therapeutic bronchoscopy is coming of age. Numerous procedures such as laser resection, argonplasma coagulation (APC), electrosurgery, cryotherapy, brachytherapy, photodynamic therapy (PDT) and stenting are now available to the endoscopist. With all these options, sometimes there is a question of what intervention is best to use on an individual patient. This is especially true in
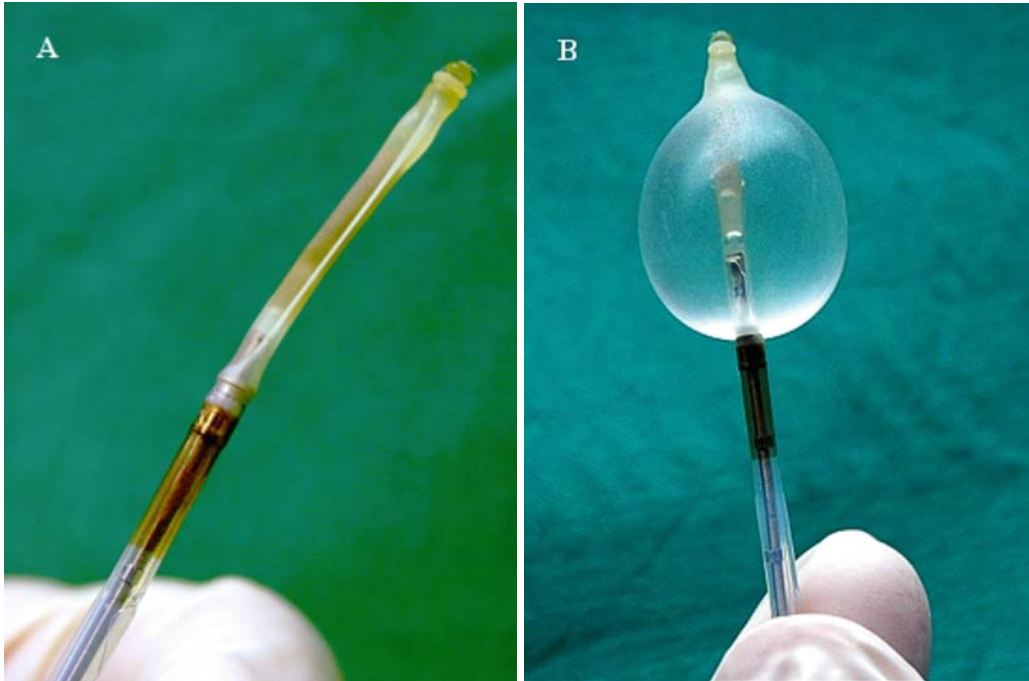
Fig. 6.1. Radial EBUS systems. (**A**) Miniature radial probe (**B**) Miniprobe with water-filled balloon.

bronchoscopic treatment of malignant tumors with curative intent such as PDT or endoluminal high-dose radiation (HDR). In these lesions, it is important to ensure that tumor growth is restricted to the bronchial wall *(4, 5)* in order to achieve a good and lasting result.

Since commercial ultrasound devices have been available for several years, this chapter will explain where experience with radial endobronchial ultrasound may be a beneficial and unique adjunct to therapeutic bronchoscopy.

1. Radial EBUS for Early Cancer Staging

With a number of recent technical developments and the availability of new instruments, the diagnosis and therapy for early-stage lung cancer have improved considerably *(8)*. Other than surgical resection, PDT or HDR may be one of the endoscopic approaches for early-stage lung cancer at this time *(9)*.

It has been confirmed that both techniques had curative potential in patients with centrally located early-stage lung cancer *(9, 10)*. Many criteria in selecting the appropriate candidates for curative intent of HDR/PDT have been reported. Bronchoscopic

diagnosis is accepted as one of the most important criteria *(11)*, based on statistical data indicating that lesions less than 1.0 cm have a high likelihood of achieving complete remission (CR) after PDT.

However, local recurrences or subsequent metastases can develop in patients with early-stage lung cancer who achieved a CR with HDR/PDT *(10, 12)*, and thus the incidence of long-term remission has been reported to be as low as 30 percent to 50 percent *(13, 14)*. Because tumors confined to the mucosa and submucosa rarely have lymph node metastases, and because laser beams cannot penetrate the exterior wall of the cartilage, it is important for the tumor to be confined within the mucosa and submucosa for successful endoscopic treatment.

Hence, improving the assessment of the depth of the tumor invasion into the bronchial wall will likely improve the quality and efficacy of techniques. Radial EBUS is a useful adjunct for this purpose *(4, 5)*.

In the bronchial system, the normal layered structure of the bronchial wall of the central airway as it appears under EBUS has been reported *(15)* (**Fig. 6.2a,b, Table 6.1**), making it possible to evaluate the depth of tumor invasion. In contrast to radiological imaging, EBUS allows even very small tumors of a few millimeters to be analyzed (**Fig. 6.3**). As Kurimoto, et al. *(16)* demonstrated EBUS is a very reliable tool for analyzing the extent of these small lesions. Herth, et al. *(17)* demonstrated that using EBUS assessment in small autofluorescence-positive lesions that were negative in white light bronchoscopy improved specificity (predicting malignancy), which rose from 50 to 90 percent. Combining EBUS with autofluorescence has proved efficient in prospective studies and has become the basis for curative endobronchial treatment of malignancies in some institutions.
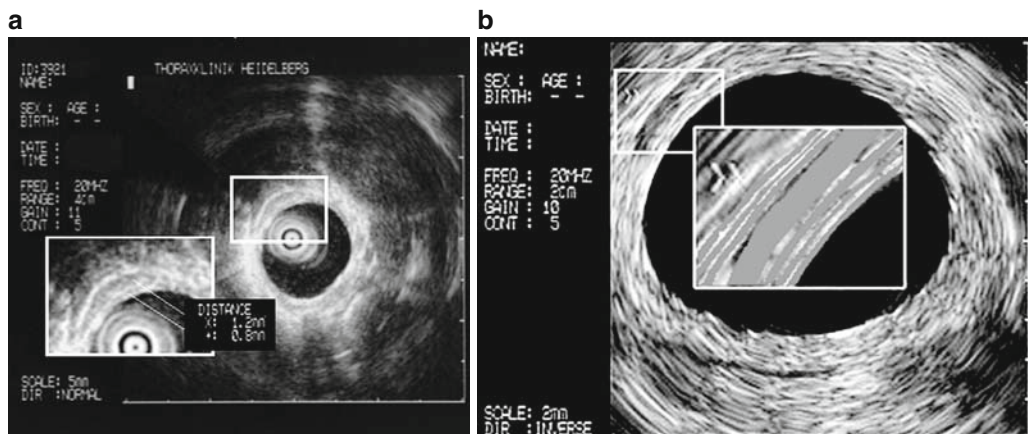
Fig. 6.2. **(a)** EBUS image of a normal tracheal wall. **(b)** EBUS image of a normal tracheal wall, in the enlarged part the different layer as described in Table 6.1 are shown.

Table 6.1
Sonographic layers of the tracheobronchial wall

Sonographic layers of the tracheobronchial wall

	Layer	Echo	Finding
Tracheobronchial tree	1st	hyperechoid	marginal echo (balloon and mucosa)
	2nd	hypo/ isoechoid	submucosa (intrapulmonary bronchi) or submucosal smooth muscle (extrapulmonary bronchi and trachea)
	3rd	hyperechoid	inner margin of the cartilage (endochondrium)
	4th	hypoechoid	Cartilage
	5th	hyperechoid	outer margin of the cartilage (perichondrium)
	6th	hypoechoid	supporting loose connective tissue
	7th	hyperechoid	Adventitia
Pars membranacea	1st	hyperechoid	marginal echo (balloon and mucosa)
	2nd	hypoechoid	smooth muscle
	3rd	hyperechoid	adventitia
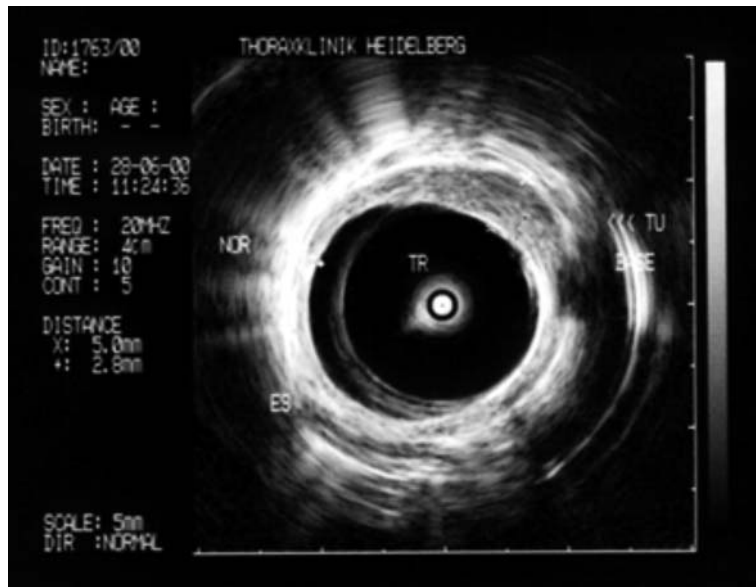
Fig. 6.3. Tumor (TU) disruption of the normal (NOR) multilayer structure of the bronchial wall in the trachea (TR), Esophagus (ES).

In the largest series Miyazu, et al. *(18)* reported the value of EBUS in selecting appropriate candidates with centrally located early-stage lung cancer for photodynamic therapy (PDT) with curative intent. In patients considered to be appropriate candidates for PDT by conventional bronchoscopy and high-resolution computed tomography, they performed EBUS before PDT biopsy-proven squamous cell carcinomas. Lesions were diagnosed even as intracartilaginous by EBUS and subsequently PDT was performed (**Fig. 6.4**). Long-term complete remission had been achieved in these patients with a median follow-up term of 32 months after PDT. The remaining lesions were diagnosed as extracartilaginous by EBUS and were considered candidates for other therapies such as surgical resection, chemotherapy, and radiotherapy (**Fig. 6.5**). The depth of tumor invasion estimated by EBUS was proven to be accurate by histopathologic findings in a couple of specimens after surgical resection. Using the EBUS findings as a decision maker, Miyazu, et al. achieved a 100 percent complete remission rate in the endoluminal-treated group. At a mean follow-up of 32 months, none of the patients have had a recurrence.
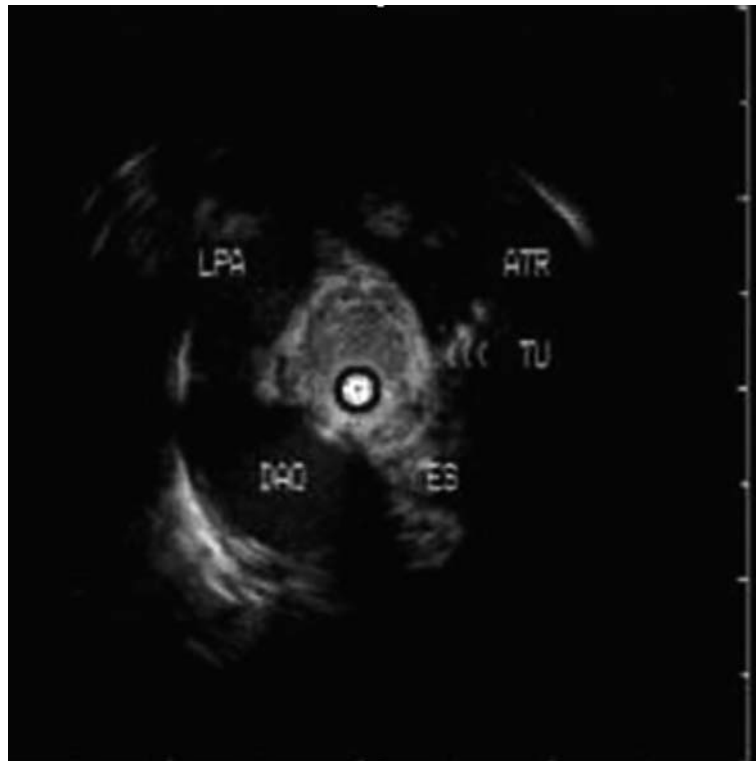
Fig. 6.4. Small, radiological invisible tumor (Tu) in the distal left main bronchus. In the 360° view, also the left atrium (ATR), the left pulmonary artery (LPA), the descending aorta (DAO) and the esophagus (ES) is visible.
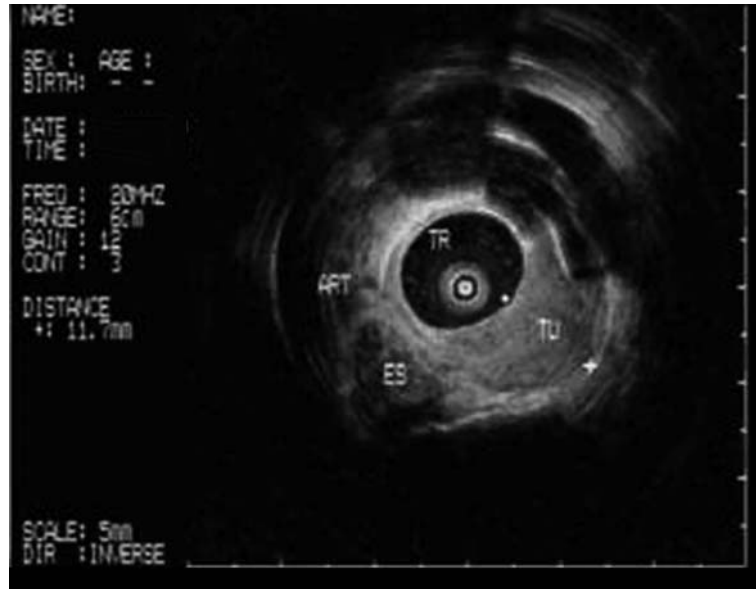
Fig. 6.5. A small, distal Tracheatumor (Tu) is invading the parabronchial space. Based on the extracartilaginous tumor grow, an endoscopic treatment is not effective. (ES = Esophagus, Art = artefact, Tr = trachea).

Earlier published trials using endoluminal techniques in early cancer lesions without EBUS assessment showed a significant failure and recurrence rate. Apparently, adding EBUS to the airway assessment in patients with presumed carcinoma in situ significantly increases the likelihood of identifying the patients best treated by endoluminal therapy.

2. Radial EBUS for Interventional Bronchoscopy

In the meantime, therapeutic bronchoscopy is an established treatment option. Numerous procedures such as laser resection, argon plasma coagulation (APC), electrosurgery, cryotherapy, and stenting are available to the endoscopist *(19)*.

With all these options, sometimes there is a question of what intervention is best to use on an individual patient. Many abnormalities leading to the need for interventional bronchoscopy arise from the airway wall and parabronchial structures *(2)*.

Radial EBUS is an addition to the bronchoscopist's diagnostic armamentarium *(20)*.

Its properties enable excellent visualization of the bronchial wall and structures surrounding the airways and, as such, add significant potential to therapeutic bronchoscopies (**Fig. 6.6**).
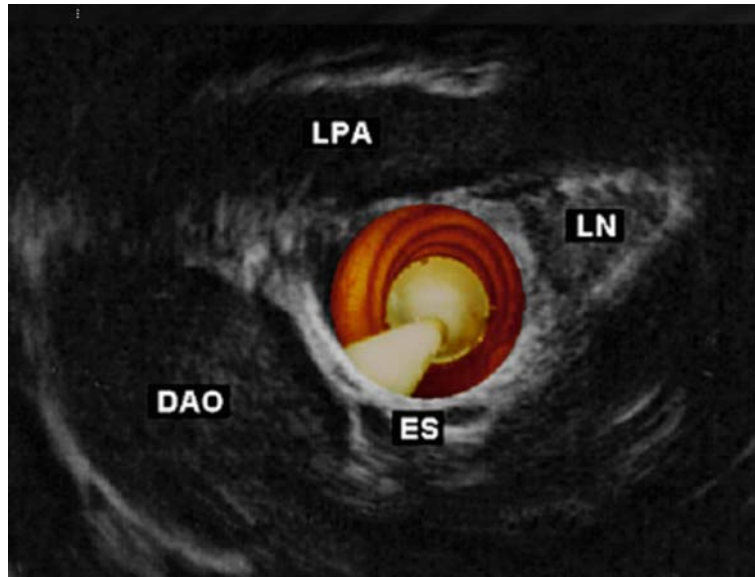
Fig. 6.6. Animation of the 360° view of a normal parabronchial space (LPA = left pulmonary artery, DAO = descending aorta, ES = esophagus, LN = Lymph node).

EBUS provides important data to consider when determining endobronchial therapy of advanced lung cancer. In complete bronchial obstruction the basis and surface of the tumor can be assessed, as well as whether the different layers of the bronchial wall are involved, how far the tumor is penetrating into the mediastinal structures and whether the airways beyond the stenosis are patent. Also, patency of the adjacent pulmonary artery can be diagnosed, which is important to predict post-interventional perfusion of the dependent lung and prevent increase of dead space ventilation (21). EBUS is also useful for exploring benign central airway stenosis to assess the extent and cause of the disease, the relationship to vessels and other surrounding structures and to make the correct decision for therapy, like mechanical dilatation, laser ablation or stent implantation and endoscopic control of the results (22).

In a large series (23) using EBUS guidance for therapeutic airway procedures was described. Within three years a total of 2,446 therapeutic bronchoscopies were performed. In 1,174 cases EBUS was used (29% mechanical tumor debridement, 20% airway stenting, 13% Neodymium:yttrium aluminium gamet [Nd:YAG] laser use, 23% argon plasma coagulation, 11% brachytherapy, 2% foreign body removal and 2% endoscopic abscess drainage). Adding EBUS to conventional bronchoscopy changed the planned intervention in 43 percent of cases. The changes ranged from altering stent sizes to guiding tumor debridement. As EBUS affords a better assessment of the airway wall, longer stents were frequently chosen when submucosal infiltration was noted. This is not often appreciated by regular bronchoscopy.

A complication feared by interventionalists when using laser debridement in the airways is bleeding through neighboring vessels or fistula formation. Since EBUS allows for exact determination of tumor penetration through the airway wall and vessels are well-visualized, debridement can be halted when nearing critical structures. As a result, neither fistula formation nor fatal bleeding was observed in this population *(23)*.

Obviously, not every therapeutic intervention requires the use of EBUS, as the information achieved may not be helpful. Skilled endoscopists currently use it in all cases of total airway obstruction before and during thermal tumor destruction, as well as in all brachytherapy and PDT applications for planning purposes.

So, it seems that radial EBUS changed or guided therapeutic decisions during therapeutic bronchoscopic procedures in a substantial number of cases. As this may result in better outcomes, it has become a standard adjunct in many centers *(24, 25)*.

Also, with the convex EBUS, unexpected findings can be discovered. Life threatening central pulmonary embolism (PE) is defined as a thrombotic occlusion of the pulmonary trunk or of a main or lobar pulmonary artery (**Fig. 6.7**). These vessels accompany the trachea, the main and lobar bronchi at a distance of less than 5 mm. Chest CT enhanced with I.V. contrast (Angio CT) has become the principal imaging modality to evaluate suspected, central PE. In a feasibility trial *(26)* the value of discovered PE via EBUS was described. In 32 consecutive patients with Angio CT documented central PE we detected 97 of 101 emboli in the central PAs via EBUS corresponding to a sensitivity rate of 96 percent and specificity rate of 100 percent. It seems that convex EBUS can also detect central pulmonary arteries (PA) and might be influence the bronchoscopic proceeding.
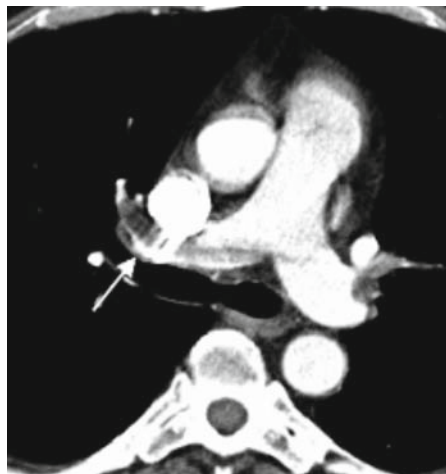
Fig. 6.7a. Angio CT: Incomplete occlusion of the upper lobe artery on the right side.

Fig. 6.7b. EBUS: Incomplete occlusion of the upper lobe artery on the right side with color power doppler.

3. Radial EBUS for Staging

Lung cancer is a common disease, and exact staging is of extreme importance in order to plan therapy and assess patients for potentially curative surgical resection *(27)*. A frequent problem in assessing the extent of tumor spread is the question of infiltration versus compression of central airways by central tumors *(28)*. Using chest CT as the general imaging procedure of choice is often not helpful with this question *(29)* as it cannot delineate the layers of the airway wall. Regular bronchoscopy also cannot reliably identify intramural disease and differentiate it from external compression. Patients in this situation often require surgical exploration to establish final staging and may find themselves non-surgical candidates who had to undergo surgical procedures in order to establish this fact.

EBUS allows detailed analysis of intraluminal, submucosal and intramural tumor spread which can be essential to determine resection margins. EBUS proved especially useful in diagnosing mediastinal tumor involvement like the great vessels such as Aorta, Cava, main pulmonary arteries and of the esophageal wall, which is frequently impossible to achieve through conventional radiology *(30)*.

In a trial *(31)* it was shown that differentiating external tumor invasion from impression of the tracheobronchial wall by EBUS is highly reliable (94%) in contrast to CT imaging (51%). One-hundred-four patients with central tumors were examined with EBUS and CT and classified into invasion or impression. All patients underwent surgery; the findings were compared to the initial classification. The sensitivity (89–25%) and specificity (100–89%)

show the superiority of the ultrasound technique in differentiating between airway infiltration and compression by tumor. Thus many patients considered to be nonresectable by the radiologist due to supposed T4 tumors could undergo curative surgery after EBUS (**Fig. 6.8a,b**). During preoperative staging, EBUS allows detailed analysis of intraluminal, submucosal, and intramural tumor spread, which can be essential for decisions on resection margins.
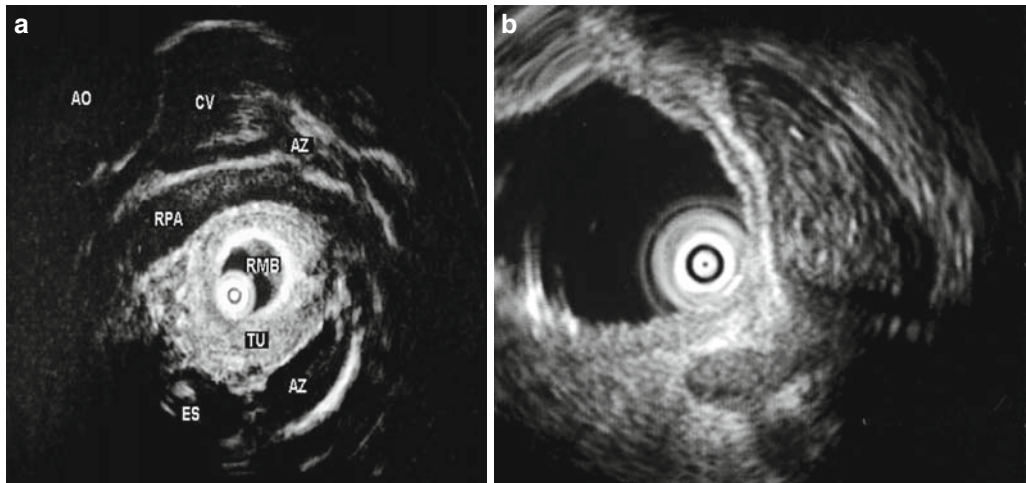
Fig. 6.8. **(a)** Tumor(tu) invasion in the right main bronchus (RMB). (CV=Vena cava, AO0 Aorta, RPA=right pulmonary artery, AZ=Vena acygos, ES=esophagus), **(b)** Tumor in the right upper lobe. The EBUS shows normal bronchial wall, the tumor is respecting the tracheal wall.

Assessing preoperative tracheobronchial invasion is also important to select the best treatment, including surgery and radiochemotherapy, and to predict prognosis in patients with thyroid or esophageal cancer. For surgical planning, the choice of procedure is dependent on several variables, including patient age, histological type, and depth and extent of invasion (**Fig. 6.9**). It is important to establish the extent of tumor spread to determine whether thyroid or esophageal cancer has invaded beyond the tracheal adventitia *(32, 33)*.

Tsushima, et al. *(34)* performed a trial to compare the usefulness of CT, MRI and EBUS for the assessment of invasion of thyroid or esophageal cancer in cases with suspected tracheobronchial invasion. In cases with suspected contact between the tumor and tracheobronchial wall, CT, MRI and EBUS indicated deformity of the tracheobronchial wall due to the adjacent mass. The final diagnosis was based on surgical and histological results, and/or clinical follow-up. Fifty-four patients were included in this study.
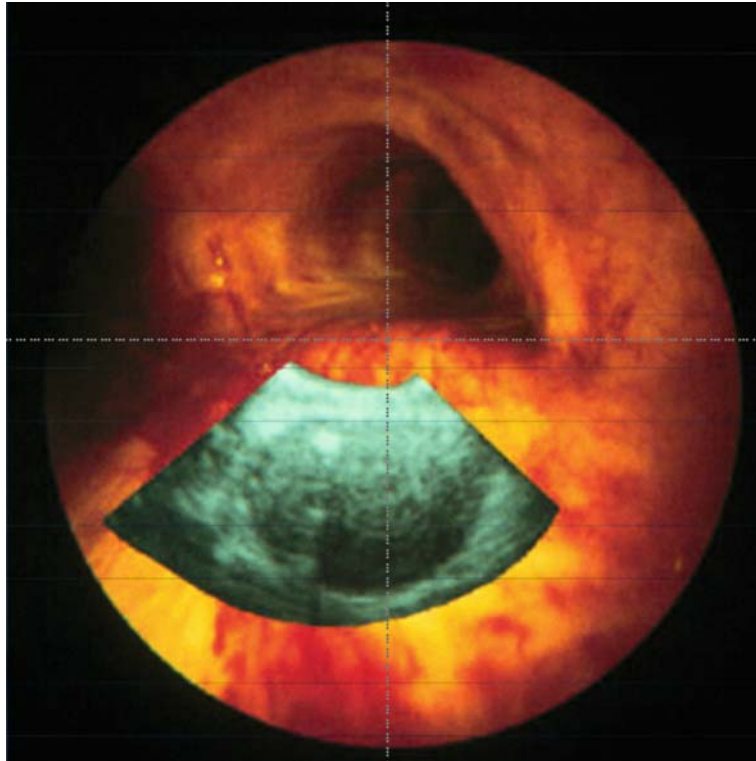
Fig. 6.9. Endoscopic image of the trachea. The elevated pars membranacea is seen, in the EBUS image the esophageal cancer is visible. The tumor respects the tracheal wall.

The sensitivity and specificity of CT, MRI and EBUS for invasion were 59 and 56, 75 and 73, and 92 and 83 percent. The accuracy of EBUS was significantly greater than that of CT and MRI.

Summary

EBUS seems to be the most useful technique for determining the depth and extent of tumor invasion into the airway wall. CT and MRI are useful to imaging techniques, and a combination of these procedures will be beneficial for surgical planning for patients with lung cancer, as well as esophageal and thyroid cancer.

Endobronchial ultrasound proved to be useful in high-resolution imaging of the multilayer structures of the bronchial wall and the adjacent mediastinal structures in a distance of up to 4 cm. In many instances it was superior for staging of lung cancer and other pathologies. Since the results of treatment of advanced bronchial carcinoma have been disappointing so far, detection

and treatment at early stages has gained new interest. Especially new methods like automated sputum cytology analysis in persons at risk and localization of radiologically and macroscopically invisible early carcinoma by fluorescence methods will be used more widely. Other pathologies such as vascular malformations, mediastinal masses, pathologies of neighboring organs and pulmonary lesions could also be correctly diagnosed. Thus we come to the conclusion that in the near future endobronchial ultrasound may play an important role in bronchology at feasible costs. Especially in on the spot decision making during diagnostic and interventional procedures it proved extremely useful.

References

1. Schreiber G, McCrory DC. Performance characteristics of different modalities for diagnosis of suspected lung cancer: summary of published evidence. Chest 2003; 123(1):115S–128S.

2. Herth FJF, Eberhardt R. The role of endobronchial ultrasound in diagnosis, staging and treatment. Therapy 2005; 2 (2): 223–228.

3. Herth F, Becker HD. Endobronchial ultrasound of the airways and the mediastinum. Monaldi Arch Chest Dis 2000; 55: 1, 36–45.

4. Falcone F, Fois F, Grosso D, Cinti C, Galetti S, Severino C. Endobronchial ultrasonography (EBUS): technique and learning curve. Giornale Italiano di echographia 2003; 6(2): 177–188.

5. Annema JT, Rabe KF. State of the art lecture: EUS and EBUS in pulmonary medicine. Endoscopy. 2006; 38(1):S118–S122.

6. Spira A, Ettinger DS. Multidisciplinary management of lung cancer. N Engl J Med 2004; 350: 379–392.

7. Sihoe AD, Yim AP. Lung cancer staging. J Surg Res 2004; 117: 92–106.

8. Sheski FD, Mathur PN. Endoscopic treatment of early-stage lung cancer. Cancer Control 2000; 7:35–44.

9. Moghissi K, Dixon K, Thorpe JA, Stringer M, Oxtoby C. Photodynamic therapy (PDT) in early central lung cancer: a treatment option for patients ineligible for surgical resection. Thorax. 2007; 62(5):391–395.

10. Vergnon JM, Huber RM, Moghissi K. Place of cryotherapy, brachytherapy and photodynamic therapy in therapeutic bronchoscopy of lung cancers. Eur Respir J. 2006; 28(1): 200–218.

11. Sutedja G, Postmus PE. Bronchoscopic treatment of lung tumors. Lung Cancer 1994; 11:1–17.

12. Kato H, Okunata T, Shimatani H. Photodynamic therapy for early stage bronchogenic carcinoma. J Clin Laser Med Surg 1996;14:235–238.

13. Nakamura H, Kawasaki N, Hagiwara M, Ogawa A, Kato H. Endoscopic evaluation of centrally located early squamous cell carcinoma of the lung. Cancer 2001;15:1142–1147.

14. Sutedja G, Golding RP, Postmus PE. High resolution tomography in patients referred for intraluminal bronchoscopic therapy with curative intent. Eur Respir J 1996; 9: 1020–1023.

15. Kurimoto N: Endobronchial Ultrasonography. Kinpodo, Kyoto, 2001:31–33.

16. Kurimoto N. M. Murayama, K. Morita et al. Assessment of usefulness of endobronchial ultrasonography in determination of depth of tracheobronchial tumor invasion. Chest 1999; 115:1500–1506.

17. Herth F, Becker HD. EBUS for early cancer detection. J Bronchol 2003; 10:249–253.

18. Miyazu Y, Miyazawa T, Iwamoto Y, Kano K, Kurimoto N: The Role of Endoscopic Techniques, Laser-Induced Fluorescence Endoscopy, and Endobronchial Ultrasonography in Choice of Appropriate Therapy for bronchial Cancer. J Bronchol 2001; 8:10–16.

19. Wahidi MM, Herth FJ, Ernst A. State of the art: interventional pulmonology. Chest. 2007; 131(1):261–274.

20. Herth F, Becker HD. Endobronchial Ultrasound (EBUS) – assessment of a new diagnostic tool in bronchoscopy. Onkologie 2001; 24:151–154.

21. Kurimoto N, Murayama M, Morita K, Kobayashi A, Uomoto M, Nishizaka T. Clinical applications of endobronchial ultrasonography in lung diseases. Endoscopy 1998; 30:8–12.

22. Irani S, Hess T, Hofer M, Gaspert A, Bachmann LM, Russi EW, Boehler A, Endobronchial ultrasonography for the quantitative assessment of bronchial mural structures in lung transplant recipients. Chest. 2006 Feb;129(2):349–355.

23. Herth F, Ernst A, Becker HD. Endobronchial ultrasound in therapeutic bronchoscopy. Eur Respir J. 2002 Jul;20(1):118–21.

24. Pungpapong S, Noh KW, Wallace MB. Endoscopic ultrasonography in the diagnosis and management of cancer. Expert Rev Mol Diagn. 2005; 5(4):585–597.

25. Shulman L, Ost D. Advances in bronchoscopic diagnosis of lung cancer. Curr Opin Pulm Med. 2007;13(4):271–277.

26. Aumiller J, Eberhardt R, Krasnik M, Herth FJF. Central pulmonary embolism diagnosed by real-time endobronchial ultrasound Eur Respir J 2007; 30(S51):S221.

27. Scott WJ, Howington J, Feigenberg S, Movsas B, Pisters K. Treatment of Non-small Cell Lung Cancer Stage I and Stage II: ACCP Evidence-Based Clinical Practice Guidelines Chest 2007; 132(33): 234–242.

28. Rivera MP, Mehta AC. Initial Diagnosis of Lung Cancer: ACCP Evidence-Based Clinical Practice Guidelines (2nd Edition). Chest 2007; 132(3):131–148.

29. Kurimoto N, Murayama M, Yoshioka S. Assessment of usefulness of endobronchial ultrasonography in tracheobronchial tumor invasion. Chest 1999; 115: 1500–1506.

30. Becker HD, Herth F: Endobronchial Ultrasound of the Airways and the Mediastinum in: C.T. Bolliger and P.N. Mathur (eds.): Progress in Respiratory Research Vol. 30, Interventional Bronchoscopy. S. Karger, Basel-Freiburg etc., 1999, pp 80–93.

31. Herth FJ, Ernst A, Schulz M, Becker HD Endobronchial Ultrasound Reliably Differentiates Between Airway Infiltration and Compression by Tumor Chest 2003 123: 458–462.

32. Wieder HA, Stahl A, Lordick F, Ott K. Esophageal cancer. Recent Results Cancer Res. 2008;170:71–79.

33. Law S, Wong J. The current management of esophageal cancer.Adv Surg. 2007; 41: 93–119.

34. Wakamatsu T, Tsushima K, Yasuo M, Yamazaki Y, Yoshikawa S, Koide N, Fujimori M, Koizumi T. Usefulness of preoperative endobronchial ultrasound for airway invasion around the trachea: esophageal cancer and thyroid cancer. Respiration. 2006; 73(5):651–7.

Endobronchial Ultrasound for Peripheral Lesions

Ralf Eberhardt

Lung cancer remains the leading cause of cancer death in both men and women, even though the risk factors for this disease have been thoroughly investigated and are well established. Despite being the most common cancer in the world, it still remains poorly diagnosed at the early stages, and the tragedy of lung cancer is directly associated with its delayed presentation. Most patients who receive an initial diagnosis of lung cancer have advanced stage disease, making cure with currently available techniques unlikely. In contrast, individuals with early stage disease can achieve cure through surgical resection *(1–5)*.

1. Solitary Pulmonary Nodule

A solitary pulmonary nodule (SPN) is defined radiologically as an intraparenchymal lung lesion that is less than 3 cm in diameter, and is not associated with atelectasis or adenopathy *(6)*. Most SPNs are benign, but more than 150,000 solitary pulmonary nodules are detected annually in the United States. Each of these could indicate the presence of lung cancer *(7)*. The increased use of computed tomography (CT) for screening could result in substantial increases in this number.

The likelihood of malignancy for SPNs between 0.8 cm and 2.0 cm was previously reported to be about 18 percent, and for nodules larger than 2.0 cm, about 50 percent *(8, 9)*. One of the challenges in the early diagnosis of lung cancer remains the

difficulty in reaching these small lung lesions - detected by X-ray or CT – and successfully obtaining adequate tissue samples for pathological diagnosis.

2. Transbronchial Biopsy Under Fluoroscopic Guidance

Bronchoscopy has been used for over 30 years to evaluate SPNs and peripheral tumors of the lung. In patients with such nodules, the diagnostic procedure is usually performed as a transbronchial biopsy (TBBx) under fluoroscopic guidance. The complication rate is generally low, but there is certainly radiation exposure to the patient and the staff. Using fluoroscopic guidance demands expensive X-ray equipment or coordination with the radiology department.

It is also known that TBBx under fluoroscopy is limited in evaluating small pulmonary nodules *(10)*. Its diagnostic yield varies from 20 percent to 84 percent in malignant lesions, and from 35 percent to 56 percent in benign cases *(11–14)*. More specifically, for peripheral lesions of less than 2 cm, it varies between 14 percent and 31 percent depending on the precise location of the lesion *(11)*. It is generally accepted that the greater the lesion size, the higher the diagnostic yield.

Several techniques were recently proposed to increase the yield of diagnosing small lung lesions. Highly invasive techniques such as CT-guided fine needle aspiration (CT-FNA), video-assisted thorascopic surgery (VATS) or thoracotomy are available, but these techniques have increased costs and complication rates *(15, 16)*.

2.1. Biopsy Tools

Different biopsy tools for diagnosing peripheral lung lesions endoscopically are available. It has been shown that the yield will increase, when a cytological sampling like brushing or transbronchial needle aspiration (TBNA) is added to the transbronchial biopsy by forceps. In particular, the sensitivity of TBNA in diagnosing peripheral lung lesions is greater than that of TBBx in all papers in which these two techniques have been compared *(17, 18)*

3. Endobronchial Ultrasound for Peripheral Lesions

3.1. Instruments and Technique

The different impedance of soft tissues has made sonography an indispensable diagnostic tool in medicine, but ultrasound, which is almost completely reflected by surrounding air and

radiological imaging, seems to be far superior in visualizing peripheral lung lesions. In contrast, small caliber, radial probes can be placed in the periphery of the lung and used to clinically apply ultrasonography to SPNs (19, 20). The probes must be inserted like a forceps into the different bronchi where the lesion is suspected. Ultrasound probes with an external diameter of 1.4 mm and 1.7 mm are available from different companies. The so-called *miniprobes* are fragile and have to be handled very delicately (see **Chapter 5**).

3.1.1. Ultrasound Imaging of Peripheral Lesions

Normal air-filled alveolar tissue typically produces a "snowstorm-like" whitish image. After reaching the lesion, the ultrasonic picture will change. The high resolution provided by 20 MHz ultrasound allows detailed imaging of the structure of lung lesions in the periphery. Solid tumors appear darker and more homogeneous. Usually they are well differentiated against the lung tissue by a bright border (**Fig. 7.1**). In contrast, the ultrasound images of inflammatory tissue or atelectasis have an inhomogeneous distribution caused by the different structures of the lung. Small bronchi containing trapped air will be visible as sharp white echo spots; fluid areas will appear dark (**Figs. 7.2**, **7.3** and **7.4**).

When such images are seen, the probe is considered to be located within the lesion.

After localization of the target the probes must be removed from the working channel to introduce a biopsy tool for taking specimens of the area of interest. A high yield for EBUS-guided TBBx can be achieved even though the probe has to be removed before inserting the biopsy forceps blindly (20, 21).

3.1.2. Fluoroscopic Guidance

The most common approach allowing for imaging while obtaining a biopsy is the additional usage of fluoroscopic guidance. This method steers the ultrasound probe in the direction of the peripheral lung nodule. After detecting the lesion by a naked ultrasound probe, confirmed by the fluoroscopic image, a forceps will be introduced through the working channel into the corresponding subsegmental bronchus and the correct way of the forceps will be controlled by fluoroscopy (**Fig. 7.5**). Biopsies will be taken under fluoroscopic sight. The major advantage of this approach is possibly obtaining a larger biopsy by using big forceps.

3.1.3. Ultrasound via Guide Sheath

The combination of endobronchial ultrasound (EBUS) technique with a guide sheath was introduced by Kurimoto (22). First, the bronchoscope is inserted as deeply as possible into the target bronchus under direct vision. Then a guide sheath-covered ultrasound probe is introduced in the working channel. A flexible bronchoscope with a 2.0 mm diameter working channel and a
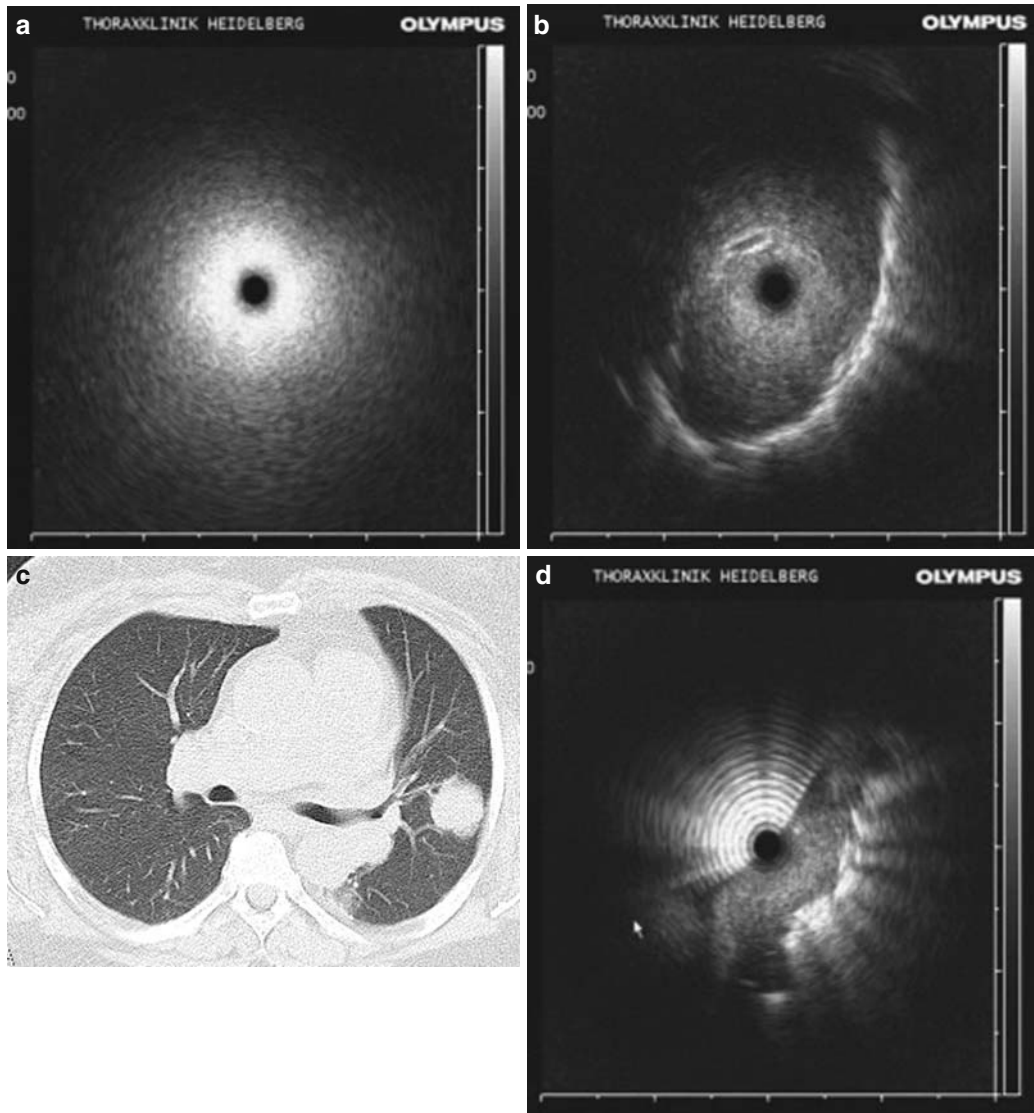
Fig. 7.1. Typical ultrasonographic images: (**a)** complete reflection of ultrasound sound waves in normal lung parenchyma; (**b)** peripheral malignant pulmonary tumor. The bright border demarcates the non-small cell lung cancer against the lung tissue, a small bronchus is visible in the tumor, (**c)** corresponding CT-scan, (Courtesy of Dr. Claus P. Heußel, Department of Diagnostic and Interventional Radiology, Thoraxklinik at the University of Heidelberg), (**d)** repeat echoes as a circular artefact between 9-òclock and 1-o'clock position: there is an insufficient contact between the probe and the bronchial wall leading to repeated reflections.

catheter with an external diameter of 1.9 mm can be used for the 1.4 mm probe, and a flexible bronchoscope with a working channel of 2.8 mm or larger and a guide sheath with an external diameter of 2.7 mm will be employed for the 1.7 mm ultrasound probe *(23)* (**Fig.** 7.6).
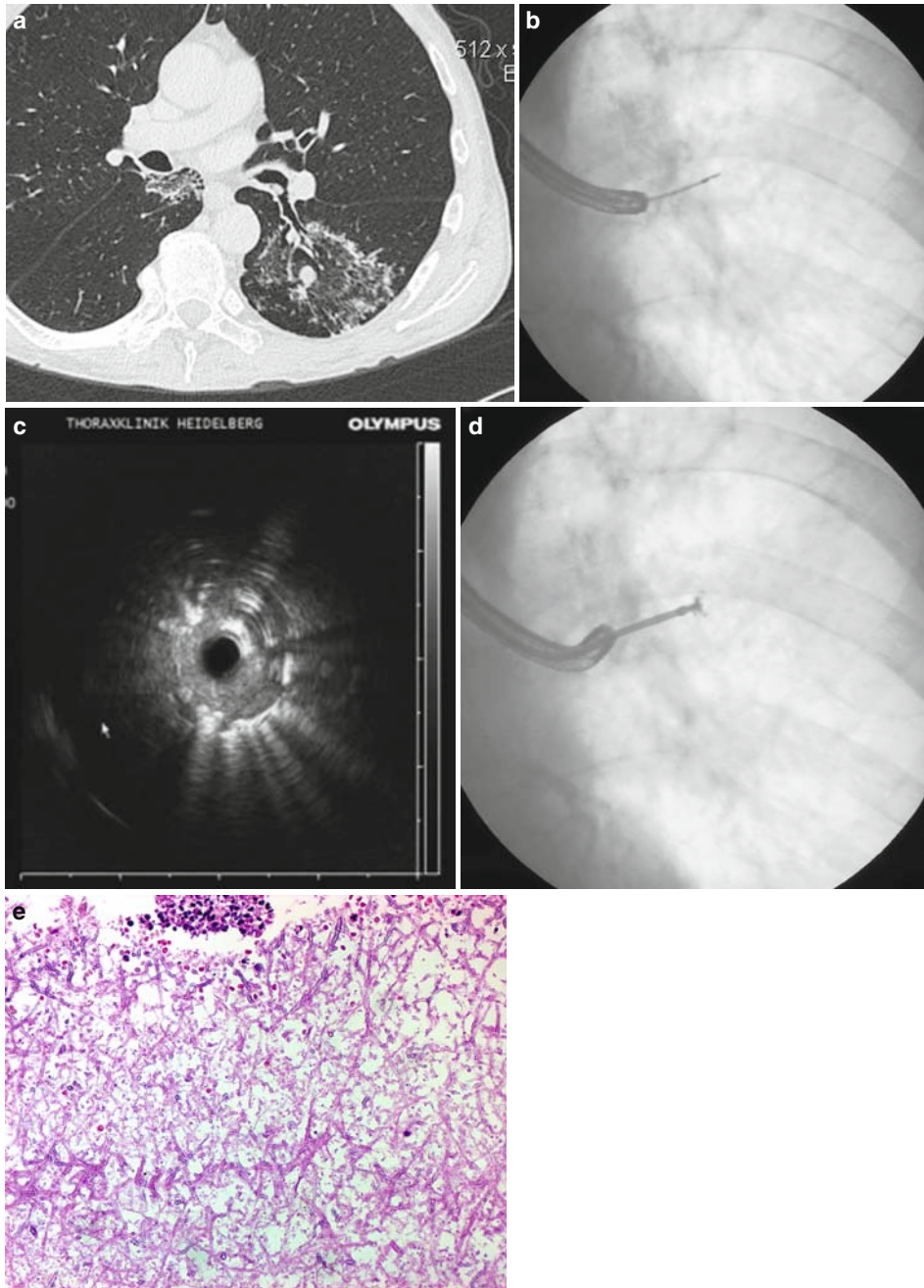
Fig. 7.2. (**a**) CT-Scan: patient with a localized fungal pneumonia in both lungs, (Courtesy of Dr. Claus P. Heußel, Department of Diagnostic and Interventional Radiology, Thoraxklinik at the University of Heidelberg), (**b**) fluoroscopy: detecting the lesion in segment 6 of the left lower lobe by ultrasound probe, (**c**) typical ultrasound image of a inflammatory tissue. White echo spots like a "positive air bronchogram" with corresponding ultrasound images are seen, (**d**) histological biopsies are taken under fluoroscopic control, (**e**) histological image of a pulmonary aspergillosis, PAS, original magnification 20×, (Courtesy of Dr. Philipp A. Schnabel, Department of Pathology, University of Heidelberg).
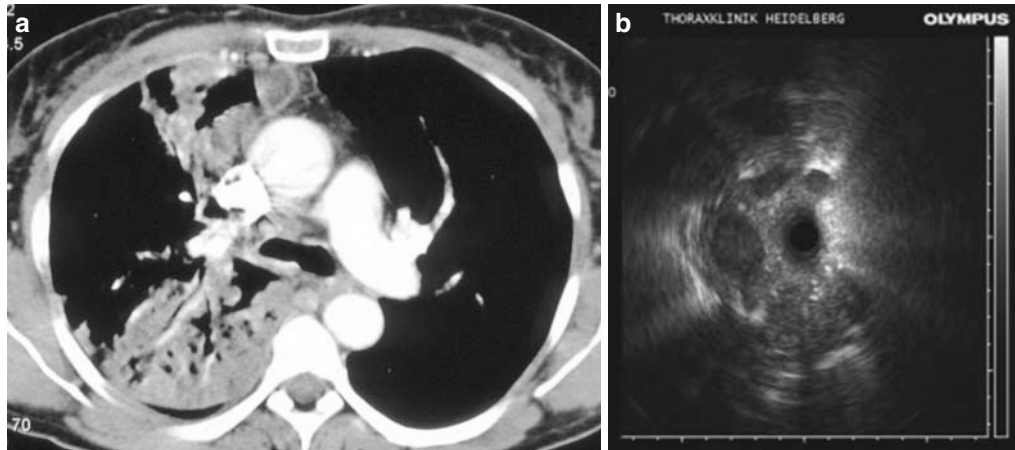
Fig. 7.3 Aspiration pneumonia in the right lower lobe. (**a**) CT-scan (Courtesy of Dr. Claus P. Heußel, Department of Diagnostic and Interventional Radiology, Thoraxklinik at the University of Heidelberg), (**b**) corresponding ultrasound image with solid inflammatory and necrotic tissue.
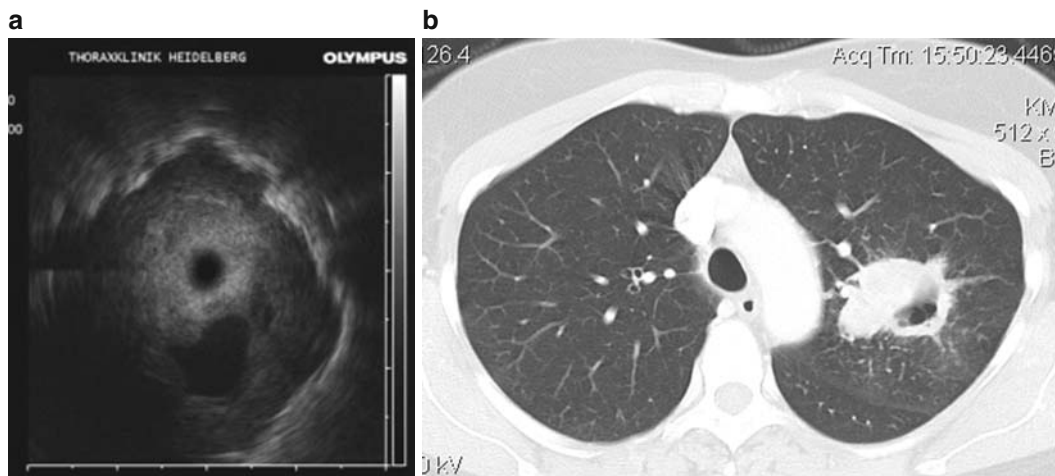
Fig. 7.4. Necrotic tumor in the left upper lobe: (**a**) ultrasound image of a non-small cell lung cancer (NSCLC) with solid and fluid parts. At 9-o'clock a sharp line is visible caused by a rotation artifact, (**b**) corresponding CT-scan.

EBUS imaging is used to confirm that the probe and guide sheath have reached the target. After locating the peripheral lesion the probe will be removed from the guide sheath and the catheter will be left in place. The guide sheath can then be used as an extended working channel for biopsy procedures with forceps, curette or brush. Then its possible to obtain specimens for cytological and/or histological examination with or without additional fluoroscopic guidance. In a retrospective analysis the optimum number of biopsy specimen attempts with ultrasound assistance has been at least five *(23)*.
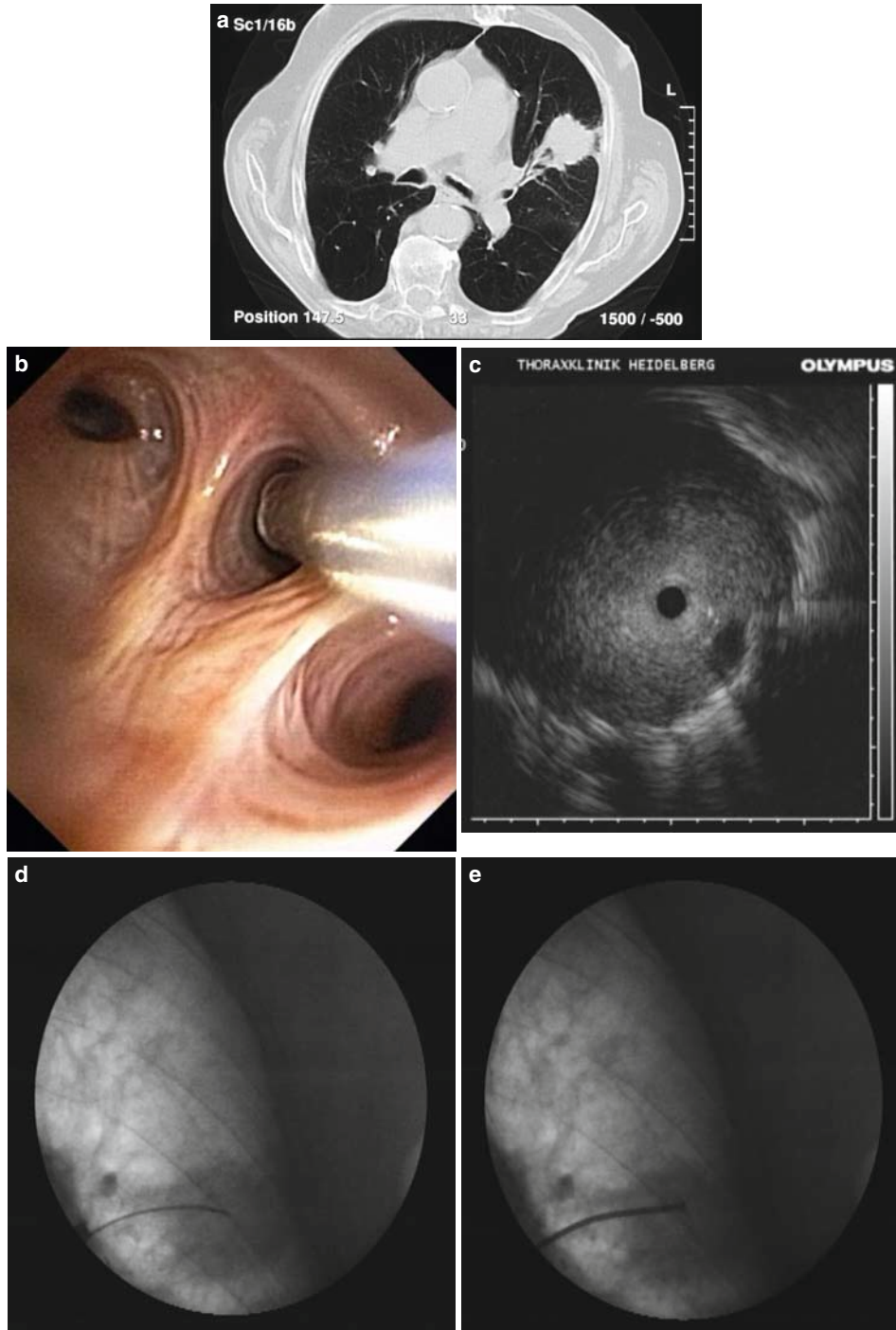
Fig. 7.5 Patient with a non-small cell lung cancer (NSCLC) in the left upper lobe (LUL): (**a**) CT-scan (Courtesy of Dr. Claus P. Heußel, Department of Diagnostic and Interventional Radiology, Thoraxklinik at the University of Heidelberg); (**b**) endoscopic view after the ultrasound probe was inserted in segment 3 of the LUL; (**c**) ultrasound image of the homogeneous lung tumor. A small vessel inside the tumor is visible in the right lower corner; (**d**) fluoroscopic control: the ultrasound probe is projecting into the tumor; (**e**) transbronchial biopsy by forceps under fluoroscopic guidance after removing the probe.
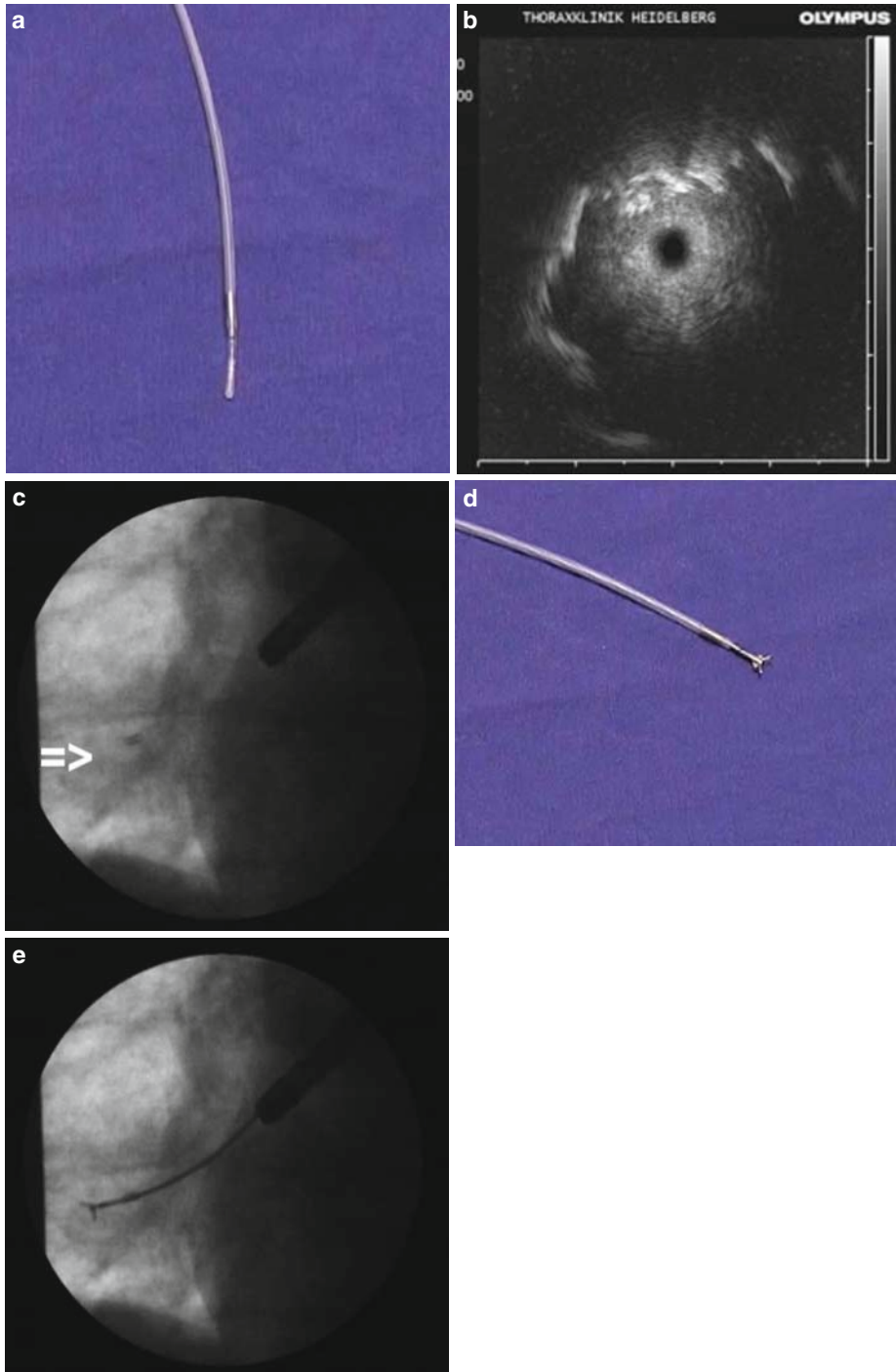
Fig. 7.6. (**a**) A sheath-covered ultrasound probe (UM-S20-17R; Olympus, Tokyo, Japan), (**b**) Ultrasound image of a homogeneous malignant lesion in the right lower lobe. Air inclusions as small sharp artifacts are seen at 12-o'clock (**c**) After removing the ultrasound probe the guide-sheath (GS) is left in place. The metallic tip of the sheath is visible in the tumor lesion (=>). (**d,e**) Small forceps (FB-44D-1; Olympus, Tokyo, Japan) is insert in the GS. It is used as an extended working channel for attempting biopsies by forceps.

If the SPN cannot be visualized by ultrasonic picture the probe will be removed from the guide sheath and a double hinged curette can be inserted. The appropriate bronchus will be selected by manipulating the curette under fluoscopy. Once the bronchus is determined, the curette must be removed from the catheter and the ultrasound probe will be inserted again to confirm the correct position by ultrasound imaging.

3.2. Clinical Results

Endobronchial ultrasound has increased the yield of flexible bronchoscopy in the diagnosis of peripheral lung lesions and solitary pulmonary nodules. Several studies have reported the efficacy and safety of this guidance technique. The first trial using radial ultrasound for diagnosing SPNs was reported in 2002 *(19)*. In this prospective study the diagnostic yields were compared for fluoroscopic-guided and EBUS-guided TBBx in random order. Diagnostic material was obtained in 80 percent of patients with EBUS, and 76 percent of patients with fluoroscopy. There was a nonsignificant trend for EBUS to be better than fluoroscopy for lesions less than 3 cm in diameter.

Recently the success rate was confirmed by different groups of bronchologists. Overall, yields for EBUS using a radial probe with or without a guide catheter have been reported to be 58.3 percent to 80.0 percent, and independent of lesion size when using a sheath (**Table** 7.1). Eleven to 24 percent of SPNs could not be localized by EBUS and all experts agree, however, that lesions smaller than 15 mm are harder to reach with the EBUS system *(20–28)*.

In a retrospective analysis of 155 patients SPNs in which the probe was positioned within the lesion on the ultrasound image had a higher diagnostic yield (83%) than SPNs in which the probe was positioned only adjacent to the target *(23)* (**Fig.** 7.7). There were no significant differences in diagnostic yield for underlying disease, location, CT scan bronchus sign, operator, or type of EBUS probe.

Nodules less than 3 cm frequently cannot be visualized fluroscopically. One prospective study assessed the diagnostic yield of EBUS-guided TBBx in fluoroscopically invisible SPNs. In 80 percent of cases the lesion with a mean diameter of 2.2 cm was localized with EBUS, and in 70 percent the biopsy established a diagnosis *(29)*. So EBUS can be used as an alternative to fluoroscopy in providing image guidance for TBBx. Yoshikawa could confirm the usefulness of endobronchial ultrasonography as a guide for diagnosing peripheral pulmonary lesions without radiographic fluoroscopy. Seventy-six of 123 SPNs (61.8%) were diagnosed by EBUS-guided sheath alone. In this study the diagnostic yield for lesions > 20 mm was significantly higher than for those ≤ 20 mm in diameter *(30)*. Moreover, the use of endobronchial ultrasound for diagnosing peripheral lung lesions avoids fluoroscopy-induced radiation exposure for patients and medical staff.

Table 7.1
Yield of Endobronchial Ultrasound–Guided Diagnosis pf Peripheral Lung Lesions

Series	Technique	N	Size (mm)	Diagnostic yield (%)
Herth et al. (19)	EBUS – transbronchial forceps biopsy	50	All	80
		21	< 30	80
		29	> 30	79
Kurimoto et al. (22)	EBUS with guide sheath and fluoroscopy	150	All	77.3
	±curette – forceps biopsy/brush	81	< 20	72.8
		43	20-30	77
		26	> 30	90
Kikuchi et al. (24)	EBUS with guide sheath and fluoroscopy	24	< 30	58.3
	±curette – forceps biopsy/brush	15	20-30	66.7
		9	< 20	53.3
Yang et al. (25)	EBUS – transbronchial forceps biopsy	122	All	65.6
		103	>20	66
		11	< 20	54.5
Asahina et al. (26)	EBUS with guide sheath, virtual bronchoscopy	30	< 30	63.3
	navigation and fluoroscopy ± curette -	12	20-30	91.7
	forceps biopsy/brush	18	< 20	44.4
Paone et al. (27)	EBUS – transbronchial forceps biopsy	87	All	78.7
			> 30	82.8
			< 30	75
			< 20	71
Herth et al. (29)	EBUS with guide sheath w/o fluoroscopy – transbronchial forceps biopsy	54	Fluoroscopically invisible, mean 22 ± 0.7	
Yoshikawa et al. (30)	EBUS with guide sheath w/o fluoroscopy	123	all	61.8
	±curette – forceps biopsy/brush	48	> 30	98.68

(continued)

Table 7.1 (continued)

Series	Technique	N	Size (mm)	Diagnostic yield (%)
		38	20-30	37.9
		37	≤20	29.7
Dooms et al. *(19)*	EBUS w/o fluoroscopy – transbronchial	50	All	68
	forceps biopsy		> 20	82
			< 20	18
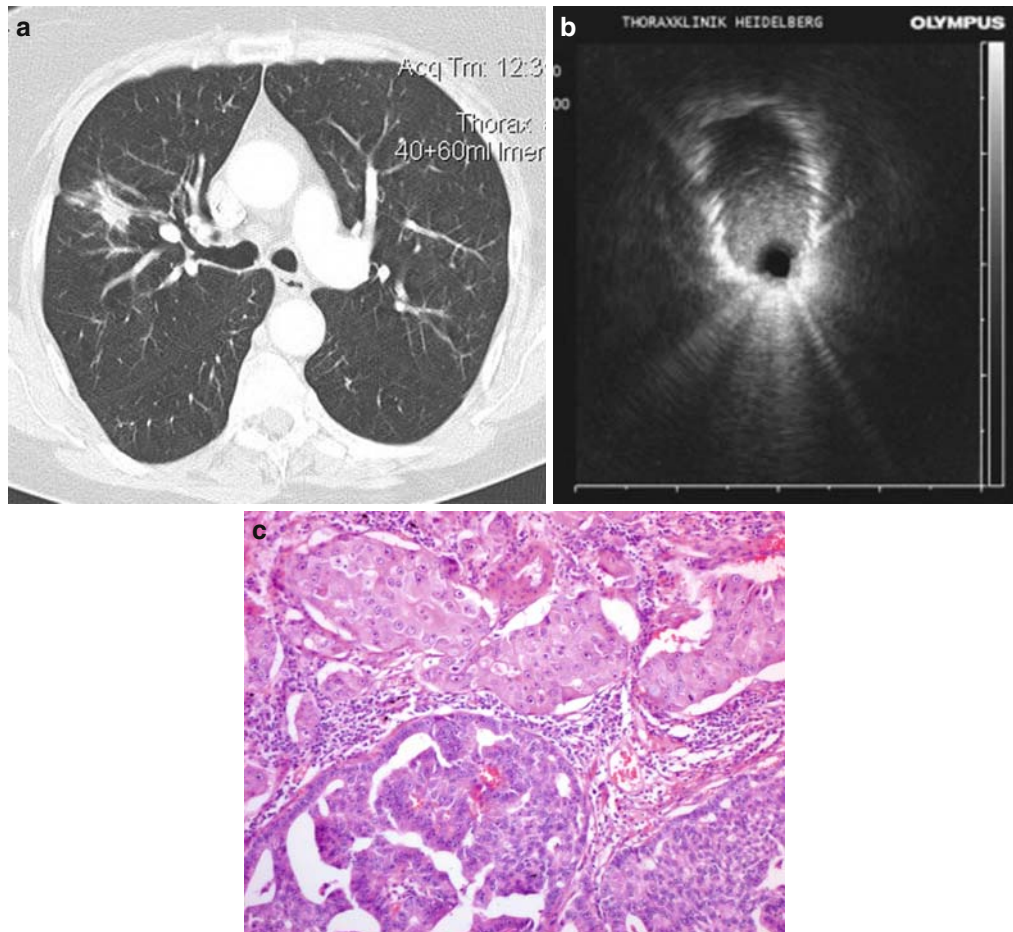
Fig. 7.7. Solitary pulmonary nodule (SPN) in the right lung, diagnosed as an adenocarcinoma of the lung. (**a**) CT-scan (Courtesy of Dr. Claus P Heußel, Department of Diagnostic and Interventional Radiology, Thoraxklinik at the University of Heidelberg). (**b**) corresponding ultrasound image: even though the probe is located in the bronchus adjacent to the SPN, the definitive diagnosis has been established by ultrasound guided TBBx, (**c**) histological image of an adenocarcinoma (mixed type), HE, original magnification 10 × , (Courtesy of Dr. Philipp A. Schnabel, Department of Pathology, University of Heidelberg).

4. Combination of Ultrasound with other Guidance Techniques

EBUS enables direct visualization of the target lesion before attempting biopsy. However, EBUS lacks a navigation system and requires the operator to maneuver the bronchoscope blindly to the lesion with the knowledge of prior radiological investigations such as CT scans.

4.1. Virtual Bronchoscopy

Virtual bronchoscopy (VB) is a novel CT-based imaging technique that allows a noninvasive intraluminal evaluation of the tracheobronchial tree. The usefulness of VB navigation has been reported for CT-guided TBBx using an ultrathin bronchoscope *(31, 32)*. However, this procedure has the disadvantages of excessive radiation exposure from CT and of occupying the CT room for approximately one hour.

Combining endobronchial ultrasound guidance by using small-caliber radial probes with virtual bronchoscopy may overcome the limitations of CT-guided TBBx. Asahina, et al. demonstrated the feasibility, safety and efficacy of this endoscopic approach *(26)*. Diagnostic sensitivities were 44.4 percent for pulmonary lesions < 20 mm, and 91.7 percent for SPNs 20–30 mm in mean diameter.

4.2. Electromagnetic Navigation

Electromagnetic navigation-guided bronchoscopy (ENB) consists of four components: an electromagnetic location board, a locatable sensor probe with a steering mechanism, an extended working channel and computer software that converts CT scans into multiplanar images with three-dimensional virtual bronchoscopy reconstruction *(33)*. This system enables navigation guidance within the lungs to endobronchially invisible targets, but it is based on a virtual environment and when used by itself, does not provide assurances that the intended lesion has indeed been reached. ENB lacks a means to directly visualize the lesion before biopsy. Combining endobronchial ultrasound and electromagnetic navigation improves the diagnostic yield of flexible bronchoscopy in peripheral lung lesions without compromising safety. We could demonstrate in a randomized trial that combined EBUS and ENB overcame each individual technique's limitation *(34)*. The diagnostic yield of the combined procedure (88%) was greater than either EBUS (69%) or ENB alone (59%).

Multimodality diagnosis with the combined use of EBUS and ENB has pushed the diagnostic yield of flexible bronchoscopic procedures closer to the sensitivity obtainable through either transthoracic CT-guided (92%) or surgical biopsies (~100%) *(35, 36)*.

These techniques may provide a means for therapeutic interventions to inoperable tumor patients. The successful treatment of a peripheral pulmonary tumor by electromagnetically navigated and EBUS-controlled brachytherapy has been reported recently *(37)* (**Fig.** 7.8).
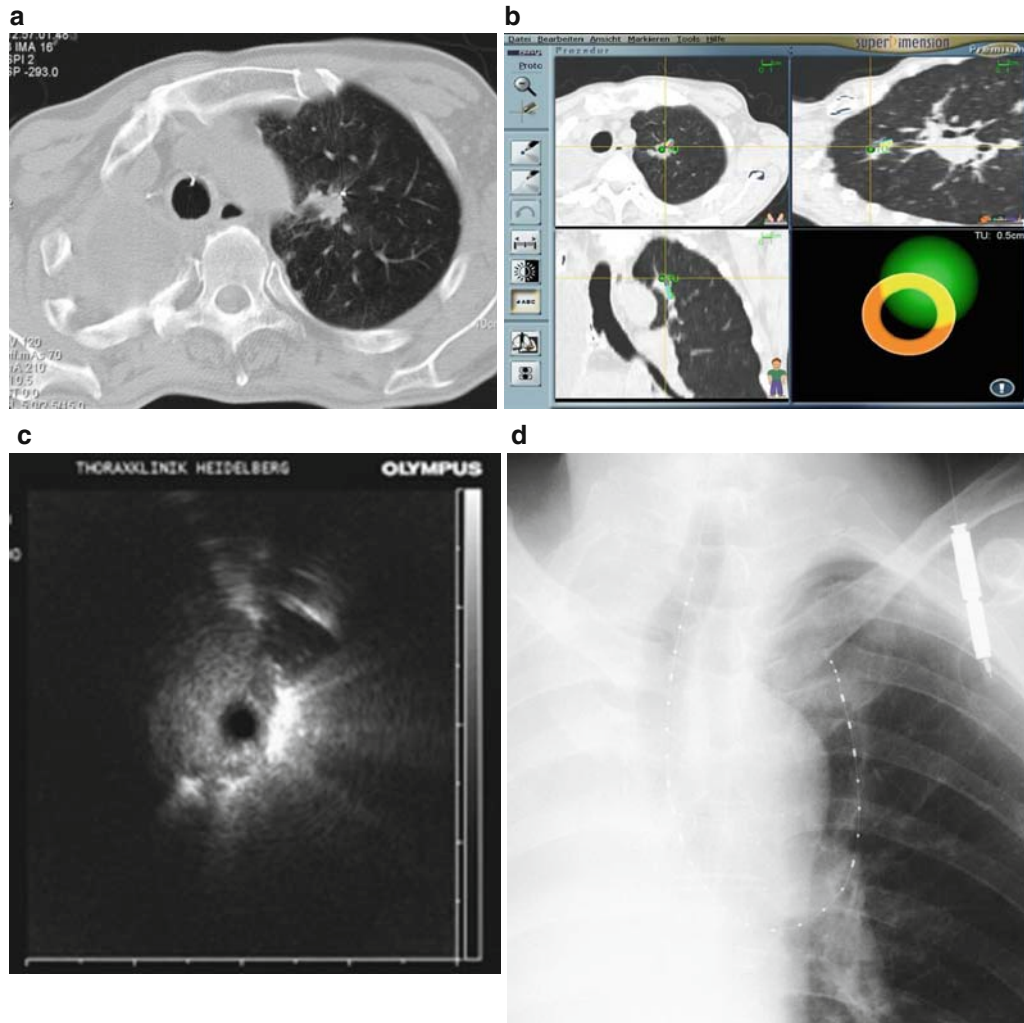
Fig. 7.8. (**a**) Small peripheral lesion suspicious for lung cancer recurrence after pneumonectomy 3 years ago (Courtesy of Dr. Claus P. Heußel, Department of Diagnostic and Interventional Radiology, Thoraxklinik at the University of Heidelberg). (**b**) typical screen of a electromagnetic navigation system (superDimension Ltd, Herzliya, Israel). The locatable guide is navigated to the lesion, the distance from the tip to the marked center (navigation error) is 0.5 cm (**c**) confirmation of the position of the extended working channel inside the lesion by EBUS radial probe, (**d**) inserted brachytherapy catheter with a dummy probe.

References

1. Parkin DM, Bray F, Ferlay J, Pisani P. Global cancer statistics, 2002. CA Cancer J Clin 2005; 55:74–108.

2. Salomaa ER, Sällinen S, Hiekkanen H, Liippo K. Delays in the diagnosis and treatment of lung cancer. Chest 2005; 128:2282–2288.

3. Henschke CI, Yankelevitz DF, Libby DM, Pasmantier MW, Smith JP, Miettinen OS. Survival of patients with stage I lung cancer detected on CT screening. N Engl J Med 2006; 355:1763–1771.

4. Bach PB, Kelley MJ, Tate RC, McCrory DC. Screening for lung cancer: a review of the current literature. Chest 2003; 123:72S–82S.

5. Tan BB, Flaherty KR, Kazerooni E, Iannettoni MD. The solitary pulmonary nodule. Chest 2003; 123:89S–96S.

6. Tuddenham, WI. Glossary of terms for thoracic radiology: recommendations of the Nomenclature Committee of the Fleischner Society. Am J Roentgenol 1984; 43:509–517.

7. Stoller JK, Ahmad M, Rice TW. Solitay pulmonry nodule. Cleve Clin J Med 1988; 55:68–74.

8. Leef JL 3rd, Klein IS. The solitary pulmonary nodule. Radiol Clin North Am 2002; 40:123–143.

9. Midthun DE, Swensen SJ, Jett JR, Hartman TE. Evaluation of nodules detected by screening for lung cancer with low dose spiral computed tomography. Lung Cancer 2003; 41(suppl 2):S40.

10. Libby DM, Smith JP, Altorki NK, Pasmantier MW, Yankelevitz D, Henschke CI. Managing the small pulmonary nodule discovered by CT. Chest 2004; 125:1522–1529.

11. Baaklini WA, Reinoso MA, Gorin AB, Sharafkaneh A, Manian P. Diagnostic yield of fiberoptic bronchoscopy in evaluating solitary pulmonary nodules. Chest 2000; 117:1049–1054.

12. Shiner RJ, Rosenman J, Kaz I, Reichart N, Hershko E, Yellin A. Bronchoscopic evaluation of peripheral lung tumours. Thorax 1988; 43:887–889.

13. Chechani V. Bronchoscopic diagnosis of solitary pulmonary nodules and lung masses in the absence of endobronchial abnormality. Chest 1996; 109:620–625.

14. Mori K, Yanase N, Kaneko M, Ono R, Ikeda S. Diagnosis of peripheral lung cancer in cases of tumors 2 cm or less in size. Chest 1989; 95:304–308.

15. Schreiber G, McCrory DC. Performance characteristics of different modalities for diagnosis of suspected lung cancer: summary of published evidence. Chest 2003; 123:115S–128S.

16. Ohno Y, Hatabu H, Takenaka D, Higashino T, Watanabe H, Ohbayashi C, Sugimura K. CT-guided transthoracic needle aspiration biopsy of small solitary pulmonary nodules. Am J Radiol 2003; 180:1665–1669.

17. Gasparini S, Ferretti M, Secchi EB, Baldelli S, Zuccatosta L, Gusella P. Integration of transbronchial and percutaneous approach in the diagnosis of peripheral pulmonary nodules or masses: experience with 1,027 consecutive cases. Chest 1995; 108:131–137.

18. Reichenberger F, Weber J, Tamm M, Bolliger CT, Dalquen P, Perruchoud AP, Soler M. The value of transbronchial needle aspiration in the diagnosis of peripheral pulmonary lesions. Chest 1999; 116: 704–708.

19. Herth FJF, Ernst A, Becker HD. Endobronchial ultrasound-guided transbronchial lung biopsy in solitary pulmonary nodules and peripheral lung lesions. Eur Respir J 2002; 20:972–974.

20. Shirakawa T, Imamura F, Hamamoto J, Honda I, Fukushima K, Sugimoto M, Shikakusa T. Usefullness of endobrochial ultrasonography for transbronchial lung biopsies of peripheral lung lesions. Respiration 2004; 71:260–268.

21. Dooms CA, Verbeken EK, Becker HD, Demedts MG, Vansteenkiste JF. Endobronchial ultrasonography in bronchoscopic occult pulmonary lesions. J Thorac Oncol 2007; 2:121–124.

22. Kurimoto N, Miyazawa T, Okimasa S, Maeda A, Oiwa H, Miyazu Y, Murayama M. Endobronchial ultrasonography using a guide sheath increases the ability to diagnose peripheral pulmonary lesions endoscopically. Chest 2004; 126:939–963.

23. Yamada N, Yamazaki K, Kurimoto N, Asahina H, Kikuchi E, Shinagawa N, Oizumi S, Nishimura M. Factors related to diagnostic yield of transbronchial biopsy using endobronchial ultrasonography with a guide sheath in small peripheral pulmonary lesions. Chest 2007; 132:603–608.

24. Kikuchi E, Yamazaki K, Sukoh N, Kikuchi J, Asahina H, Imura M, Onodera Y, Kurimoto N, Kinoshita I, Nishimura M. Endobronchial ultrasonography with guide sheat-sheath for peripheral pulmonary lesions. Eur Respir J 2004; 24:533–537.

25. Yang MC, Liu WT, Wang CH, Lin HC, Chen HC, Chou CL, Hsuch S, Kuo HP. Diagnostic value of endobronchial ultrasound-guided transbronchial lung biopsy in peripheral lung cancers. J Formos Med Assoc 2004; 103:124–129.

26. Asahina H, Yamazaki K, Onodera Y, Kikuchi E, Shinagawa N, Asano F, Nishimura M. Transbronchial biopsy using endobronchial ultrasonography with a guide-sheath and virtual bronchoscopic navigation. Chest 2005; 128:1761–1765.

27. Paone G, Nicastri E, Lucantoni G, Dello Iacono R, Battistoni P, D'Angeli AL, Gallucio G. Endobronchial ultrasoun-driven biopsy in the diagnosis of peripheral lung lesions. Chest 2005; 128:3551–3557.

28. Herth FJF. Endobronchial ultrasound-guided biopsy of coin lesions. Future Oncol 2007; 3:273–275.

29. Herth FJF, Eberhardt R, Becker HD, Ernst A. Endobronchial ultrasound-guided

transbronchial lung biopsy in fluoroscopically invisible solitary pulmonary nodules: a prospective trial. Chest 2006; 129:147–150.

30. Yoshikawa M, Sukoh N, Yamazaki K, Kanazawa K, Fukumoto S, Harada M, Kikuchi E, Munakata M, Nishimura M, Isobe H. Diagnostic value of endobronchial ultrasonography with a guide sheath for peripheral pulmonary lesions without x-ray fluoroscopy. Chest 2007; 131:1788–1793.

31. Shinagawa N, Yamazaki K, Onodera A. CT-guided transbronchial biopsy using an ultrathin bronchoscope with virtual bronchoscopic navigation. Chest 2004; 123:1138–1143.

32. Asano F, Matsuno Y, Matsushita T, Kondo H, Saito Y, Seko A, Ishihara Y. Transbronchial diagnosis of a pulmonary peripheral small lesion using an ultrathin bronchoscope with virtual bronchoscopic navigation, J Bronchol 2002; 9:108–111.

33. Schwarz Y, Greif Y, Becker H, Ernst A, Mehta A. Real-time electromagnetic navigation bronchoscopy to peripheral lung lesions using overlaid CT images: the first human study. Chest 2006; 129: 988–994.

34. Eberhardt R, Anantham D, Ernst A, Feller-Kopman D, Herth F. Multimodality bronchoscopic diagnosis of peripheral lung lesions: a randomized controlled trial. Am J Respir Crit Care Med 2007; 176:36–41.

35. Yeow KM, Su IH, Pan KT, Tsay PK, Lui KW, Cheung YC, Chou ASB. Risk factors of pneumothorax and bleeding: multivariate analysis of 660 CT-guided coaxial cutting needle biopsies. Chest 2004; 126:748–754.

36. DeCamp MM Jr, Jaklitsch MT, Mentzer SJ, Harpole DH Jr, Sugarbaker DJ. The safety and versatility of videothoracoscopy: a prospective analysis of 895 consecutive cases. J An Coll Surg 1995; 181:113–120.

37. Harms W, Krempien R, Grehn C, Hensley F, Debus J, Becker HD. Electromagnetically navigated brachytherapy as a treatment option for peripheral pulmonary tumors. Strahlenther Onkol 2006; 182:108–111.

Chapter 8

EBUS-TBNA Bronchoscopy

Kazuhiro Yasufuku

The development and introduction of the new convex probe endobronchial ultrasound (CP-EBUS) that performs endobronchial ultrasound-guided transbronchial needle aspiration (EBUS-TBNA) has changed the practice of bronchoscopic biopsy of the mediastinum in respiratory diseases. In particular, the role of EBUS-TBNA in the diagnosis and mediastinal lymph node staging of lung cancer, the leading cause of death from malignant disease worldwide *(1)*, is becoming an interest to pulmonologists as well as thoracic surgeons.

In the management of patients with lung cancer, mediastinal lymph node staging is one of the most important factors affecting patient outcome. Accurate staging of the disease is important not only to determine the prognosis, but also to determine the most suitable treatment plan. Mediastinal staging can be divided into noninvasive staging (imaging) and invasive (sampling) staging. Computed tomography (CT), magnetic resonance imaging (MRI), positron emission tomography (PET) and PET-CT are used for noninvasive imaging *(2)*. Other imaging modalities include the use of transesophageal ultrasonography (EUS) and endobronchial ultrasound (EBUS) using a radial probe for detecting even small mediastinal lymph nodes *(3, 4)*.

Invasive staging provides definitive tissue diagnosis either by surgical biopsy or needle biopsy *(5)*. Mediastinoscopy is still the gold standard for mediastinal lymph node staging *(6)*. However, it requires general anesthesia and complications cannot be ignored. Different needle biopsy techniques exists which include conventional bronchoscopic transbronchial needle aspiration (TBNA),

EUS-guided fine needle aspiration (EUS-FNA), CT fluoroscopy-guided TBNA, and EBUS-guided TBNA using the radial probe *(5)*. However, each of these methods has its limitations.

There has been a need for a new modality with a high yield which enables pulmonologists and thoracic surgeons to assess the mediastinum easily and safely. In 2002, the authors started to develop the new convex probe endobronchial ultrasound with the ability to perform real-time EBUS-guided TBNA (EBUS-TBNA). This new endoscope, with a built-in linear probe ultrasound on the tip, enables real-time guidance during TBNA. Compared to the radial probe EBUS, the linear ultrasound images are easier to understand. After preliminary studies showing the efficacy of CP-EBUS in surgical lung specimens *(7)*, the clinical use of CP-EBUS for assessing mediastinal and/or hilar lymph nodes under local anesthesia was reported *(8)*. EBUS-TBNA is now performed by trained interventional pulmonologists and thoracic surgeons in selected centers around the world (**Fig. 8.1**). Publications concerning the use of EBUS-TBNA in respiratory disease indicate the effectiveness of this new modality *(7–25)*.

Fig. 8.1. Bronchoscopist performing endobronchial ultrasound-guided transbronchial needle aspiration under local anesthesia. A two-screen display is preferable for endobronchial images as well as ultrasound images during the procedure.

EBUS-TBNA was initially developed for lymph node staging of lung cancer. However, from our experience, there are many other uses in clinical practice. This chapter will discuss in detail the actual procedure of EBUS-TBNA and clinical application of EBUS-TBNA in the management of respiratory disease.

1. History

Endobronchial application of the ultrasound was first described in 1992 *(26)*. After solving technical difficulties for the application of the ultrasound in bronchoscopic practice, the radial probe EBUS was commercially introduced in 1992. Currently, EBUS has gradually been introduced into the field of respiratory diseases, which has broadened the diagnostic possibilities for bronchial and mediastinal pathology. The radial probe EBUS was initially developed to seek high resolution imaging of processes within the airway wall and outside the airways. The structure of special importance was lymph nodes, walls of the central airways and the mediastinum. After the development of miniaturized radial probes with flexible catheters with a balloon at the tip, it has been applied to aid the bronchoscopist during biopsy in respiratory diseases *(27–31)*. In particular, the radial probe EBUS-guided TBNA has increased the yield of TBNA of mediastinal lymph nodes *(28, 29)*. However, it was still not a real-time procedure with target visualization. The new CP-EBUS with the ability to perform real-time EBUS-guided TBNA (EBUS-TBNA) has emerged to overcome these problems.

The history of CP-EBUS goes back to 1992 when the use of bronchoscopic ultrasonography in the diagnosis of lung cancer was first reported *(32)*. The device used in this early report comprises an Echo-camera, SSD-630, and a transbronchial ultrasonic probe (Aloka). The maximum diameter of the probe head is 6.3 mm. The probe head has a convex type transducer 5.0 mm in maximum diameter with a frequency of 7.5 MHz and an effective image field of 34° with good resolution. The scanning direction is parallel to the axis. It also provides a front view with a built-in optical quartz fiber bundle, 2 mm in diameter, for image transmission. It is very similar to the current CP-EBUS widely being used, however it lacked an injection catheter or TBNA for real-time EBUS-guided procedures. Unfortunately, this was a single report without further investigations that discussed the use of the Echo-camera.

In 2002, a new device was developed by integrating a convex transducer with a frequency of 7.5 MHz at the tip of a flexible bronchoscope (XBF-UC40P, Olympus, Tokyo, Japan). This new CP-EBUS is a linear curved array transducer that scans parallel to the insertion direction of the bronchoscope. Images can be obtained by directly contacting the probe or by attaching a balloon on the tip and immersing with saline. The outer diameter of the insertion tube of the flexible bronchoscope is 6.7 mm and that of the tip is 6.9 mm. The ultrasound image is processed in an ultrasound processor and is visualized along with the conventional

bronchoscopy image on the same monitor. XBF-UC40P was mainly used in preliminary studies in surgically resected specimens *(7)*. It was also a bronchofiberscope.

The newest CP-EBUS now being used in clinical practice is a hybrid bronchofibervideoscope which features a unique optical system that exploits both video and fiber-optic technologies (BF-UC160F-OL8, Olympus, Tokyo, Japan) (**Fig. 8.2**). The built-in CCD in the control section allows sharp images similar to those of regular videoscopes and allows a slimmer insertion tube of 6.2 mm. The dedicated 22-gauge needle is used for EBUS-TBNA.
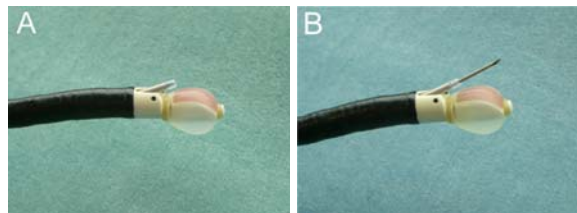
Fig. 8.2. Tip of the new convex probe endobronchial ultrasound (CP-EBUS, BF-UC160F-OL8, Olympus, Tokyo, Japan). The outer diameter of the insertion tube of the flexible bronchoscope is 6.2 mm. CP-EBUS has a linear curved array ultrasonic transducer of 7.5 MHz. The balloon attached to the tip of the bronchoscope is inflated with normal saline (**A**). The dedicated TBNA needle is inserted through the working channel (**B**).

2. Instrument

2.1. Convex Probe Endobronchial Ultrasound (CP-EBUS)

The current available CP-EBUS is an ultrasound puncture bronchoscope with a 7.5 MHz convex transducer placed at the tip of a flexible bronchoscope (**Table 8.1**) (**Fig. 8.3**). This CP-EBUS is a linear curved array transducer that scans parallel to the insertion direction of the bronchoscope. Images can be obtained by directly contacting the probe (**Fig. 8.2A**) or by attaching a balloon on the tip and inflating with saline (**Fig. 8.2B**). The outer diameter of the insertion tube of the CP-EBUS is 6.2 mm, and that of the tip is 6.9 mm. The angle of view is 80° and the direction of view is 35° forward oblique. The unique optical system exploits both video and fiber-optic technologies. With the built-in CCD in the control section, it allows sharp images similar to those of regular video bronchoscopes. The inner diameter of the instrument channel is 2.0 mm. A dedicated 22-gauge needle is used to perform EBUS-TBNA (**Fig. 8.3**).

Table 8.1
Convex probe endobronchial ultrasound (CP-EBUS, BF-UC160F-OL8) Specifications

Endoscopic functions	Optical system	Field of view	80°
		Direction of view	35° forward oblique
		Depth of field	2–50 mm
	Insertion tube	Distal end diameter	6.9 mm
		Insertion tube diameter	6.2 mm
		Working length	600 mm
	Instrument channel	Channel inner diameter	2.0 mm
	Bending section	Angulation range	up 120°, down 90°
	Total length	890 mm	
Ultrasonic functions	Display mode	B-mode	
		Color Power Doppler mode	
	Scanning method	Electrical curved linear array	
	Scanning direction	Parallel to insertion direction	
	Frequency	7.5 MHz	
	Scanning range	50°	
	Contact method	Balloon method	
		Direct contact method	

Fig. 8.3. The convex probe endobronchial ultrasound (CP-EBUS, BF-UC160F-OL8, Olympus, Tokyo, Japan).

2.2. Ultrasound
Processor

The ultrasound image is processed in a dedicated ultrasound processor (EU-C60/EUC2000, Olympus, Tokyo, Japan) (Table 8.2) (**Fig. 8.4**) and is visualized along with the conventional bronchoscopy image. The display mode includes the B-mode as well as the Color Power Doppler mode. The display range covers 2–24 cm. The ultrasound images can be frozen and the size of lesions can be

Table 8.2
Ultrasound processor (EU-C60) Specifications

Size	Dimensions	$313 \times 220 \times 93$ mm
	Weight	2.4 kg
Monitor observation	Display mode	B-mode, Color Power Doppler mode
	Display polarity	Positive display
	Scanning display	Convex type
	Display range	2–24 cm
Measurement	Distance	Measures distance
	Area/Circumference	Measures area/circumference

Fig. 8.4. The dedicated ultrasound processor (EU-C60/EU-C2000, Olympus, Tokyo, Japan). The ultrasound images can be frozen and the size of lesions can be measured in two dimensions by the placement of cursors. It is also equipped with the Color Power Doppler mode.

measured in two dimensions by the placement of cursors. The area and the circumference enclosed by caliper tracking can be measured as well.

2.3. Dedicated 22-Gauge Needle

The dedicated 22-gauge needle (NA-201SX-4022) is used to perform EBUS-TBNA (**Fig. 8.5**). The needle is a single use aspiration needle with echogenic dimpled tip design to improve visibility on ultrasound images. This needle has various adjuster knobs which work as a safety device to prevent damage to the channel. The maximum extruding stroke is 40 mm and to prevent excessive protrusion, a safety mechanism stops the needle at the stroke of 20 mm. The needle is attached onto the working channel of the bronchoscope which allows the operator to actually perform EBUS-TBNA (**Fig. 8.6**). The needle is also equipped with an internal sheath which is withdrawn after passing the bronchial wall, avoiding contamination during TBNA. This internal sheath is also used to clear out the tip of the needle after passing the bronchial wall. The use of this sheath has significantly increased the yield of EBUS-TBNA. The exit of the needle is at 20° with respect to the outer covering of the insertion tube. The needle can be visualized through the optics and on the ultrasound image.
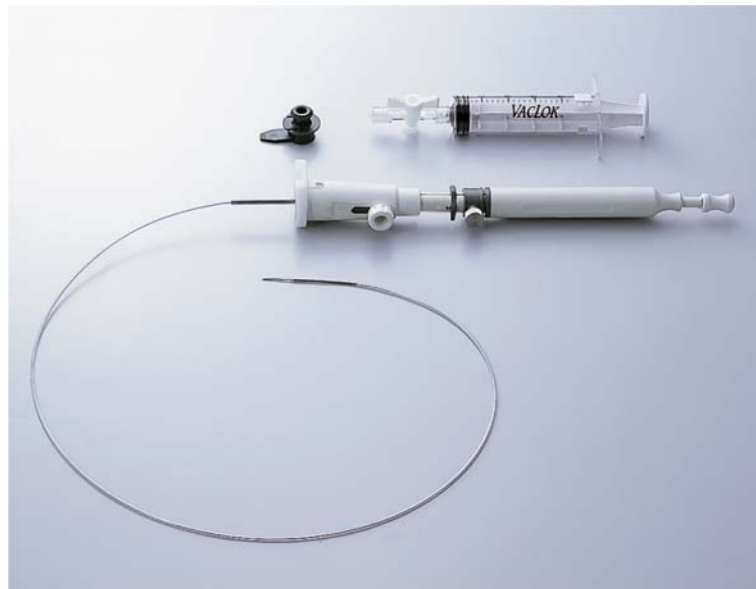
Fig. 8.5. Dedicated 22-gauge needle (NA-201SX-4022, Olympus, Tokyo, Japan) and the Vaclok syringe used to create negative pressure.

Fig. 8.6. Dedicated 22-gauge needle attached to the working channel of the EBUS-TBNA bronchoscope. The maximum extruding stroke is 40 mm and to prevent excessive protrusion, a safety mechanism stops the needle at the stroke of 20 mm. (Olympus, Tokyo, Japan).

3. Anatomic Considerations

It is important to understand the mediastinum and the lymph nodes that occur throughout the mediastinum and hilum. For descriptive purposes, lymph nodes are classified according to the lymph node map by Naruke, et al. and its revisions by Mountain (Table 8.3) *(33)*. The main mediastinal lymph node regions include superior mediastinal nodes (stations #1, #2, #3, and #4), aortic nodes (stations #5 and #6) and inferior mediastinal nodes (stations #7, #8, and #9). Ni nodes are found at the hilar (#10), interlobar (#11), lobar (#12), segmental (#13) and subsegmental (#14) stations. Mediastinoscopy is able to access the paratracheal (station #2 and #4) and subcarinal (#7) lymph node station, while anterior mediastinotomy (Chamberlain's procedure) or VATS is needed to access the aortic nodes (station #5 and #6). The reach of EBUS-TBNA is similar to mediastinoscopy, but extends down to the N1 nodes (#10, #11,

and #12), thus providing maximal sampling flexibility. EUS-FNA can access part of the paratracheal and the inferior mediastinal nodes. The reach of EBUS-TBNA and EUS-FNA is shown in **Fig. 8.7**.

Table 8.3
Regional lymph node stations for lung cancer staging

Superior Mediastinal Nodes	Highest Mediastinal	1
	Upper Paratracheal	2
	Pre-vascular and Retrotracheal	3
	Lower Paratracheal	4
Aortic Nodes	Subaortic (A-P window)	5
	Para-aortic (ascending aorta or phrenic)	6
Inferior Mediastinal Nodes	Subcarinal	7
	Paraesophageal	8
	Pulmonary Ligament	9
N1 Nodes	Hilar	10
	Interlobar	11
	Lobar	12
	Segmental	13
	Subsegmental	14

Adapted from Mountain et al. *(33)*

4. Procedural Technique

4.1. Anesthesia

In the author's practice, EBUS-TBNA is performed on an outpatient basis under midazolam-induced conscious sedation. Local anesthesia is achieved with 5-ml nebulized 1 percent lidocaine solution in the pharynx. A 2-ml bolus dose of 2 percent lidocaine is used during the procedure. The bronchoscope is usually inserted orally, since the ultrasound probe on the tip will limit nasal insertion. ECG, pulse oximetry, and blood pressure monitoring is required without the presence of an anesthesiologist.

Although EBUS-TBNA can be performed in an ambulatory setting under conscious sedation, some investigators prefer using the endotracheal tube or rigid bronchoscopy under general
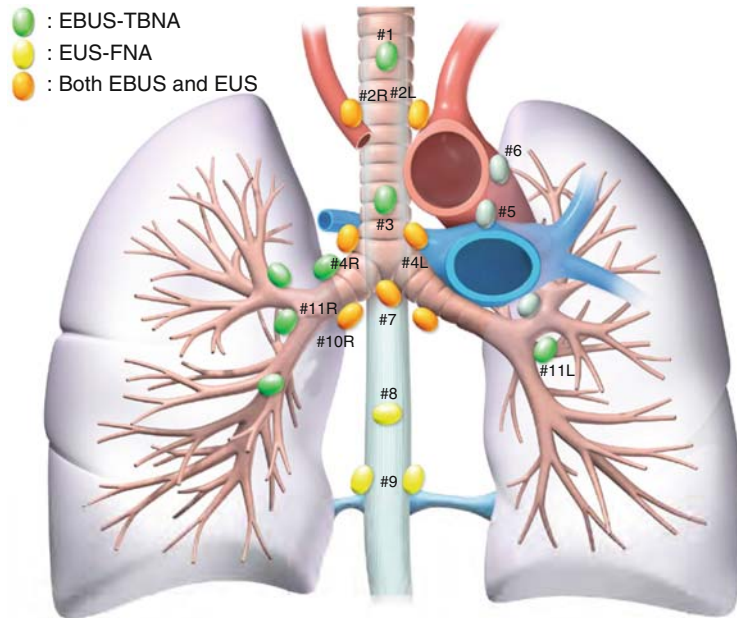
Fig. 8.7. Regional lymph node map for lung cancer staging. EBUS-TBNA: endobronchial ultrasound guided transbronchial needle aspiration. EUS-FNA: endoscopic ultrasound-guided fine needle aspiration.

anesthesia. Since the EBUS-TBNA scope is larger than a regular bronchoscope, an endotracheal tube larger or equal to size 8 is required. Cough reflex is minimal under general anesthesia, which may be an advantage during the procedure. However, operators should be careful not to put excessive pressure with the probe onto the airway. The disadvantage of the endotracheal tube is that is causes the bronchoscope to lie in the central position within the airway which creates difficulty to bring its tip in close proximity to the trachea or bronchus. Stations #1 and #2 require higher endo-tracheal tube placement. The use of the laryngeal mask airway can be helpful during EBUS-TBNA *(34)*.

4.2. Insertion to Visualization of Lymph Nodes

Although many centers have adopted this new modality for lymph node staging in lung cancer, little has been described concerning the actual procedure of EBUS-TBNA *(35)*. The bronchoscopist must be aware of the fact that the optical system of the CP-EBUS provides an 80° field of view at a 35° forward oblique angle. Therefore, in order to obtain a straight view, the bronchoscope needs to be slightly flexed down. One should also note that the ultrasound probe attached on the tip of the bronchoscope is not visible without the inflation of the balloon. Thus, the tip should not be accidentally forced onto the airway, which may cause trauma.

Since the endobronchial images obtained by the CP-EBUS are not as clear as the conventional flexible bronchovideoscope image, the authors prefer to examine the tracheobronchial tree using the conventional video bronchoscope prior to EBUS-TBNA. After achieving local anesthesia and conscious sedation, the CP-EBUS is inserted orally into the trachea. The bronchoscope should be passed through the vocal cords by visualizing the anterior angle of the glottis (**Fig. 8.8A**). Do not force the scope into the glottis, since the tip is not visible and may cause dislocation of the cartilage. The bronchoscope is introduced into the airway until the desired position is reached for EBUS imaging, and the balloon is inflated with normal saline to provide an ultrasonic transparent
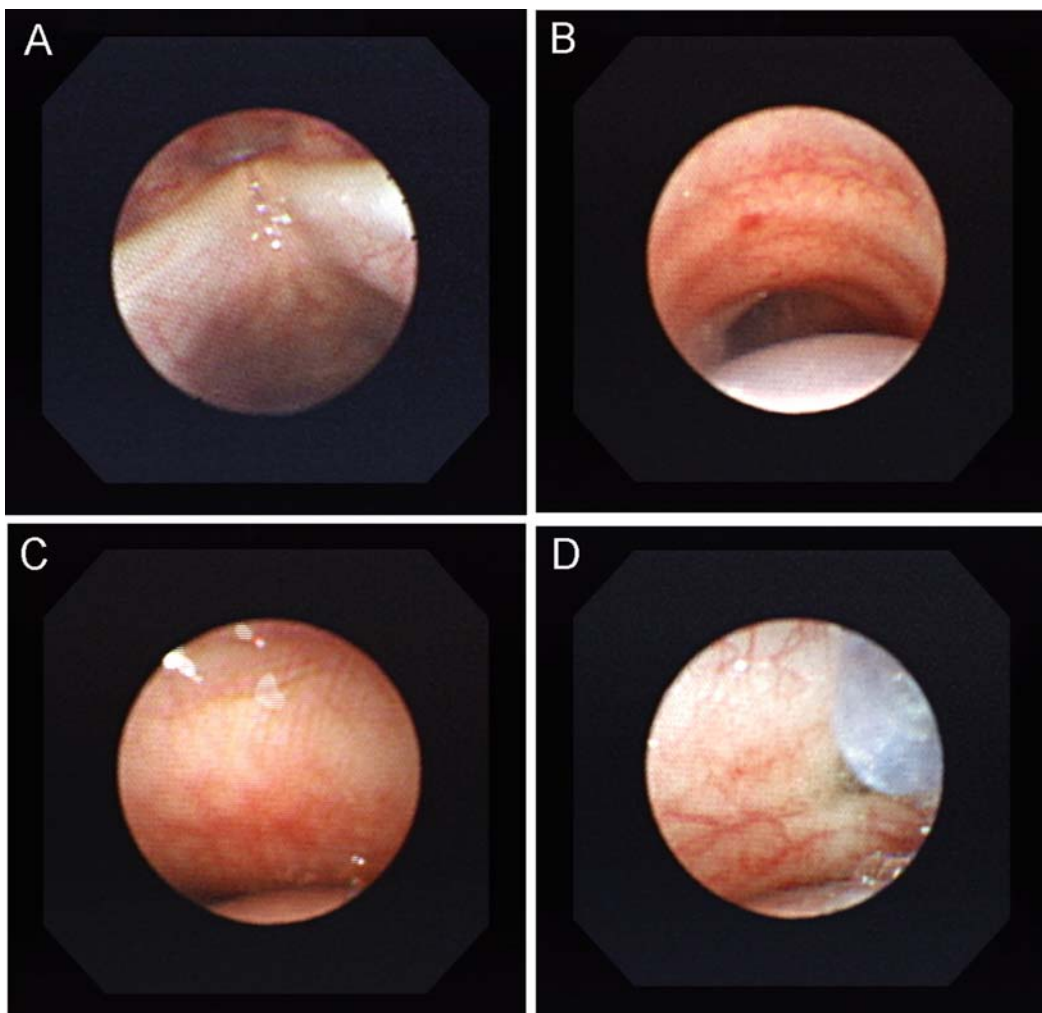
Fig. 8.8. Endobronchial images of the EBUS-TBNA procedure. (**A**) The bronchoscope is passed through the vocal cords by visualizing the anterior angle of the glottis. (**B**) The balloon is inflated with normal saline for maximum contact. (**C**) The tip is gently pressed onto the airway. (**D**) The needle is passed through the intercartilage space.

fluid coupling medium to achieve a maximum contact with the tissue of interest (**Fig. 8.8B**). The tip of the CP-EBUS is flexed and gently pressed onto the airway (**Fig. 8.8C**). A two-screen display is used to provide an endoscopic image of the airway and the corresponding ultrasound image underlying the tip of the bronchoscope simultaneously (**Fig. 8.9**). By moving the tip of the CP-EBUS in small motion, the lesion of interest is localized. The tip of the bronchoscope should be carefully adjusted so that the maximum diameter of the lymph node is visualized in the center of the ultrasound image. Ultrasonically visible vascular landmarks are used to identify the specific lymph node stations according to the Mountain classification system *(33)*. The Doppler mode is used to confirm and identify surrounding vessels as well as the blood flow within lymph nodes (**Fig. 8.10A**). The lymph node station, size, number and the ultrasound characteristics of each lymph node are recorded (**Fig. 8.10B**). Lymph nodes larger than 1 cm in short axis, round shaped, distinct margins without the presence of central hilar structures are suspicious for malignancy and need to be biopsied.

4.3. Endobronchial Ultrasound-Guided Transbronchial Needle Aspiration (EBUS-TBNA)

After identifying the lesion of interest with the CP-EBUS, the bronchoscopic image of the airway is simultaneously visualized to localize the insertion point of the needle. The tip should repeatedly be flexed up for contact for ultrasound image and down away from the airway for endoscopic visualization. Once the point of entry is decided using small landmarks on the
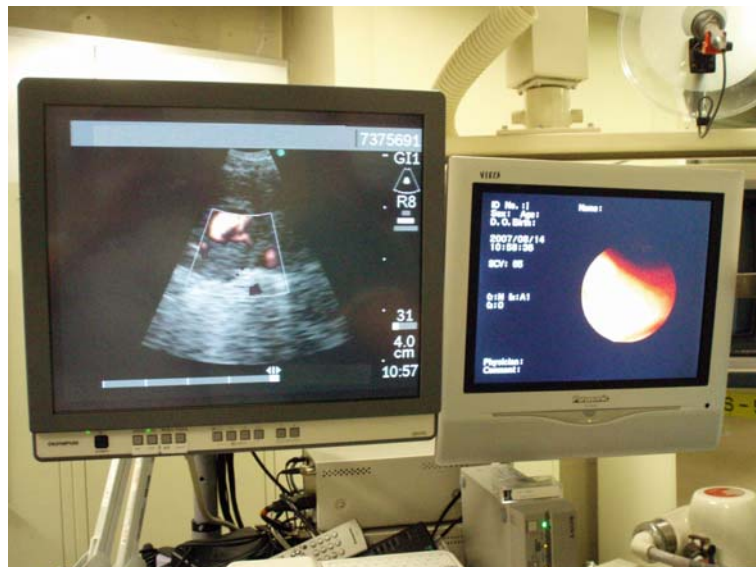
Fig. 8.9. Two-screen display of the endoscopic image and the corresponding ultrasound image.
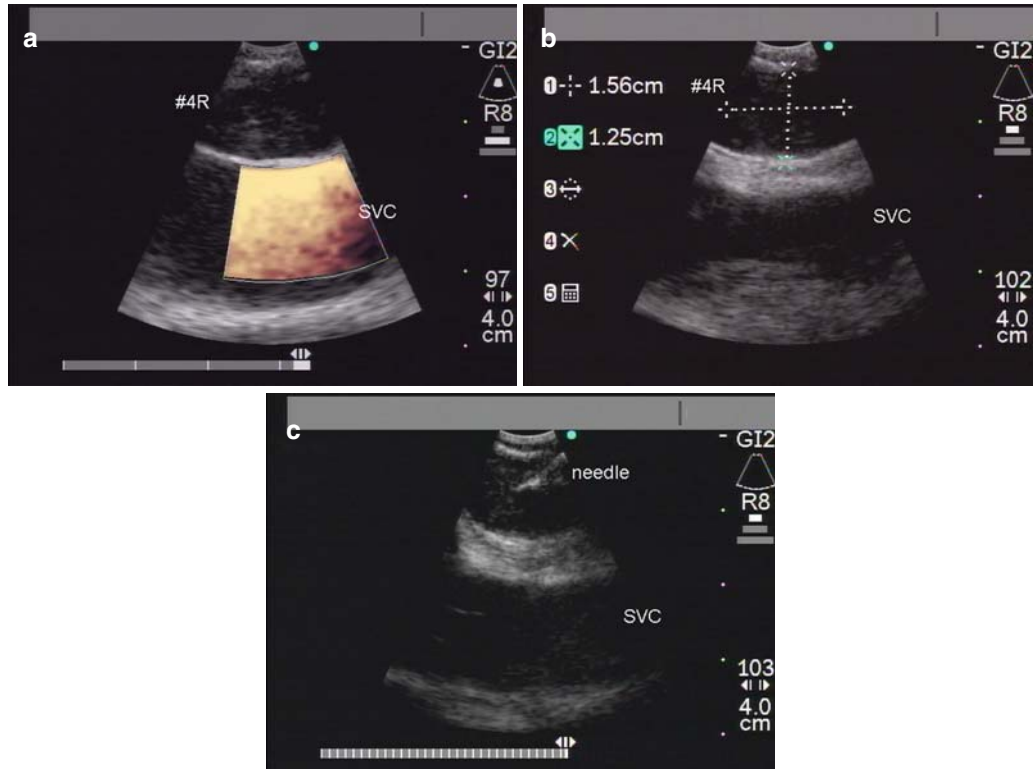
Fig. 8.10. A representative case of EBUS-TBNA. (**A**) EBUS scan demonstrates lymph node station #4R (#4R) and SVC. (**B**) EBUS-TBNA of lymph node station #4R. (**C**) The 22-gauge needle is seen within the lymph node.

airway, the dedicated 22-gauge TBNA needle is fastened onto the working channel of the bronchoscope (**Fig. 8.6**). The manipulation of the needle is a very important element of performing EBUS-TBNA, and is shown in Fig. 8.11. The tip of the bronchoscope is straightened to allow the sheath to easily come out of the channel. The sheath adjuster knob is loosened and the length of the sheath is adjusted so that the sheath can be visualized on endoscopic image. The tip of the bronchoscope is flexed up for contact and the lymph node is visualized again on ultrasound image. After the needle adjuster knob is loosened, real-time endobronchial ultrasound-guided transbronchial needle aspiration (EBUS-TBNA) can be performed (**Fig. 8.10C**). In case a cartilage ring is encountered during TBNA, the bronchoscope is moved slightly up or down so that the needle will go through the intercartilage space (**Fig. 8.8D**). After the initial puncture, the internal stylet is used to clear out the internal lumen, which may become clogged with bronchial membrane. The internal sheath is then removed and negative pressure is applied with the Vaclok syringe. After the needle is moved back and forth inside the lymph node, the needle is
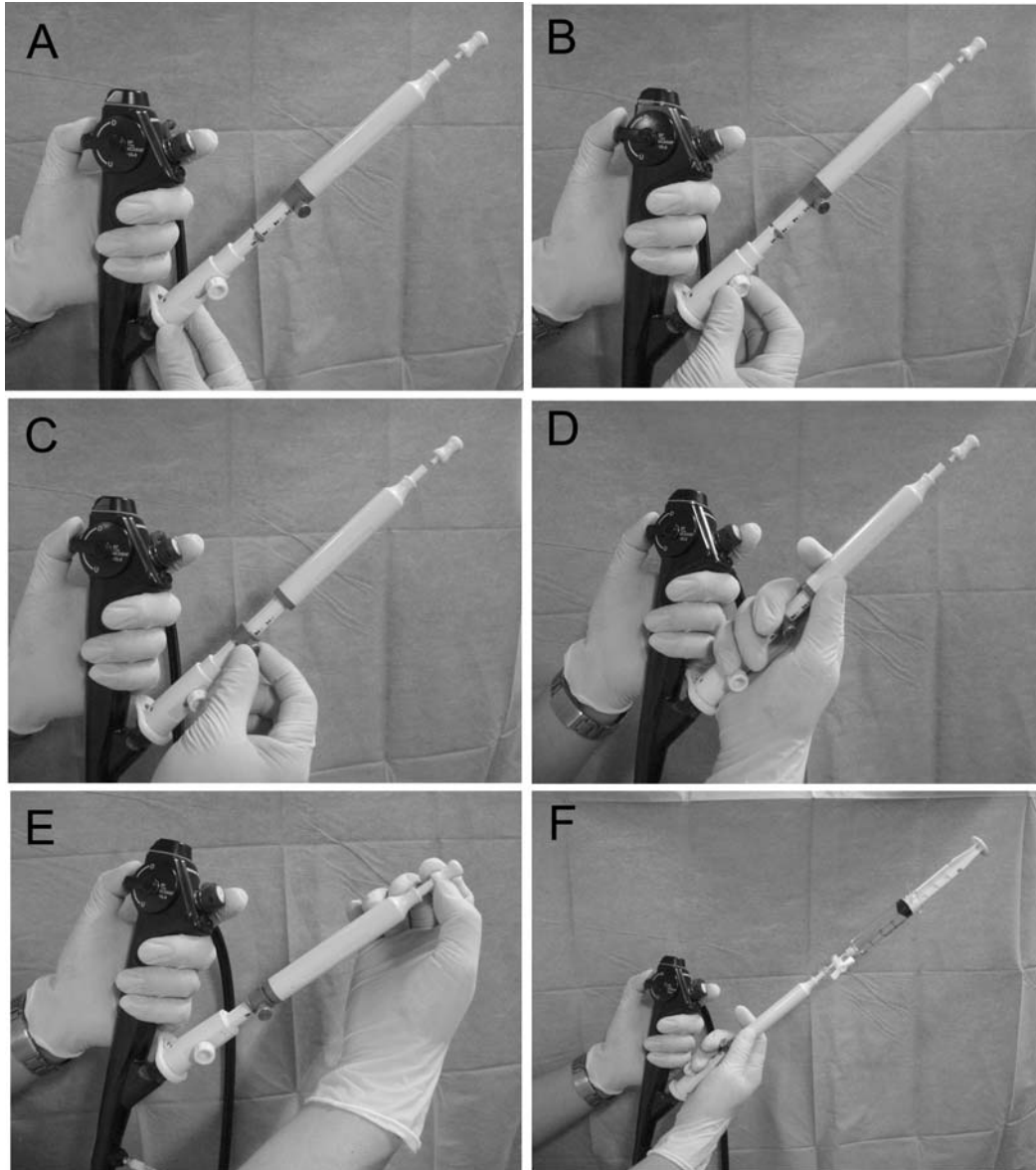
Fig. 8.11. Manipulation of the dedicated needle (NA-201SX-4022, Olympus, Tokyo, Japan). (**A**) The needle is fastened onto the working channel. (**B**) The sheath adjuster knob is loosened and the length adjusted. (**C**) The needle adjuster knob is loosened. (**D**) EBUS-TBNA is performed. (**E**) After the initial puncture, the internal stylet is used to clear out the internal lumen. (F) Negative pressure is applied with the Vaclok syringe.

retrieved and the internal sheath is used once again to push out the histological core. With this method, histological cores as well as cytological specimens can be obtained. The aspirated material is smeared onto glass slides, and smears are air-dried and immediately stained using Diff-Quik for immediate

interpretation by an on-site cytopathologist to confirm adequate cell material. Furthermore, Papanicolaou staining and light microscopy is performed. Histological cores are fixed with formalin and stained with hematoxylin and eosin. Immunohistochemistry can also be performed if needed.

4.4. Systematic Assessment of Mediastinal and Hilar Lymph Nodes

In patients with lung cancer, the mediastinal and hilar lymph nodes should be assessed in a systematic way so that all lymph nodes are identified and characterized. The basic principal is to identify the specific lymph node stations according to the Mountain classification system *(33)*. The authors prefer to start the lymph node assessment from the hilum (the side of the primary lung cancer), working up into the mediastinum and ending in the contralateral hilum. To avoid contamination and upstaging, EBUS-TBNA should be performed from the N3 nodes, followed by N2 nodes and N1 nodes.

Representative lymph node stations, bronchoscopic landmarks for optimal ultrasound visualization, and ultrasound images of lymph nodes and surrounding vessels are shown in **Fig. 8.12** and explained in detail below.

4.4.1. Station #12R

Advance the bronchoscope into the right main bronchus, the intermediate bronchus and into the middle and lower lobe bronchus. Press the tip against the lower lobe bronchus just proximal to where the basal bronchus branches. Station #12R can be visualized adjacent to the interlobar pulmonary artery.

4.4.2. Station #11R

Straighten and withdraw the bronchoscope to the intermediate bronchus. Turn to the two o'clock position and press the tip just distal the entrance of the right upper lobe bronchus. Station #11R can be visualized with the interlobar pulmonary artery running distal to the lymph node.

4.4.3. Station #10R

Withdraw the bronchoscope to the right main bronchus. Turn the tip to the three o'clock position and press the tip to visualize station #10R. Station #10R also lies just distal to station #7 along the right main bronchus. This part is visualized after identifying station #7 at the nine o'clock position at the right main bronchus.

4.4.4. Station #7

Station #7 can be visualized from either the right or the left main bronchus. On the right side, turn to the 12 o'clock position and press the tip against the right main bronchus where the main stem of the pulmonary artery is visualized. After confirmation with the Doppler mode, turn the tip to the nine o'clock position to visualize station #7. Lymph node distal to station #7 along the main bronchus is station #10R.
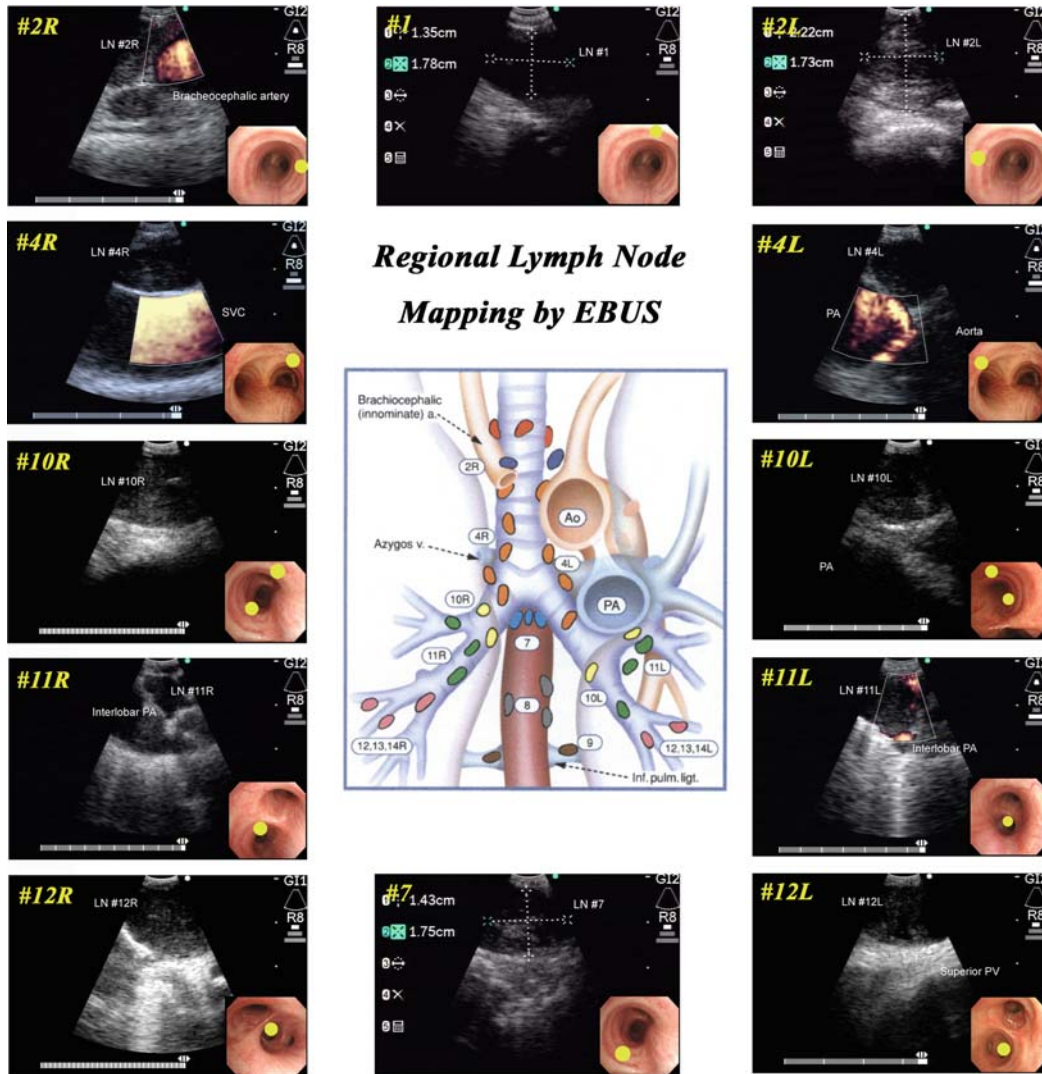
Fig. 8.12. Regional lymph node mapping by EBUS. EBUS images and bronchoscopic landmarks of representative lymph node stations are shown.

4.4.5. Station #4R

Withdraw the bronchoscope to the trachea looking straight towards the main carina. Turn to the two o'clock position and press the tip just proximal to the main carina. Look for the SVC and the azygos vein branching from the SVC. Station #4R is close to the SVC and the azygos vein.

4.4.6. Station #2R

While visualizing the SVC on the ultrasound image, withdraw the bronchoscope maintaining contact with the trachea at the two to three o'clock position. The SVC will bifurcate to the left and right bracheocephalic veins. Any lymph node distal to the bifurcation along the right side of the trachea is station #2R.

4.4.7. Station #1	Withdraw the bronchoscope further to visualize the right bracheo-cephalic artery. Any lymph node above the bifurcation of the right and left bracheocephalic vein along the trachea is station #1.
4.4.8. Station #2L	Once again visualize the right bracheocephalic artery on the ultrasound image. The tip is located at the two to three o'clock position in the upper trachea. Maintaining contact with the trachea and following the bracheocephalic artery on the ultrasound image, push the broncho-scope back distally into the trachea. By following the bracheocephalic artery, the tip will consequently be turned counterclockwise. At the mid-trachea level 12 o'clock position, the bracheocephalic artery will run into the aortic arch. The aortic arch is the vascular landmark for differentiating station #2L and #4R. Lymph node present on the left side of the trachea above the aortic arch is station #2L.
4.4.9. Station #4L	Facing the main carina, turn the bronchoscope to the 10 o'clock position and press the tip just proximal to the main carina and scan the area for station #4L. The aortic arch can be followed to the aorto-pulmonary window. The aortic arch is proximal and the left main pulmonary artery is distal.
4.4.10. Station #10L	Advance the bronchoscope into the left main bronchus at the 10 o'clock position by following the left pulmonary artery on ultrasound image. This is the area of station #10L. Similar to station #10R, #10L can be visualized distal to station #7 at the three o'clock position on the left main bronchus.
4.4.11. Station #11L	Further advancing the bronchoscope into the left lower lobe bronchus, press the tip at the two o'clock position in the carina of the upper and lower lobe bronchus. Station #11L is visualized adjacent to the interlobar pulmonary artery.
4.4.12. Station #12L	By advancing the bronchoscope further into the basal segmental bronchus or the upper lobar bronchus, station #12L can be visua-lized. However, due to the angle of the left upper lobe bronchus, oftentimes it is difficult to identify these nodes. There is no rule for the visualization of lymph nodes around the airway; however, the authors find that the whole mediastinum and hilum can be fully assessed by this method.

5. Indications

Indications for EBUS-TBNA are the assessment of mediastinal and hilar lymph nodes, diagnosis of lung tumors and diagnosis of

mediastinal tumors. All of the mediastinal lymph nodes, except for the subaortic and paraesophageal lymph nodes (levels 5, 6, 8, and 9), are assessable by EBUS-TBNA. Since the outer diameter of the tip of the CP-EBUS is 6.2 mm, stations #10 and #11 are approachable. However, part of station #12 is not accessible (**Fig. 8.7**).

From our experience there are various clinical applications of EBUS-TBNA in pulmonary medicine as shown in Table 8.4.

Table 8.4
Indications for EBUS-TBNA in Pulmonary Medicine

Indications in Pulmonary Medicine
Mediastinal and hilar lymph node staging of lung cancer
Mediastinal restaging of lung cancer
Diagnosis of lung tumors adjacent to large airwrays
Diagnosis of mediastinal tumor
Diagnosis of sarcoidosis
Diagnosis of lymphoma
Molecular evaluation of mediastinal lymph nodes

6. Lymph Node Staging by EBUS-TBNA

The treatment of non-small cell lung cancer (NSCLC) is determined by accurate definition of the stage. The status of the mediastinal lymph nodes is critical, if there are no distant metastases. Recently, a new ACCP evidence-based practice guideline (2nd edition) for invasive staging of lung cancer was published *(36)* only four years after the initial publication in *(37)*. This is due to the pace of discovery and development of technology in the diagnosis and management of lung cancer. EBUS-TBNA is one of the new technologies that has been newly introduced as evidence-based practice for invasive staging.

Conventional bronchoscopic TBNA would be the preferred method for patients with radiographic evidence of enlarged mediastinal lymph nodes that are adjacent to the airways, since bronchoscopy is usually performed in lung cancer patients and assessment for endobronchial lesions can be performed during the same procedure. However, conventional TBNA is a blind procedure preventing target visualization and, therefore, the yield for TBNA varies widely *(2)*. Before the availability of the

CP-EBUS, the radial probe EBUS has been used for TBNA guidance of mediastinal lymph nodes *(28, 29)*. Although a high diagnostic yield has been reported, it is still not a real-time procedure with target visualization. EBUS-TBNA has emerged as a new modality to overcome these problems allowing real-time TBNA of mediastinal and hilar lymph nodes.

The first article to report the diagnostic yield of EBUS-TBNA in a prospective study for mediastinal staging of lung cancer not only showed the high yield and safety of the procedure, but also the impact of this procedure on patient management *(10)*. In 105 patients, EBUS-TBNA was successfully performed to obtain samples from 163 lymph nodes. With respect to the correct prediction of lymph node stage, EBUS-TBNA had a diagnostic accuracy rate of 96.3 percent. In the 20 suspected lung cancer cases, mediastinal lymph node was used for tissue diagnosis of malignancy as well as staging. In addition, as a result of EBUS-TBNA, 29 mediastinoscopies, eight thoracotomies, four VATS, and nine CT-guided PCNB were avoided. EBUS-TBNA spared invasive staging procedures which had a major impact on patient management in lung cancer.

As explained previously, the reach of EBUS-TBNA is similar to the "gold standard" mediastinoscopy, but extending to the hilum. However, as so with mediastinoscopy, the subaortic and paraesophageal lymph nodes are not accessible. By combining EBUS-TBNA and EUS-FNA, most of the mediastinum can be evaluated *(12, 13, 16)*. EBUS has better access to anterior and superior mediastinal lymph nodes, whereas EUS has better access to posterior and inferior mediastinal lymph nodes. However, lymph node stations #5 and #6 need to be evaluated by VATS, anterior mediastinotomy, or extended mediastinoscopy *(5)*.

A study comparing EBUS-TBNA, CT, and PET for lymph node staging of lung cancer showed a high yield through the use of the CP-EBUS *(11)*. One–hundred-two potentially operable patients with proven (n = 96) or radiologically suspected (n = 6) lung cancer were included in the study. CT, PET, and EBUS-TBNA were performed prior to surgery to evaluate mediastinal and hilar lymph node metastasis. EBUS-TBNA was successfully performed in all 102 patients (mean age 67.8 years) from 147 mediastinal and 53 hilar lymph nodes. The sensitivities of CT, PET, and EBUS-TBNA for the correct diagnosis of mediastinal and hilar lymph node staging were 76.9 percent, 80.0 percent, and 92.3 percent, respectively. Specificities were 55.3 percent, 70.1 percent, and 100 percent. The diagnostic accuracies were 60.8 percent, 72.5 percent, and 98.0 percent. EBUS-TBNA was proven to have a high sensitivity as well as specificity compared to CT or PET, for mediastinal staging in patients with potentially resectable lung cancer.

The yield of EBUS-TBNA for mediastinal lymph node staging in lung cancer ranges from 89 percent to 98 percent (average 94.5%) *(8–16, 25)*. However, there have been no studies directly

comparing the "gold standard" mediastinoscopy and EBUS-TBNA for lymph node staging. There is an ongoing study comparing the yield of mediastinoscopy and EBUS-TBNA for mediastinal lymph node staging in patients with confirmed or suspected lung cancer *(38)*. In this prospective trial, patients with resectable lung cancer who require a mediastinoscopy for mediastinal staging underwent EBUS-TBNA followed by mediastinoscopy under general anesthesia in the same setting. The diagnostic yield was compared between the two procedures.

Out of 45 patients enrolled in the study, the diagnostic accuracy of EBUS-TBNA and mediastinoscopy for analysis of each lymph node station were 95.6 percent and 96.6 percent. The sensitivity, specificity, and diagnostic accuracy for the correct mediastinal lymph node staging for EBUS-TBNA and mediastinoscopy were 76.9 percent, 100 percent, 90.9 percent and, 84.6 percent, 100 percent and 93.9 percent, respectively. EBUS-TBNA was uneventful and there were no complications. These preliminary results show that EBUS-TBNA may reduce the number of mediastinoscopy needed for the staging of the mediastinum in NSCLC. However, due to the possibility of micrometastases, it is not clear that EBUS-TBNA will completely replace mediastinoscopy for mediastinal staging.

Restaging of the mediastinum is another area of growing interest for the treatment strategy of lung cancer. In case of advanced lymph node stage lung cancer, induction chemotherapy prior to surgical resection is an option. Mediastinoscopy is considered the "gold standard" in staging the mediastinum. However, remediastinoscopy can be technically difficult and is, therefore, not commonly performed. The ability of multiple, repeat biopsies using EBUS-TBNA allows restaging of the mediastinum after the introduction of chemotherapy.

One-hundred-twenty-four consecutive patients with tissue proven IIIA-N2 disease that were treated with induction chemotherapy underwent mediastinal restaging by EBUS-TBNA. Sensitivity, specificity, positive predictive value, negative predictive value and diagnostic accuracy of EBUS-TBNA for mediastinal restaging following induction chemotherapy were 76 percent, 100 percent, 100 percent, 20 percent and 77 percent, respectively. EBUS–TBNA is an accurate and minimally invasive test for mediastinal restaging of patients with NSCLC. However, due to the low negative predictive value, tumor negative findings should be confirmed by surgical staging *(39)*.

7. EBUS-TBNA for the Diagnosis of Lung Tumors

The current biopsy techniques widely performed for small lung nodules are bronchoscopic biopsy, percutaneous needle biopsy, and surgical resection either by VATS or thoracotomy.

Transbronchial biopsy (TBB) and TBNA for solitary lung nodules have been reported to have a high diagnostic yield in specialized centers (40). However, TBB and TBNA of peripheral nodules that are smaller than 3 cm have a lower diagnostic yield in general and, therefore, are not performed in most centers. CT-guided percutaneous needle biopsy has become a very important diagnostic technique and is widely being performed with good results. However, CT-guided needle biopsy of small peripheral lung nodules can be difficult and the tissue obtained is often nondiagnostic.

A new approach for diagnosing peripheral nodules has been recently highlighted. The radial probe EBUS has been shown to be effective with a high yield in EBUS-guided biopsy of peripheral nodules without the exposure of radiation (30, 31). However, these procedures are not "real-time" biopsies.

CP-EBUS can be used for the diagnosis of intrapulmonary nodules as well as mediastinal and hilar lymph nodes. The limitation is the reach of CP-EBUS which is dependent on the size of the bronchus. Usually the CP-EBUS can be inserted down to the lobar bronchus. For lower lobes, it can be inserted into the basal segmental bronchus. Lung tumors that are located adjacent to the airway within the reach of CP-EBUS can be diagnosed with EBUS-TBNA. We have experienced many cases where tumors are located adjacent to the bronchus, but conventional bronchoscopic biopsy procedures ended in inconclusive results (**Fig. 8.13**). Lung mass located in the apex adjacent to the trachea can also be easily diagnosed by EBUS-TBNA (**Fig. 8.14**).

8. EBUS-TBNA for the Diagnosis of Mediastinal Tumors

Diagnosis of mediastinal tumors is another area of potential use for EBUS-TBNA. We have experienced EBUS-TBNA of mediastinal tumors suspected of malignancy in various patients. Mediastinal processes diagnosed by EBUS-TBNA include bronchogenic cyst, malignant lymphoma, thymic cancer, mediastinal goiter, and chondrosarcoma (8). The role of EBUS-TBNA for the diagnosis of sarcoidosis has also been reported with a high yield (17, 23). There is also evidence that EBUS-TBNA can be used to diagnose lymphoma (24). Compared to diagnosis of lymph node metastasis in lung cancer patients, cytological diagnosis of mediastinal tumors is often-times more difficult. Histological diagnosis is the preferred choice. Although the current 22-gauge needle is capable of obtaining specimen suitable for histological examination, a larger needle that allows better tissue sampling is needed.
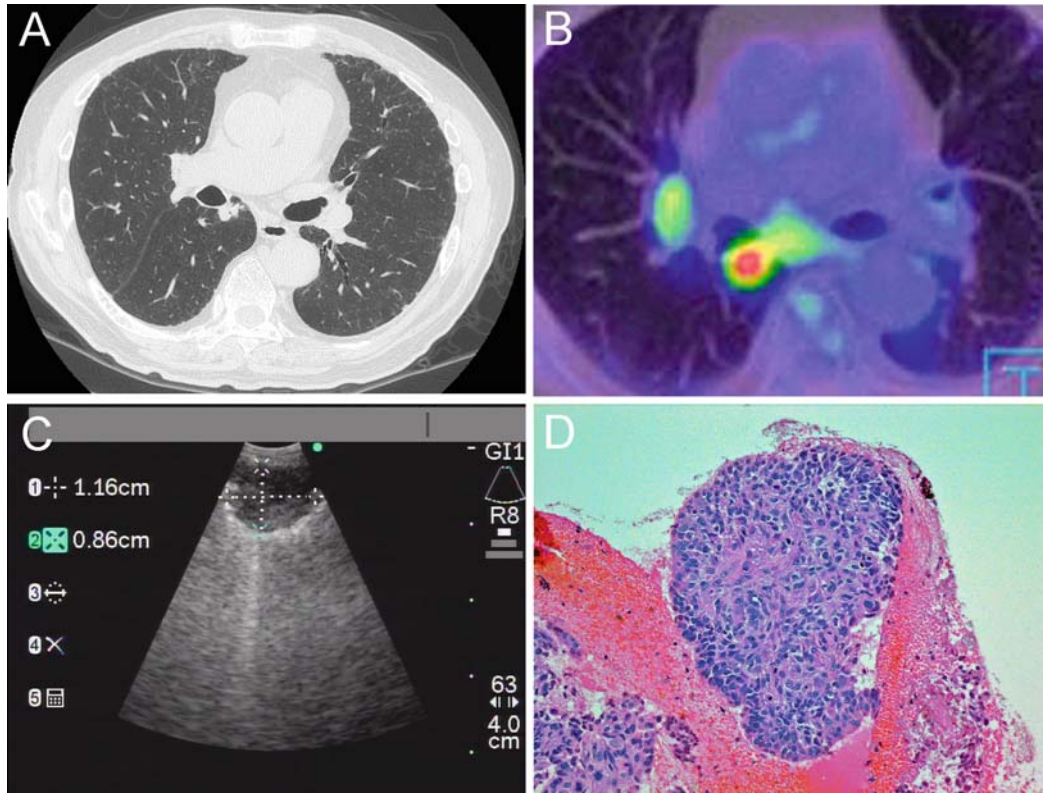
Fig. 8.13. Chest CT (**A**), methionine PET (**B**), EBUS scan (**C**), and histology (**D**) obtained in an 84-year-old patient with an intrapulmonary tumor suspected of lung cancer. (**A**) CT scan demonstrates a small lesion along the right lower lobe adjacent to the intermediate bronchus. (**B**) Methionine PET showed an accumulation in the lesion. (**C**) EBUS scan demonstrates the tumor 1.16 × 0.86 cm in diameter. (**D**) EBUS-TBNA resulted in the diagnosis of squamous cell carcinoma.

Currently newer technology is being incorporated into the endobronchial ultrasound system. The dedicated 21-gauge needle will be useful for obtaining larger histological samples. By combining the CP-EBUS to a high-end ultrasound scanner (Aloka alpha 5, Tokyo, Japan), an even clearer image and Doppler sonographic assessment will be possible (**Fig.** 8.15).

9. Complications

The authors have successfully performed EBUS-TBNA on more than 1,000 patients on an outpatient basis without major complications. EBUS-TBNA is considered a safe procedure and, to date, there are no major complications reported in the literature (7–25). However, complications related to the procedure are always
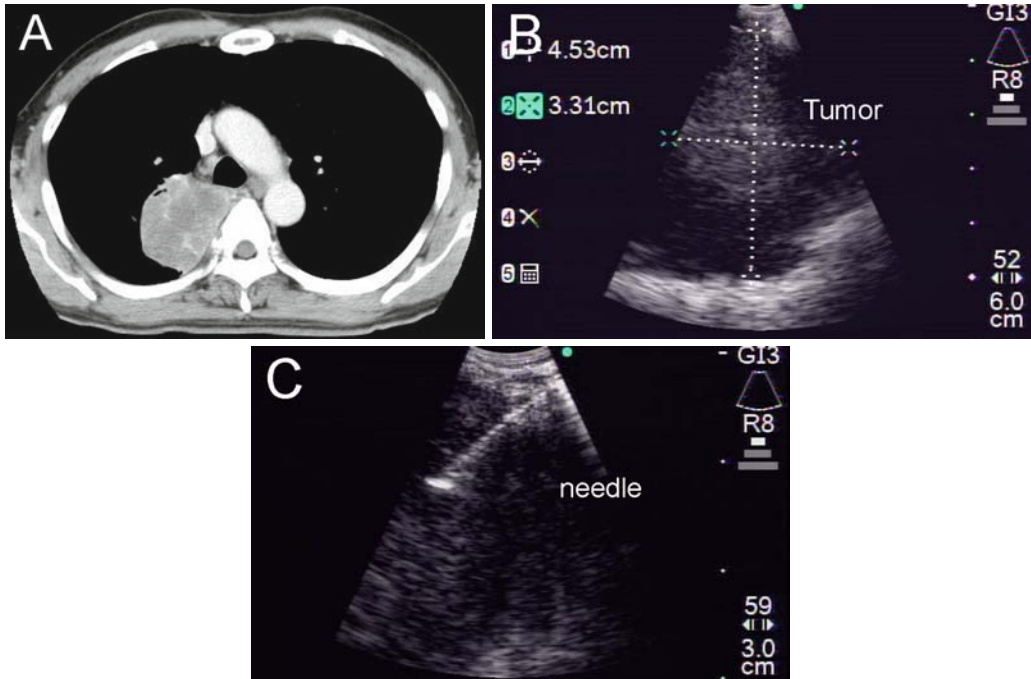
Fig. 8.14. Chest CT (**A**) and EBUS scans (**B, C**) obtained in a 69-year-old patient referred to our hospital for the diagnosis of a right lung tumor with negative study from bronchoscopy. (**A**) CT scan demonstrates a tumor along the trachea (Tumor). (**B**) EBUS scan demonstrates a 4.53 × 3.31 cm in diameter tumor. (**C**) EBUS-TBNA resulted in the diagnosis of adenocarcinoma. The 22-gauge needle is seen within the lymph node.

possible, and are similar to those in conventional TBNA, including bleeding from major vessels, pneumomediastinum, mediastinitis, peumothorax, bronchospasm and laryngospasm.

Bleeding from major vessels is unlikely due to the nature of the procedure, using real-time ultrasound guidance. Pneumomediastinum due to EBUS-TBNA is also unlikely since the needle used is 22-gauge and is too small to cause a significant leak of air into the mediastinum. The possibility of pneumothorax is very low because the pleura is rarely punctured by EBUS-TBNA.

Conclusion

CP-EBUS has emerged as a new instrument that enables real-time TBNA of the mediastinum, hilum as well as intrapulmonary nodules. It is a minimally invasive and safe procedure that is useful and effective for the diagnosis and staging of NSCLC. Further prospective data describing diagnostic yield of EBUS-TBNA

Fig. 8.15. The high-end ultrasound scanner (Aloka alpha 5, Tokyo, Japan) in combination with the convex probe endobronchial ultrasound.

compared to conventional tools will be needed to support the value of this new modality. However, from our current experience, CP-EBUS can be used as the first test for patients with undiagnosed mediastinal lymphadenopathy either with or without lung mass. It is an attractive procedure allowing simultaneous lymph node staging as well as diagnosis.

References

1. American Cancer Society. Cancer facts and figures, 1998. Atlanta, GA: American Cancer Society, 1998.

2. Silvestri GA, Gould MK, Margolis ML, et al. Noninvasive staging in non-small cell lung cancer: ACCP evidenced-based clinical practice guidelines (2nd edition). Chest. 2007; 132: 178–201.

3. Bhutani MS, Hawes RH, Hoffmann BJ. A comparison of the accuracy of echo features during endoscopic ultrasound (EUS) and EUS-guided fine-needle aspiration for diagnosis of malignant lymph node invasion. Gastrointest Endosc. 1997; 31: 550–553.

4. Okamoto H, Watanabe K, Nagatomo A, et al. Endobronchial ultrasonography for mediastinal and hilar lymph node metastases of lung cancer. Chest. 2002; 121: 1498–1506.

5. Yasufuku K, Fujisawa T. Staging and diagnosis of non-small lung cancer: Invasive modalities. Respirology. 2007; 12: 173–183.

6. Margaritora S, Cesario A, Galetta D, Granone P. Mediastinoscopy as a standardized procedure for mediastinal lymph-

node staging in non-small cell carcinoma. Do we have to accept the compromise? Eur J Cardiothorac Surg. 2001; 20: 652–654.

7. Yasufuku K, Chhajed PN, Sekine Y, et al. Endobronchial ultrasound using a new convex probe: a preliminary study on surgically resected specimens. Oncol Rep. 2004; 11: 293–296.

8. Yasufuku K, Chiyo M, Sekine Y, et al. Real-time endobronchial ultrasound guided transbronchial needle aspiration of mediastinal and hilar lymph nodes. Chest. 2004; 126: 122–128.

9. Krasnik M, Vilman P, Larsen SS, Jacobsen GK. Preliminary experience with a new method of endoscopic transbronchial real time ultrasound guided biopsy for diagnosis of mediastinal and hilar lesions. Thorax. 2003; 58: 1083–1086.

10. Yasufuku K, Chiyo M, Koh E, et al. Endobronchial ultrasound guided transbronchial needle aspiration for staging of lung cancer. Lung cancer. 2005; 50:347–354.

11. Yasufuku K, Nakajima T, Motoori K, et al. Comparison of endobronchial ultrasound, positron emission tomography, and computed tomography for lymph node staging of lung cancer. Chest. 2006; 130: 710–718.

12. Rintoul RC, Skwarski KM, Murchison JT, et al. Endobronchial and Endoscopic ultrasound-guided real-time fine-needle aspiration for mediastinal staging. Eur Respir J. 2005; 25: 416–421.

13. Vilmann P, Krasnik M, Larsen SS, et al. Transesophageal Endoscopic ultrasound-guided fine-needle aspiration (EUS-FNA) and endobronchial ultrasound-guided transbronchial needle aspiration (EBUS-TBNA) biopsy: a combined approach in the evaluation of mediastinal lesions. Endoscopy. 2005; 37: 833–839.

14. Herth FJ, Ernst A, Eberhardt R, et al. Endobronchial ultrasound-guided trasnbronchial needle aspiration of lymph nodes in the radiologically normal mediastinum. Eur Respir J. 2006; 28: 910–914.

15. Herth FJ, Eberhardt R, Vilmann P, et al. Real-time endobronchial ultrasound guided transbronchial needle aspiration for sampling mediastinal lymph nodes. Thorax. 2006; 61: 795–798.

16. Herth FJ, Rabe KF, Gasparini S, Annema JT. Transbronchial and transoesophageal (ultrasound-guided) needle aspirations for the analysis of mediastinal lesions. Eur Respir J. 2006; 28: 1264–1275.

17. Wong M, Yasufuku K, Nakajima T, et al. Endobronchial ultrasound: new insight for the diagnosis of sarcoidosis. Eur Respir J. 2007; 29: 1–6.

18. Nakajima T, Yasufuku K, Suzuki M, et al. Assessment of epidural growth factor receptor mutation by endobronchial ultrasound-guided transbronchial needle aspiration. Chest 2007; 132: 597–602.

19. Nakajima T, Yasufuku K, Shibuya K, Fujisawa T. Endobronchial ultrasound-guided transbronchial needle aspiration for the treatment of central airway stenosis caused by a mediastinal cyst. Eur J Cardiothorac Surg. 2007; 32: 538–540.

20. Yasufuku K. Endobronchial Ultrasound guided transbronchial needle aspiration for the evaluation of the mediastinum. Kyoubu Geka. 2007; 60: 711–717.

21. Nakajima T, Yasufuku K, Iyoda A, et al. The evaluation of lymph node metastasis by endobronchial ultrasound-guided transbronchial needle aspiration: crucial for selection of surgical candidates with metastatic lung tumors. J Thorac Cardiovasc Surg. 2007; 134: 1485–1490.

22. Yasufuku K, Nakajima T, Chiyo M, et al. Endobronchial Ultrasound: Current status and future directions. J Thorac Oncol. 2007; 2: 970–979.

23. Garwood S, Judson MA, Silvestri G, et al. Endobronchial ultrasound for the diagnosis of pulmonary sarcoidosis. Chest. 2007; 132: 1298–1304.

24. Kennedy MP, Jimenez CA, Bruzzi JF, et al. Endobronchial Ultrasound Guided Transbronchial Needle Aspiration in the Diagnosis of Lymphoma. Thorax. 2008; 63(4): 360–365.

25. Vincent BD, El-Bayoumi E, Hoffman B, et al. Real-time endobronchial ultrasound-guided transbronchial lymph node aspiration. Ann Thorac Surg. 2008; 85: 224–230.

26. Hurter T, Hanrath P. Endobronchial sonography: feasibility and preliminary results. Thorax. 1992; 47: 565–567.

27. Baba M, Sekine Y, Suzuki M, et al. Correlation between endobronchial ultrasonography (EBUS) images and histologic findings in normal and tumor-invaded bronchial wall. Lung Cancer. 2002; 35: 65–71.

28. Herth, FJ, Becker, HD, Ernst, A. Ultrasound-guided transbronchial needle aspiration: an experience in 242 patients. Chest. 2003; 123: 604-607.

29. Herth F, Becker HD, Ernst A. Conventional vs endobronchial ultrasound-guided transbronchial needle aspiration: a randomized trial. Chest. 2004; 125: 322–325.

30. Kurimoto N, Murayama M, Yoshioka S, et al. Analysis of the internal structure of peripheral pulmonary lesions using endo-bronchial ultrasonography. Chest. 2002; 122: 1887–1894.

31. Kikuchi E, Yamazaki K, Sukoh N, et al. Endobronchial ultrasonography with guide-sheath for peripheral pulmonary lesions. Eur Respir J. 2004; 24: 533–537.

32. Ono R, Suemasu K, Matsunaga T. Broncho-scopic ultrasonography in the diagnosis of lung cancer. Jpn J Clin Oncol. 1993; 23: 34–40.

33. Mountain CF, Dresler CM. Regional lymph node classification for lung cancer staging. Chest. 1997; 111: 1718–1723.

34. Sarkiss M, Kennedy M, Riedel B, et al. Anesthesia technique for endobronchial ultrasound-guided fine needle aspiration of mediastinal lymph nodes. J Cardiothorac Vasc Anesth. 2007; 21: 892–896.

35. Herth F, Krasnik M, Yasufuku K, et al. Endobronchial Ultrasound-guided Trans-bronchial Needle Aspiration – How I Do It. J Bronchol. 2006; 13(2): 84–91.

36. Detterbeck FC, Jantz MA, Wallace M, et al. Invasive mediastinal staging of lung cancer: ACCP evidence-based clinical practice guidelines (2nd edition). Chest. 2007; 132: 202S–220S.

37. Detterbeck FC, DeCamp MM, Kohman LJ, Silvestri GA. Invasive staging: The guide-lines. Chest. 2003; 123:167S–175S.

38. Ernst A, Anantham D, Eberhardt R, Krasnik M, Herth FJ. Diagnosis of mediastinal ade-nopathy-real-time endobronchial ultra-sound guided needle aspiration versus mediastinoscopy. J Thorac Oncol. 2008; 3(6): 577–582.

39. Herth FJ, Ernst A, Yasufuku K, et al. Endobronchial ultrasound with transbron-chial needle aspiration for restaging the mediastinum. J Thorac Oncol. 2007; 2: 361S–362S.

40. Iyoda A, Baba M, Shibuya K, et al. Trans-bronchial fine needle aspiration cytological examination: a useful tool for diagnosing primary lung cancer. Thorac Cardiovasc Surg. 2006; 54: 117–119.

Chapter 9

Comparing EUS and EBUS-Guided Needle Aspirations

Armin Ernst and Mandeep S. Sawhney

Endobronchial ultrasound has established itself as a powerful tool for guiding transbronchial needle aspiration and, therefore, the diagnosis of thoracic lesions and staging of cancer. All aspects of EBUS TBNA are described in detail in other chapters of this book. It is important to consider EUS FNA in this context. Gastroenterologists have been using ultrasound-guided needle aspirations for longer than pulmonologists have been using EBUS.

EUS FNA has established itself not just for diagnosis of abdominal lesions, but also extensively for the diagnosis of lesions within the thorax. This obviously does make sense, since the esophagus runs alongside the trachea and many mediastinal abnormalities are within reach of the EUS FNA procedure.

Many times, bronchoscopic procedures are preceded by similar technology offered within the GI tract. The main reason for this phenomena is the fact that instruments can usually be larger when used through the esophagus rather than when being advanced though the airways. The need for additional miniaturization to allow ventilation around the instruments, as well as the ability to advance into more distal airways, generally adds years of development time. The size difference is easily visible when comparing EUS FNA and EBUS TBNA scopes side by side (**Fig.** 9.1). It is clear that the basic architecture of the instruments is the same, with a linear ultrasound scanner at the distal end and an oblique working channel used for needle aspiration using dedicated needle systems.

Similar to endobronchial ultrasound, two basic techniques for ultrasound examinations are available.

Fig. 9.1. Example of an EUS and EBUS scope next to each other. Note that the EUS scope is significantly larger, but similar in appearance and architecture.

Radial scanning is used mainly to assess paraesophageal and wall abnormalities within the GI tract, as for example is needed for esophageal cancer staging (**Fig.** 9.2 MS). The image is obtained using a 12 Mhz echoendoscope and is similar to the images obtained with the radial EBUS miniprobe.

Originally, radial EUS scanning was used to find and biopsy mediastinal lymph nodes, but similar to endobronchial applications, linear scanning has for the most part replaced this approach.

Fig. 9.2. Normal mediastinum using a radial echoendoscope with transducer located in the mid-esophagus. The spine [posterior], descending aorta (*right*), azygos vein (*left*) and air artifact from the bronchus [anterior] are seen.

Linear esophageal scanning is probably of more interest to the pulmonary enodoscopist, as it resembles EBUS TBNA. The GI instrument has a 7.5 Mhz scanner and is frequently coupled with a full capability ultrasound processor and imaging system. The needles most frequently used are 22-gauge dedicated systems similar to the EBUS TBNA needles that require fixation to the instrument handle at the introduction site. The puncture is done under real-time guidance. EUS FNA is generally performed in a standardized fashion on an outpatient basis under moderate sedation and usually takes 20–30 min of procedure time.

Similar to EBUS TBNA, EUS FNA can be used to diagnose not just cancers, but also hematologic malignancies such as lymphoma and benign lymph node enlargement caused by sarcoidosis. Gastroenterologists generally avoid needle biopsies of suspected cysts for fear of infection and mediastinitis.

The biggest difference between EBUS TBNA and EUS FNA is the reach of stations for cancer staging. Since EUS FNA must follow the esophageal trajectory, hilar station and precarinal stations cannot be accessed. Another problem may be station 4R if the esophagus has a more left-sided location. However, the GI approach also has significant advantages of over EBUS TBNA: EUS FNA allows for sampling of station 8 nodes (**Fig.** 9.3), as well as sampling of the left adrenal (**Fig.** 9.4) and left lobe of the liver (**Fig.** 9.5), enabling partial

Fig. 9.3. 64-year-old was found to have a right hilar lung mass. On CT scan of the chest, no enlarged lymph nodes were found. A lymph node was seen at station 8 [R] using a linear echoendoscope with the transducer located in the lower third of the esophagus. The lymph node was hypoechoic, homogenous with well-defined border. Fine-needle-aspirate of this node was performed and cytology was consistent with carcinoma. Based on these findings the patient was offered neo-adjuvant therapy.
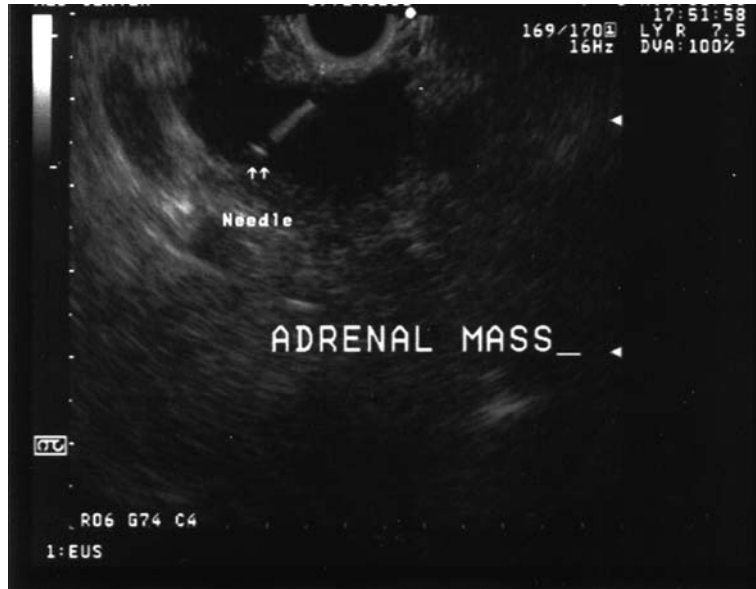
Fig. 9.4. 70-year-old man presented with hemoptysis. On CT scan a large left lower lobe lung mass was seen. The left adrenal gland was noted to be irregular and enlarged. Fine needle aspiration of left adrenal mass was performed using a linear echoendoscope with transducer located along the greater curvature of the stomach. Aspirating needle is seen within the adrenal mass. Cytology from the adrenal mass was consistent with carcinoma. A tissue diagnosis and staging was thus obtained from a single procedure.

Fig. 9.5. 88-year-old found to have a right upper lobe mass on a routine preoperative chest X-ray obtained prior to prostate surgery. CT scan showed possible metastasis in the liver. A metastasis was seen in the left lobe of the liver using a linear echoendoscope with the transducer located along the lesser curvature of the stomach. Fine-needle-aspiration was performed. Cytology was consistent with carcinoma. A tissue diagnosis and staging was thus obtained from a single procedure.

extrathoracic staging of cancer patients. The overlapping and complementary regions of access between EUS FNA and EBUS TBNA are shown in **Fig. 8.8**.

EUS FNA has a proven track record for evaluating mediastinal abnormalities and cancer staging. Multiple publications have found that EUS FNA is beneficial after nondiagnostic conventional TBNA and that it can prevent unnecessary surgical staging procedures or futile thoracotomies aimed at resection. The sensitivity and specificity for lymph node sampling in highly selected patient populations (proven or presumed lung cancer with either CT or PET abnormalities in the mediastinum) have been reported in the 0.7–1.0 range and as 1.0, respectively. EUS FNA and mediastinoscopy have been compared in a randomized fashion as first-line mediastinal staging procedures and, as expected, many surgical procedures could be avoided if EUS FNA were used as a first-line approach.

Most of these studies do not take into account the reach beyond cervical mediastinoscopy. Less is known about how EUS FNA compares to mediastinoscopy when evaluating a patient with nonenlarged lymph nodes. Similar to EBUS TBNA the negative predictive value of samples not containing tumor cells is too low and such results need to be followed with more definitive procedures.

The current body of literature supports EUS FNA as a highly viable option for a first-line staging procedure. Realistically, though, gastroenterologists are not primary care givers for patients with thoracic malignancies and do not have easy access to the patient population. Additionally, not all relevant thoracic lymph node stations can be reached and maybe most importantly, most patients still do need a bronchoscopy before any surgical procedure is planned in order to define the presurgical anatomy, perform additional procedures such as transbronchial biopsy or bronchia alveolar lavage and ensure that no endobronchial disease is present. Therefore, the discussion about which endoscopic staging technology is the superior one remains ongoing.

The most intriguing question currently asked is if EUS FNA and EBUS TBNA should be looked at as complementary procedures, rather than competitive ones. Taking it a step further: should EUS- and EBUS-guided biopsy be performed in the same setting as a preferred first-line staging procedure for lung cancer patients? Intuitively, it would make sense. The bronchoscopic component would allow for mandatory airway evaluation as well as the performance of additional procedures as indicated, for example transbronchial biopsy. The hilar lymph nodes can be accessed as well as anterior tracheal nodes and station 4R. From the esophageal route the additional reach to stations 8 and 9 as well as subdiaphragmatic abnormalities would be very attractive. A combined procedure would also be attractive from a logistical point of view by minimizing patient inconvenience and resource use associated with two independent procedures.

Preliminary data lends credence to this thought. In a trial comparing EUS FNA and EBUS TBNA a post hoc analysis found that the combined yield compared favorably with historical results reported for cervical mediastinoscopy. In that trial by Eberhardt, et al. the regions beyond the reach of the surgical mediastinoscope were not even considered, an ability that could sway any opinion towards endoscopic first-line staging.

Obviously, more data evaluating a combined approach is needed, but endoscopic staging using modern technology and image guidance certainly has a good chance of becoming a first-line diagnostic and staging procedure. It is unclear in this context which procedure should be performed first (EUS vs. EBUS) and if nodes within reach of both should only be punctured with one modality.

One of the most important issues to address is that of training and credentialing. It seems highly unlikely that institutions may have skilled GI and pulmonary echoendoscopists in the first place and then arrange for them to be in the same procedure room at the same time serving the same patient. Endoscopy started out as bronchoesophagology and we may want to consider moving back to this model. Endoscopy in the GI tract and within the airways are very similar procedures and the necessary basic skill sets can be found in advanced GI as well as pulmonary endoscopists. With proper additional training and oversight it should be more than feasible for bronchoscopists to add EUS FNA to their armamentarium and vice versa. Cardiologists have certainly proven that even non-endoscopists can safely and expertly use an esophageal echoendoscope. This potential trend would be supported by the fact that processing and ultrasound equipment is becoming compatible, making combined procedures much more easily arranged.

As procedural medicine is becoming less and less invasive and is starting to replace older conventional surgical procedures, it should be a reasonable assumption that centers will perform around thoracic oncology management. In those centers hybrid endoscopy is the next logical step in patient care.

References

1. Wiersema M, Wiersema L, Khusro Q, et al. Combined endosonography and fine-needle aspiration cytology in the evaluation of gastro- intestinal lesions. Gastrointest Endosc 1994;40:199–206.

2. Herth FJF, Rabe KF, Gasparini S, Annema JT. Transbronchial and transoesophageal (ultrasound guided) needle aspirations for the analysis of mediastinal lesions. Eur Resp J 2006;28:1264–1275.

3. Tournoy KG, Praet MM, Van Maele G, van Meerbeeck JP. Esophageal endoscopic ultrasound with fine- needle aspiration with an on- site cytopathologist: high accuracy for the diagnosis of mediastinal lymphadenopathy. Chest 2005;128:3004–3009.

4. Vilman P, Krasnik M, Larsen SS, Jacobson GK, Clementson P. Transesophageal endoscopic ultrasound- guided fine- needle aspiration (EUS FNA) and endobronchial

ultrasound- guided transbronchial needle aspiration (EBUS TBNA) biopsy: a combined approach in the evaluation of mediastinal lesions Endoscopy 2005;37:833–839.

5. Herth FJF, Lunn W, Eberhardt R, Becker HD, Ernst A. Transbronchial versus transesophageal ultrasound-guided aspiration of enlarged mediastinal lymph nodes. Am J Resp Crit Care Med 2005;171:1164–1167.

6. Annema JT, Rabe KF. State of the art lectures: EUS and EBUS in pulmonary medicine. Endoscopy 2006;38:S118–122.

7. Janes SM, Spiro SS. Esophageal endoscopic ultrasound/Endobronchial ultrasound-guided fine needle aspiration. A new dawn for the respiratory physician? Am J Resp Crit Care Med 2007;175:297–299.

Chapter 10

Ultrasound as a Therapeutic Instrument

Mark Krasnik

Since the first publication describing EUS TBNA was published the developments have been tremendous. Endoscopic ultrasound as a tool in diagnosing and staging is a relatively new method first described in 1992 in Copenhagen. Since then different methods of endoscopic ultrasound have gained a footing in the evaluation of lung cancer patients.

The primary aim of introducing EUS FNA in this area was to access the mediastinum posterior and the left adrenals. During the first examinations we learned that, via the oesophagus, we could also access lymph nodes at station 7 and often at stations 2 and 4 on both sides. The feasibility of this method has been established over the years and, in 2007, a systematic review and meta-analysis in Chest *(1)* involving 18 studies showed a pooled sensitivity of EUS FNA of 83 percent and a pooled sensitivity of 97 percent. We therefore were convinced that we had a method that could compete with mediastinoscopy to some extent. After that several studies using EUS in different contexts were published. When Annema *(2)* compared EUS FNA to mediastinoscopy it was seen that the combination of EUS-FNA and mediastinoscopy identified more patients with tumor invasion or lymph node metastases (36%), compared with either mediastinoscopy alone (20%) or EUS-FNA (28%) alone. This was not surprising when observing the areas in the mediastinum that are covered by the different methods. In the same year Larsen, et al. *(3)* also indicated that EUS-FNA and mediastinoscopy were complementary.

One of the advantages of EUS is also that it is possible to obtain tru-cut biopsies of lesions in the mediastinum. However, in point of view of endoscopic ultrasound the anterior part of the mediastinum was still unreachable.

1. Endobronchial Ultrasound (EBUS)

This problem was solved with the miniprobe which made it possible to demonstrate lymph nodes in the anterior parts of the mediastinum and the hilar regions.

1.1. EBUS and the Bronchial Wall

It soon became obvious that it was possible to visualize the bronchial wall and structures surrounding the airways and, as such, have the significant potential to add to diagnostic bronchoscopies *(4, 5)*. It became possible to recognize if changes in the mucosa were carcinoma in situ or an invasive cancer. The probe also made it possible to determine if cancer in other structures in the mediastinum invaded the bronchial tree *(6–8)*. The consequence of using the EBUS probe in daily routine is seen in **Fig.** 10.1.

With the use of EBUS in 2,446 patients Felix Herth, et al. *(9)* showed that in 43 percent of the cases where EBUS was used, it resulted in a change of therapy or better guidance of the intervention. The indications for these bronchoscopies were mechanical tumor destruction, stent placement, Nd: YAG laser resection Argon-plasma coagulation, brachytherapy, foreign body removal, and abscess drainage.

Changes in treatment were, for example, the use of longer stents for endoscopically unappreciated submucosal or parabronchial tumor extension. Tumor debridement with laser or argon-plasma coagulation was stopped when EBUS demonstrated close relationships with vessels (**Fig.** 10.2). When used for brachytherapy in patients with suspected early stage carcinoma, EBUS revealed local disease extension or lymph node metastasis which escaped all other imaging methods in 28 percent of patients (**Fig.** 10.3).
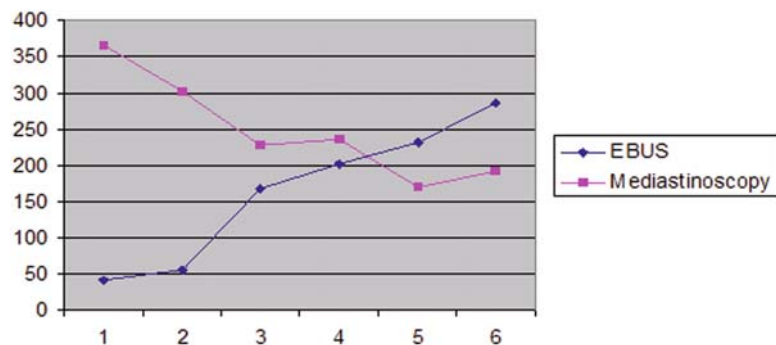
Fig. 10.1. The use of EBUS and mediastinoscopy. (Thoraxklinik, Heidelberg).
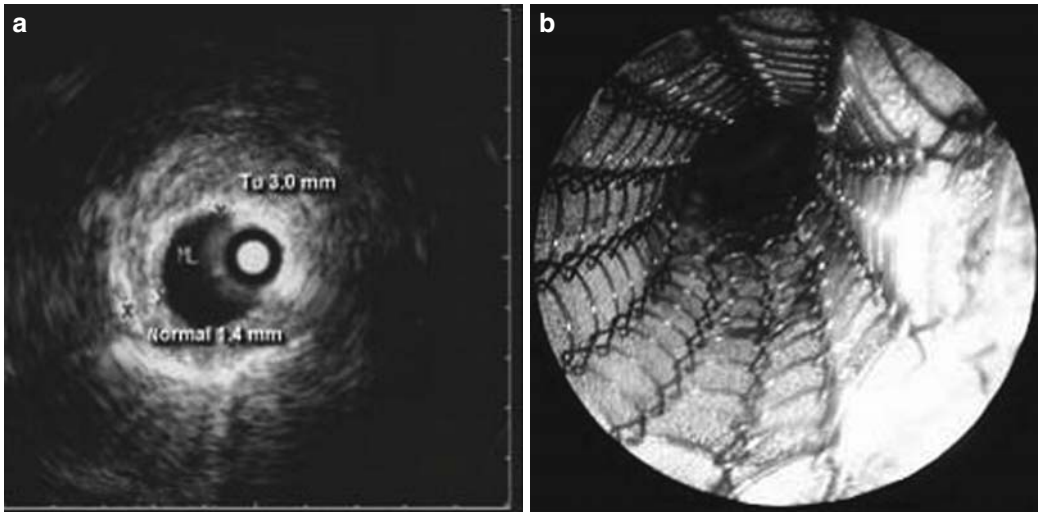
Fig. 10.2. (**a**) Endobronchial ultrasound image of a bronchus adjacent to an area with endobronchial obstruction. Submucosal tumor extension, which was not visible with conventional endoscopy, is documented. Normal thickness of the wall is compared to the infiltrated area. (**b**) Endoscopic image of the stented airway (Ultraflex, Boston Scientific, Natick, MA, USA). A longer stent was used covering the airway portion involved with submucosal disease. Tu: tumor; X: border of the bronchial wall.
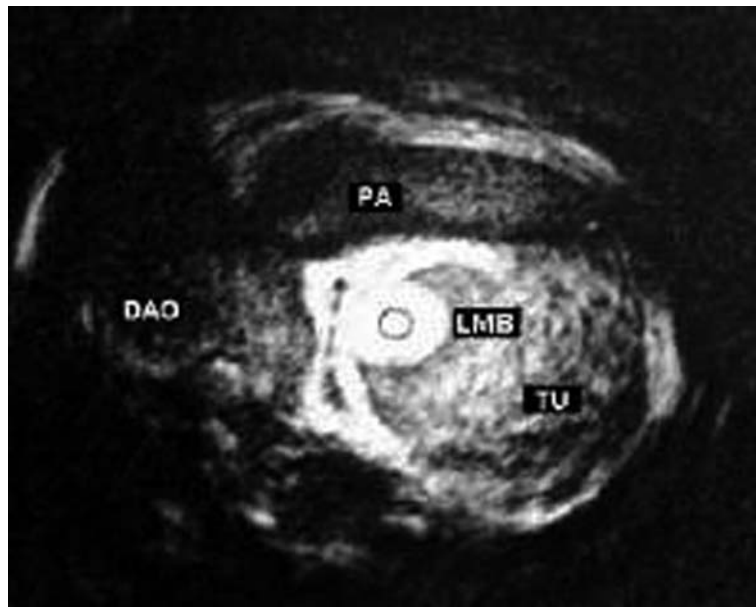
Fig. 10.3. Endobronchial ultrasound image of a left mainstem bronchus (LMB) obstructed by malignant tumor (TU). The tumor is growing through the wall in very close proximity to the pulmonary artery (PA). Thermal tumor destruction can lead to the formation of a fistula and life threatening bleed. The descending aorta (DAO) is also shown.

1.2. EBUS in Staging

When used in staging EBUS-guided TBNA, when compared to traditional TBNA, showed improved results. The yield in a randomized trial *(10, 11, 12)* showed improvement from 66 percent to 85 percent with the use of EBUS guidance, especially for stations 2 and 4.

1.3. EBUS in Peripheral Lesions

It has been seen that such peripheral intrapulmonary lesions can be approached by EBUS guidance with the same success rate of approximately 75 percent as fluoroscopic or CT guidance *(13)*. These results were confirmed by Shirakawa, et al. *(14)*, who also achieved a diagnostic yield of 75 percent using the miniprobe as the guidance tool for the forceps. The rate of pneumothorax was below 1 percent in all trials.

A later trial *(15)* used EBUS-guided transbronchial lung biopsy (TBB) in fluoroscopically invisible solitary pulmonary nodules using a monoplane C-arm. In 48 out of 54 (89%) cases, the lesion could be reached with EBUS, in 38 (70%); the biopsy established the diagnosis. Especially the results from the latest study are of interest because the possible algorithms for these patients is either thoracotomy/scopy or just waiting until the lesion gets big enough to be biopsied by traditional methods.

2. EBUS AND EUS in Lung Cancer Management

The limitation of the EBUS is that real-time puncture is not possible with this method. Therefore, the EBUS TBNA system was developed. With the EBUS TBNA it is possible to target lesions in the mediastinum anterior and the hilar regions not reachable with EUS FNA so, theoretically, the whole mediastinum can be examined with the combination of EBUS TBNA, and soon after the introduction of the EBUS TBNA scope publications showed the benefits of EBUS TBNA. It was safe, easy, noninvasive, highly acceptable, and had high sensitivity, specificity, NPV and PPV *(16–22)*.

Published results stated that the combination of EUS FNA and EBUS TBNA covered the whole mediastinum, with better results than either EUS FNA or EBUS TBNA alone could produce *(20, 23, 24)*.

In the same period studies with neoadjuvant and adjuvant therapy in lung cancer were introduced. This aspect increased the demand for accurate staging and restaging, not only to establish a basis for correctly analyzing results from the different studies, but also to establish a basis for planning the right treatment protocols for each individual patient to receive the best possible multimodality treatments.

When introducing new techniques it should be evaluated not only on the quality of the results, but also according to the benefit patients gain from the new techniques.

Up to 10 percent of operations for non-small cell lung cancer (NSCLC) result in explorative thoracotomies without tumor resection, and an additional 25–35 percent of the operations are unsuccessful because of postoperative recurrent disease. *(25, 26)* Therefore, surgery may be regarded as futile or unnecessary in up to 45 percent of patients, apparently because the stage of the disease is more advanced than expected preoperatively.

Could this aspect be improved by introducing endoscopic ultrasound?

The traditional final preoperative staging is based on cervical mediastinoscopy. This method only reaches mediastinum anterior and the superior part of the subcarinial region, i.e., stations 2, 4 and 7. Mediastinum posterior and the hilar regions cannot be reached by traditional mediastinoscopy.

The results of mediastinoscopy in a meta-analysis show a PPV of 1.00 and NPV on 0.91. Other studies show a sensitivity of 0.81. *(27)* New methods should show better results than this.

3. Endoscopic Ultrasound (EUS FNA)

The early publications concerning EUS FNA and EBUS TBNA showed results that equal the results for mediastinoscopy, and some publications even showed better results than mediastinoscopy *(17–22, 28)*, but most important is the impact these methods had on the treatment of these patients. The aim was to develop methods which were noninvasive, could be performed under local anesthesia and were based on an outpatient program and showed better results.

Larsen, et al. *(29)* conducted a study involving 104 patients randomly assigned to either a conventional workup including EUS-FNA only for selected patients, or a strategy where all patients were offered EUS-FNA (routine EUS-FNA) in addition to conventional workup. Patients were followed up for a median period of 1.3 years (range 0.2–2.4 years). Thoracotomy was regarded as futile if the patient had an explorative thoracotomy without tumor resection or if a resected patient had recurrent disease or died from lung cancer during follow-up.

Fifty-three patients were randomly assigned to routine EUS-FNA and 51 patients to conventional workup. EUS-FNA was performed in 50 patients (94%) in the routine EUS-FNA group, and in 14 patients (27%) in the CWU group. In the routine EUS-FNA group five patients (9%) had a futile thoracotomy, compared

with 13 (25%) in the conventional workup group, $p = 0.03$. They could conclude that the addition of routine EUS-FNA to the standard workup in routine clinical practice improved selection of surgically curable patients with NSCLC because it resulted in a 16 percent reduction of futile thoracotomies.

The same year Annema, et al. published his results *(30)*. Two-hundred-forty-two consecutive patients with suspected or proven lung cancer and enlarged (> 1 cm) mediastinal LNs at chest computed tomography were scheduled for mediastinoscopy/tomy (94%) or exploratory thoracotomy (6%). Before surgery all patients underwent EUS-FNA.

They found that EUS-FNA prevented 70 percent of scheduled surgical procedures due to the demonstration of LN metastases in non-small cell lung cancer (52%), tumor invasion (T4) (4%), tumor invasion and LN metastases (5%), SCLC (8%), or benign diagnoses (1%). Sensitivity, specificity, and accuracy for EUS in mediastinal analysis were 91 percent, 100 percent and 93 percent, respectively. So endoscopic ultrasound has proven to have a major impact on decision making in the treatment of lung cancer, even though EUS FNA only reaches the mediastinum posterior and inferior.

4. Endobronchial Ultrasound Transbronchial Fine Needle Aspiration (EBUS TBNA)

Therefore, the expectations for EBUS TBNA were very high when introduced in the staging and diagnostics of lung cancer. One-hundred-ten patients with suspected lung cancer and an intrapulmonary tumor located near or adjacent to the central part of the bronchial tree, or with suspected metastases to the mediastinum or to the hilar lymph nodes, and who had undergone a nondiagnostic broncho-scopy combined with TBNA underwent EBUS-FNA. Diagnoses based on EBUS-FNA biopsies were verified by mediastinoscopy or EUS FNA, and if these procedures were nondiagnostic during surgical resection if the biopsy indicated non-small cell lung cancer.

A specific diagnosis in 103 of 110 patients (97%) were obtained and lung cancer was found in 82 patients (72%). Eighteen patients had a cancer ruled out and seven patients had equivocal biopsy results. No complications occurred. In 17 patients the malignant diagnosis was obtained by puncture of N1 lymph modes**.** The 103 patients could have avoided the mediastinoscopy and three of the patients could have avoided diagnostic thoracotomy/scopy. Two of the patients were found with N3 disease in the contralateral hilar region**.** One-hundred patients scheduled for mediastinoscopy or thoracotomy underwent EBUS TBNA and mediastinoscopy in the same anesthesia. The characteristics of the patients are seen in **Tables 10.1 and 10.2**. In three cases we

Table 10.1
Characterization of the patient: EBUS TBNA and mediastinoscopy

Variable	No.
Total No. of patients	100
Age, years	
Mean	62
Range	38–79
Sex, %	
Male	63
Female	37
Nodal status based on CT, %	
N0	27
N1	8
N2	41
N3	24
Scheduled for, %	27
Mediastinoscopy	75
Thoracotomy	25

Table 10.2
Characterization of the patient: EBUS TBNA, EUS FNA and mediastinoscopy

Variable	No.	%
Total no. of EUS FNA/EBUS TBNA procedures	90	100
EUS-FNA results		
No lymph node metastases	40	44
N1 metastases	3	3
N2 metastases	33	37
N3 metastases	8	9
Tumors	6	7
SCLC	5	6
Other diagnoses	2	2
Surgery could have been prevented Mediastinoscopy/thoracotomy	75	7

found a false-negative mediastinoscopy and EBUS TBNA (one station 6, one metastases in the adrenals and one in station 8). In 11 cases the mediastinoscopy was false–negative, and in four patients EBUS TBNA was false-negative. The results of EBUS TBNA and mediastinoscopy are shown in **Table** 10.3.

Table 10.3
Results of EBUS TBNA and Mediastinoscopy in 100 patients

Stage	EBUS TBNA	Mediastinoscopy
N0	49	49
N2 false-negative	7	14
N2	37	31
N3	7	6

In many centers patients with CT T1-2N0-1M0 are referred directly to thoracotomy. On this background 25 patients would have been referred directly to thoracotomy. Patients with N0 after mediastinoscopy were referred to thoracotomy/thoracoscopy. Nine thoracotomies could therefore have been avoided with the use of EBUS TBNA because of false-negative CT N0-1.

Of the 75 patients scheduled for mediastinoscopy, seven patients would have undergone an unnecessary primary thoracotomy with EBUS TBNA alone. With mediastinoscopy alone the numbers would have been 14 unnecessary thoracotomies. Because of positive EBUS TBNA 51 mediastinoscopies could be avoided.

The actual guidelines recommend mediastinoscopies when EBUS TBNA is without malignancies. Following these guidelines 49 medistinoscopies should be performed with the results of finding four false-negative EBUS TBNAs (8%).

5. EBUS TBNA Combined with EUS FNA in Exploration of the Mediastinum

In 90 of these patients EBUS TBNA and medistinoscopy were combined with EUS FNA. **Table** 10.4 shows the results which included just two cases of false-negative endoscopic ultrasound examinations (2%). This is a much better result than presented by mediastinoscopy alone or mediastinoscopy and EUS combined.

Table 10.4
Results of EBUS TBNA, Mediastinoscopy and EUL FNA in 90 patients

Stage	EBUS TBNA	Mediastinoscopy/ thoracotomy	EUL FNA	Combined EBUS TBNA and EUS TBNA
N0	42	42	42	42
N2 false-negative	7	13	10	2
N2	28	23	24	33
N3	6	6	5	6
Tumor	6	6	6	6
Adrenal			1	1

5.1. Ultrasound in Treatment of Mediastinal Lesions

Because it is possible to visualize and reach lesions by EBUS, EBUS TBNA, and EUS FNA new indications for these methods have been proposed. EBUS TBNI and EUS TBNI (needle injection) is a possibility in treating cancers and metastases, but only one study *(31)* is reporting the results of local injections in vitro. It described the relationship between tumor physiology and the pharmacokinetics of gemcitabine, and concluded that their experimental model provides useful new insight into metabolism and intratumor pharmacokinetics of chemotherapeutic agents in solid tumors. However, no clinical studies in this area exist.

The challenge is to develop a drug which can diffuse throughout the tumor. However, combining EUS and EBUS with radio ablation is also a possibility. EBUS TBNA has only recently been introduced into clinical practice and we have only seen the "tip of the iceberg" concerning the benefits this method will bring patients in daily clinical work.

References

1. Micames et al. EUS-FNA for NSCLC staging: A systematic review and metaanalysis. Chest 2007;131:539–548.
2. Annema JT, Versteegh MI, Veselic M et al. Endoscopic ultrasound added to mediastinoscopy for preoperative staging of patients with lung cancer. JAMA 2005;294:931–936.
3. Endoscopic Ultrasound Guided Biopsy versus mediastinoscopy for analysis of paratracheal and subcarinal lymph nodes in lung cancer staging. Lung Cancer 2005;48:85–92.
4. Herth F, Becker HD. Endobronchial ultrasound of the airways and the mediastinum. Monaldi Arch Chest Dis 2000;55(1):36–45.
5. Falcone F, Fois F, Grosso D. Endobronchial ultrasound. Respiration 2003;70(2):179–194.
6. Kurimoto N, Murayama M, Yoshioka S. Assessment of usefulness of endobronchial ultrasonography in tracheobronchial tumor invasion. Chest 1999;115:1500–1506.
7. Herth F, Becker HD. EBUS for early cancer detection. J Bronchol 2003;10:249–253.
8. Miyazu Y, Miyazawa T, Kurimoto N, Iwamoto Y, Kanoh K, Kohno N. Endobronchial ultrasonography in the assessment of centrally located earlystage lung cancer before photodynamic therapy. Am J Respir Crit Care Med 2000;165(6):832–837.

9. Herth F, Becker HD, LoCicero J, Ernst A. Endobronchial ultrasound in therapeutic bronchoscopy. Eur Respir 2002; J 20:118–121.

10. Herth FJ, Becker HD, Ernst A. Ultrasound-guided transbronchial needle aspiration: an experience in 242 patients. Chest 2003;123:604–607.

11. Herth F, Becker HD, Ernst A. Conventional vs endobronchial ultrasound-guided transbronchial needle aspiration: a randomized trial. Chest 2004;125(1):322–325.

13. Herth F, Ernst A, Becker HD. Endobronchial Ultrasound (EBUS)-guided transbronchial lung biopsy(TBBX) in solitary pulmonary nodules and peripheral lesions. Eur Respir J 2002;20:972–975.

14. Shirakawa T, Imamura F, Hamamoto J, Honda I, Fukushima K, Sugimoto M, Shirkakusa T. Usefulness of endobronchial ultrasonography for transbronchial lung biopsies of peripheral lung lesions. Respiration 2004;71(3):260–268.

15. Herth FJ, Eberhardt R, Becker HD, Ernst A. Endobronchial ultrasound-guided transbronchial lung biopsy in fluoroscopically invisible solitary pulmonary nodules: a prospective trial. Chest 2006;129(1):147–150.

16. Krasnik M, Vilmann P, Larsen SS, Jacobsen GK. Preliminary experience with a new method of endoscopic transbronchial real time ultrasound guided biopsy for diagnosis of mediastinal and hilar lesions. Thorax 2003;58:1083–1086.

17. Yasufuku K, Chiyo M, Sekine Y Chhajed PN, Shibuya K, Iizasa T, Fujisawa T. Real-time endobronchial ultrasound-guided transbronchial needle aspiration of mediastinal and hilar lymph nodes. Chest 2004;126:122–128.

18. Herth FJ, Eberhardt R, Vilmann P, Krasnik M, Ernst A. Real-time, endobronchial ultrasound-guided, transbronchial needle aspiration: a new method for sampling mediastinal lymph nodes. Thorax 2006;61:795–798.

19. Herth FJF, Ernst A, Eberhardt R, et al. Endobronchial ultrasoundguided transbronchial needle aspiration of lymph nodes in the radiologically normal mediastinum. Eur Respir J 2006;28:910–914.

20. Rintoul RC, Skwarski KM, Murchison JT, Wallace WA, Walker WS, Penman ID. Endobronchial and endoscopic ultrasound-guided real-time fine-needle aspiration for mediastinal staging. Eur Respir J 2005;25:416–421.

21. Herth FJF, Eberhardt R, Vilman P, Krasnik M. EBUS-TBNA-a new device for endoscopic transbronchial real time ultrasound guided biopsy for diagnosis and staging of mediastinal lymph nodes. Thorax 2006 Sep;61(9):795–798.

22. Herth FJF, Krasnik M, Eberhardt R, Ernst A, Vilman P, Dienemann H. EBUS guided biopsy for the staging of mediastinal lymph nodes in a radiologically normal mediastinum. Eur Respir J 2006 Nov;28(5):910–914.

23. Herth FJ, Lunn W, Eberhardt R, Becker HD, Ernst A. Transbronchial vs transesophageal ultrasound-guided aspiration of enlarged mediastinal lymph nodes. B Am J Respir Crit Care Med 2005;171:1164–1167.

24. Vilmann P, Krasnik M, Larsen SS, Jacobsen GK, Clementsen P. Endoscopic trans-esophageal and endoscopic ultrasound guided biopsy: a combined approach in the evaluation of mediastinal lesions. Endoscopy 2005;37:833–839.

25. Herder GJ, Verboom P, Smit EF, van Velthoven PC, van den Bergh JH, Colder CD, van Mansom I, van Mourik JC, Postmus PE, Teule GJ, Hoekstra OS. Practice, efficacy and cost of staging suspected non-small cell lung cancer: a retrospective study in two Dutch hospitals. Thorax 2002;57:11–14.

26. van Tinteren H, Hoekstra OS, Smit EF, van den Bergh JH, Schreurs AJ, Stallaert RA, van Velthoven PC, Comans EF, Diepenhorst FW, Verboom P, van Mourik JC, Postmus PE, Boers M, Teule GJ. Effectiveness of positron emission tomography in the preoperative assessment of patients with suspected non-small-cell lung cancer: the PLUS multicentre randomised trial. Lancet 2002;359:1388–1393.

27. Toloza EM, Harpole L, Detterbeck F, McCrory DC. Invasive staging of non-small cell lung cancer: a review of the current evidence. Chest 2003 Jan;123(1 Suppl):157S–166S.

28. Tournoy KG, De Ryck F, Vanwalleghem LR, Vermassen F, Praet M, Aerts JG, Van Maele G, van Meerbeeck J. Endoscopic ultrasound reduces surgical mediastinal staging in lung cancer: a randomized trial. Am J Respir Crit Care Med. 2008;177(5):531–535.

29. Larsen SS, Vilmann P, Krasnik M, Dirksen A, Clementsen P, Maltbaek N, Lassen U, Skov BG, Jacobsen GK. Endoscopic ultrasound guided biopsy performed routinely in lung cancer staging spares futile thoracotomies: preliminary results from a randomised clinical trial. Lung Cancer 2005 Sep;49(3):377–385.

30. Annema JT, Versteegh MI, Veselič M, Voigt P, Rabe KF. Endoscopic ultrasound-guided fine-needle aspiration in the diagnosis and staging of lung cancer and its impact on

surgical staging. J Clin Oncol 2005 Nov 20;23(33):8357–8361.

31. Kristjansen PE, Brown TJ, Shipley LA, Jain RK. Intratumour pharmacokinetics, flow resistance, and metabolism during gemcitabine infusion in ex vivo perfused human small cell lung cancer. Clin Cancer Res 1996;2(2):359–367.

Index